**UNIVERSITÀ DEGLI STUDI DI MILANO**

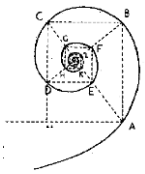

**DOTTORATO IN MEDICINA MOLECOLARE**

**E TRASLAZIONALE**

CICLO XXXI

Anno Accademico 2016/2017

TESI DI DOTTORATO DI RICERCA

MED26

# ASSESSING THE PATHOGENESIS OF MULTIPLE SYSTEM ATROPHY THROUGH CELLULAR MODELS


**Dottorando: Giacomo MONZIO COMPAGNONI**

Matricola N° R11289

TUTORE: Prof. Giacomo Pietro COMI

CO-TUTORE: Dott. Alessio DI FONZO

Coordinatore del dottorato: Prof. Riccardo GHIDONI

**SOMMARIO**

L'Atrofia Multisistemica (MSA) è una malattia neurodegenerativa grave con un'incidenza di 0,6 casi per 100000 persone/anno, ad insorgenza in età adulta e con una sopravvivenza di 6-9 anni dalla diagnosi. Clinicamente, la MSA è caratterizzata da parkinsonismo, atassia cerebellare, disautonomia e segni piramidali. In base alla prevalenza dei sintomi parkinsoniani o cerebellari si identificano due sottotipi di malattia, rispettivamente MSA-P e MSA-C. Dal punto di vista neuropatologico, la MSA rientra nell'ambito delle alfa-sinucleinopatie. Tuttavia, a differenza della malattia di Parkinson e della demenza a corpi di Lewy, nell'MSA l'alfa-sinucleina non si accumula tanto a livello neuronale quanto a livello oligodendrogliale.

Al momento non esistono terapie efficaci.

La patogenesi della malattia è quasi del tutto sconosciuta e i modelli attualmente disponibili, prevalentemente animali transgenici ottenuti overesprimendo alfa-sinucleina umana sotto il controllo di promotori di geni specificamente espressi a livello oligodendrogliale, non ne ricapitolano pienamente i meccanismi patogenetici.

Lo scopo di questo progetto è stato la generazione e lo studio di nuovi modelli sperimentali mirati alla valutazione dei meccanismi patogenetici della malattia e all'identificazione di nuovi obiettivi terapeutici.

Lo studio si è basato sull'utilizzo di cellule di sangue periferico, colture primarie di fibroblasti, neuroni dopaminergici derivati da cellule staminali pluripotenti indotte (iPSCs) e tessuto cerebrale. Le tematiche esaminate sono state molteplici, comprendendo l'autofagia, la funzionalità mitocondriale e l'espressione di alfa sinucleina.

Le principali alterazioni riscontrate nei pazienti sono state: un aumento della quantità di DNA mitocondriale nelle cellule di sangue periferico e nel tessuto

cerebrale, selettivamente nella forma cerebellare di malattia; una compromissione dell'attività della catena respiratoria mitocondriale nei fibroblasti e nei neuroni; un incremento della massa mitocondriale e della quantità di complesso II, un incremento dell'espressione di geni mitocondrio-correlati, un incremento della quantità di numerosi enzimi coinvolti nella sintesi del Coenzima Q10 nei neuroni; un'alterazione dell'autofagia nei neuroni; una ridotta espressione di marcatori neuronali nelle fasi avanzate del differenziamento dopaminergico; l'ipometilazione di una CpG island collocata nell'introne 1 del gene dell'alfa-sinucleina.

E' di particolare rilievo la generazione e la caratterizzazione del modello neuronale derivato da iPSCs, in quanto rappresenta il primo modello completo di MSA basato su questa tecnica.

Nel complesso, questo progetto ha portato all'identificazione di numerosi difetti nelle cellule e nei tessuti di pazienti affetti da MSA che suggeriscono una disfunzione di specifici processi molecolari e contribuiscono alla comprensione dei sottostanti meccanismi patogenetici. Inoltre, questo studio pone le basi per numerose linee di ricerca e il modello qui descritto può presentare notevoli applicazioni in campo terapeutico, grazie all'opportunità di valutare l'efficacia e la tollerabilità di nuovi composti farmacologici.

**ABSTRACT**

Multiple System Atrophy (MSA) is a severe adult-onset neurodegenerative disease, with an incidence of 0.6 per 100000 persons/year and a survival rate of 6-9 years from the onset. MSA is clinically characterized by parkinsonism, cerebellar ataxia, dysautonomia and pyramidal signs. Two subtypes of the disease can be distinguished, MSA-P and MSA-C, on the basis of the predominant symptomatology, parkinsonian or cerebellar respectively. From a neuropathological point of view, MSA is classified as an alpha-synucleinopathy. However, differently from Parkinson's disease and Dementia with Lewy bodies, the main intracellular localization of alpha-synuclein aggregates in MSA is not the neuron, but the oligodendrocyte.

An effective therapy is not available yet.

The pathogenesis of the disease is almost completely unknown and the available models, mainly transgenic animals overexpressing human alpha-synuclein under the promoter of genes specifically expressed in oligodendrocytes, do not fully recapitulate the pathogenic mechanisms.

The aim of the present project was the generation and study of new experimental models for the identification of the molecular mechanisms of the disease and new therapeutic targets.

The study has taken advantage from the use of peripheral blood cells, fibroblasts' primary cultures, iPSC-derived dopaminergic neurons and brain tissue and has focused on several topics, including autophagy, mitochondrial functioning and alpha-synuclein expression.

The main findings in patients have been: an increase of mtDNA amount in peripheral blood cells and in brain tissue, selectively in the cerebellar subtype; an impairment of mitochondrial respiratory chain activity in fibroblasts and iPSC-derived neurons; an increase of mitochondrial mass

and of complex II amount, an increased expression of mitochondria-related genes, an increase of the amount of many enzymes involved in the synthesis of Coenzyme Q10 in neurons; an impairment of the autophagic pathway in neurons; a reduced expression of neuronal markers in advanced stages of dopaminergic differentiation; hypomethylation of a CpG island located in alpha-synuclein intron 1.

The generation and characterization of the iPSC-derived neuronal model is particularly remarkable because it represents the first comprehensive model of MSA based on this technique.

In conclusion, this project has led to the identification of several defects in MSA cells and tissues, suggesting the impairment of specific molecular pathways and contributing to the understanding of the underlying pathogenic mechanisms. Furthermore, this study lays the foundations for several lines of investigation and the proposed model can also have remarkable therapeutic implications for the assessment of effectiveness and tolerability of new pharmacological compounds.

**TABLE OF CONTENTS**

## INTRODUCTION

Multiple System Atrophy (MSA) is a progressive adult-onset neurodegenerative disorder which affects several areas of the nervous system. The clinical presentation is heterogenous and is characterized by parkinsonian, cerebellar, autonomic and pyramidal features. An effective therapy is not available yet. Alpha-synuclein accumulation, mainly in oligodendroglia, is the main neuropathological finding, but almost nothing is known about the pathogenic mechanisms. The purpose of the present thesis project is the development and study of innovative models which may help to dissect the pathological mechanisms of this invalidating disorder and lay the basis for the future development of new drugs.

### Clinical presentation and diagnosis

Multiple System Atrophy (MSA) is a severe and progressive neurodegenerative disease, which is clinically characterized by parkinsonism, cerebellar ataxia, dysautonomia and pyramidal signs in different combinations. (Fanciulli and Wenning, 2015; Krismer and Wenning, 2017)

Estimated incidence is 0.6 per 100000 person-years, but a considerable variability has been observed in different geographical areas. Being MSA a late-onset disease, incidence is highly age-dependent and reaches the value of 3 per 100000 person-years over 50 years of age.

Onset is usually in the sixth decade of life and mean survival is 6-9 years.

The denomination “Multiple System Atrophy” is of recent use and it denotes a spectrum of disorders which were previously denominated striatonigral degeneration, olivopontocerebellar atrophy and Shy-Drager syndrome.

Two diffferent subtypes of the disease can be distinguished (MSA-P and MSA-C) on the basis of the predominant symptomatology at onset, parkinsonian or cerebellar respectively.

MSA-P is the widely most common form in Western countries, representing 80 % of cases, whereas MSA-C is the most diffuse presentation in the Japanese population.

Parkinsonism usually manifests with a rapidly progressive akinetic-rigid symptomatology comprehending muscle stiffness, resistance to passive movements and slow movements.

Cerebellar symptomatology is characterized by gait and limb ataxia, scanning dysarthria and oculomotor symptoms.

Dysautonomia is always found in MSA patients and includes a wide spectrum of signs and symptoms. Urogenital dysfunction is characterized by urinary incontinence, urinary frequency and urgency, incomplete bladder emptying and erectile dysfunction. Neurogenic orthostatic hypotension is another common invalidant autonomic symptom. Recurrent syncopes, weakness, headache, dizziness and nausea are common findings. Hypohydrosis and anhydrosis can also occur.

Generalized hyperreflexia and abnormal plantar reflex are the main pyramidal signs that can be detected in MSA. MSA-C is more often interested by the pyramidal involvement.

Many other clinical features can occur during the progression of disease, including axial deformities, dysphagia, sialorrhea, respiratory stridor and REM sleep behaviour disorder.

The heterogeneity of clinical presentation makes the diagnostic procedure difficult and differential diagnosis with other diseases is often required, in

particular with DLB, PD, PSP and sporadic adult onset ataxia. Other disorders that are less commonly involved in differential diagnosis are toxin-induced ataxias, vitamin B1 deficiency-related ataxias, immune-mediated ataxias, genetic ataxias (e.g. SCA6 and Friedreich ataxia). Only 62 % of clinically-diagnosed MSA patients have diagnosis confirmed at autopsy.

“Definite” diagnosis can be performed only post-mortem, whereas clinical diagnosis can only be defined as “probable” or “possible”.

The diagnostic criteria for definite, probable and possible MSA have been published by Gilman et al. in 2008 and are the following (quoted from the guidelines):

- “Definite MSA”. Neuropathological finding of widespread and abundant central nervous system alpha-synuclein-positive glial cytoplasmic inclusions (Papp Lantos inclusions) in association with neurodegenerative changes in striatonigral and olivopontocerebellar structures.
- “Probable MSA”. A sporadic, progressive, adult onset disease characterized by: autonomic failure involving urinary incontinence (inability to control the release of urine from the bladder, with erectile dysfunction in males) or an orthostatic decrease of blood pressure within 3 minutes of standing by at least 30 mmHg systolic or 15 mmHg diastolic AND poorly levodopa-responsive parkinsonism (bradykinesia with rigidity, tremor or postural instability) OR a cerebellar syndrome (gait ataxia with cerebellar dysarthria, limb ataxia or cerebellar oculomotor dysfunction).
- “Possible MSA”. A sporadic, progressive, adult onset disease chracterized by: parkinsonism (bradykinesia with rigidity, tremor or postural instability) OR a cerebellar syndrome (gait ataxia with cerebellar dysarthria, limb ataxia or cerebellar oculomotor

dysfunction) AND at least one feature suggesting autonomic dysfunction (otherwise unexplained urinary urgency, frequency or incomplete bladder emptying, erectile dysfunction in males or significant orthostatic blood pressure decline that does not meet the level required in probable MSA) AND at least one of the listed additional features (Babinski sign with hyperreflexia, stridor, rapidly progressive parkinsonism, poor response to levodopa, postural instability within 3 years of motor onset, gait ataxia, cerebellar dysarthria, limb ataxia or cerebellar oculomotor dysfunction, dysphagia within 5 years of motor onset, atrophy on MRI of putamen, middle cerebellar peduncle, pons or cerebellum, hypometabolism on FDG-PET in putamen, brainstem or cerebellum, parkinsonism, atrophy on MRI of putamen, middle cerebellar peduncle or pons, hypometabolism on FDG-PET in putamen, presynaptic nigrostriatal dopaminergic denervation on SPECT or PET).

Furthermore, many tools can be of help in the diagnostic procedure.

Atrophy of putamen, pons and middle cerebellar peduncle and dilation of the fourth ventricle can be observed at MRI images. Furthermore, two MRI signs at T2 weighted images are indicative of MSA: the “putaminal slit” (hyperintensity of putaminal margin) and the “hot cross bun” (pontine cruciform hyperintensity).

$^{18}$F-FDG-PET images display a reduced striatal glucose metabolism, whereas SPECT shows areas of reduced perfusion in striatum, brainstem and cerebellum in MSA patients. (Tang et al., 2010; Poston et al., 2012; Poston and Eidelberg, 2012)

The evaluation of D2 receptor ligands aimed to assess post-synaptic dopaminergic function can be useful for differential diagnosis with PD (Brooks and Seppi, 2009), whereas the degeneration of pre-synaptic

striatonigral terminals in both PD and MSA reduces the usefulness of the assessment of presynaptic dopaminergic function with $^{18}$F-fluorodopa-PET or $^{123}$I-β-CIT-SPECT.

## Therapeutic approaches

An effective therapy is not available yet, but some symptomatic treatments are currently in use. (Krismer and Wenning, 2017)

Parkinsonian symptoms are usually treated with dopamine agents and levodopa is the agent of choice, since 40 % of MSA patients have shown a beneficial response to the administration of this compound. Dopamine agonists, such as ropinirole, pramipexole, lisuride, cabergoline or rotigotine have shown lower tolerability and poorer efficacy in patients.

Amantadine effect has been assessed in two trials, without positive results.

Local dystonia can be treated with botulin toxin injections

Botulin toxin injections and anticholinergic drugs can be used to treat sialorrhea, despite the adverse effects of anticholinergic compounds (confusion, impaired concentration, drowsiness, memory impairment and attention defict).

Anticholinergic drugs can also be used for the treatment of urogenital symptoms, in particular for detrusor hyperreflexia and detrusor-sphyncter dyssynergia.

Regular clean intermittent catheterization can be necessary in case of increased post-mictutrition volumes whereas urethral obstructions can require transcutaneous suprapubic catheterization.

Erectile dysfunction can benefit from cGMP specific phosphodiesterase type 5 inhibitors (e.g. sildenafil), although orthostatic hypotension is exacerbated by such compounds.

Constipation should be treated with non-pharmacological measures (high fluid and fibre intake and exercise) and with the administration of laxatives (e.g. calcium polycarbophil and mosepride citrate).

Also cardiovascular autonomic dysfunction requires several therapeutic interventions, both non-pharmacological and pharmacological. Physical counter-manoeuvres should be used for orthostatic hypotension, such as stockings and abdominal binders. Large meals should be discouraged and sufficient fluid intake and high-salt diet are warranted. Moreover, night-time head-up tilt reduces supine hypertension, nicturia and orthostatic hypotension in the morning. The α1-receptor agonist compound midodrine alleviates hypotension, as well as the noradrenaline precursor droxidopa, the corticosteroid fludrocortisone and the acetylcholinesterase inhibitor pyridostigmine. Blood pressure elevating drugs should be avoided in late afternoon or evening to avoid night-time hypertension. Nicturia can be alleviated by the administration of the antidiuretic compound desmopressin.

Several pharmacological trials have been completed or are ongoing for the treatment of MSA.

In particular, 7 interventional trials have already been completed and have assessed the effect of mesenchymal stem cell autologous transplantation (Lee et al., 2012), riluzole (Bensimon et al., 2009), minocycline (Dodel et al., 2010), growth hormone (Holmberg et al., 2007), rifampicin (Low et al., 2014), lithium (Sacca et al., 2013) and rasagiline (Poewe etal., 2015) in MSA patients. However, none of these trials have provided positive results, with the exception of the one assessing the effect of mesenchymal stem cell transplantation. In that case, autologous mesenchymal stem cells were

delivered intra-arterially at day 0 and intra-venously at days 30, 60 and 90. A p value of 0.047 was obtained, assessing changes in the Unified Multiple System Atrophy Rating Scale (UMSARS) as primary outcome. However, the UMSARS improvement was also accompanied by the finding of multiple small cerebral infarcts at MRI, in one case clinically symptomatic.

The ongoing interventional trials are related to the assessment of the myeloperoxidase inhibitor AZD3241 (phase II), autologous mesenchymal stem cell transplantation (phase I), epigallocatechin gallate (phase II) and alpha-synuclein immunization (phase I).

However many therapeutic strategies are being studied, mainly related to alpha-synuclein pathology. In particular, alpha-synuclein-related therapeutic strategies may target alpha-synuclein expression, alpha-synuclein aggregation, alpha-synuclein degradation and clearance and alpha-synuclein cell-to-cell propagation (Valera et al., 2016).

The effect of antisense small interfering RNA (siRNA) or short hairpin RNA (shRNA) has already been tested on animal and in vitro models of PD overexpressing *SNCA* gene with encouraging results, but not in MSA. (Takahashi et al., 2015; Zharikov et al., 2015)

Alpha-synuclein aggregation could be targeted through specific agents, such as the inhibitor Anle 138b, already studied in animal models of PD, or the iron chelation agent epigallocatechin gallate whose effect in MSA is being assessed in a clinical trial. (Wagner et al., 2013; Lorenzen et al., 2014)

Apha-synuclein degradation and clearance can be targeted through various stratategies, such as the stimulation of autophagy, the modulation of phagocytic activty of microglia and the administration of extracellular degrading enzymes.

Furthermore alpha-synuclein accumulation has been found to be reduced by antiinflammatory agents, in particular some antidepressants (Valera et al., 2014; Ubhi et al., 2012) and immunomodulatory compounds (Valera et al., 2015), in animal models of synucleinopathies. Also the immunomodulatory and anticancer drug lenalidomide has been tested on the MBP-tg-mouse-model of MSA, showing a reduction of alpha-synuclein positive cells in striatum and a normalization of proinflammatory microglial phenotype (Valera et al., 2016). Furthermore, as myeloperxidase inhibition has been found to be associated with an improvement of both clinical and pathological features of the 3NP model of MSA (Stefanova et al., 2012) a phase II clinical trial is currently ongoing in MSA patients with the compound AZD3241.

The last pharmacological mechanisms which are under consideration for MSA are related to alpha-synuclein cell-to-cell propagation: extracellular alpha-synuclein degrading enzymes (e.g. matrix metalloproteinases, plasmin or neurosin, which has shown to reduce alpha-synuclein in oligodendrocytes and alpha-synuclein spread to glial cells in a mouse model of MSA) (Tatebe et al., 2010; Spencer et al., 2013; Spencer et al., 2015; Park et al., 2013) and immunization against alpha-synuclein, both passive and active. The tool of immunization is particularly promising, having been widely assessed in pre-clinical models and being now tested in clinical trials. (Masliah et al., 2011; Valera et al., 2013; Mandler et al., 2014; Mandler et al., 2015) Passive immunization is already undergoing a phase I trial aiming to assess the effect of anti-alpha-synuclein antibodies PRX002 and BIIB054 in patients. Also active immunization is being investigated through the administration of small peptides which mimic alpha-synuclein C-terminus.

## Neuropathology

The complexity of MSA clinical phenotype finds a pathological correlate in the large number of areas of the nervous system which are affected.

From the macroscopic point of view, putaminal atrophy, brainstem nuclei pale pigmentation and cerebellar and pontine atrophy are the main neuropathological findings. (Jellinger, 2014)

Microscopically, glial cytoplasmic inclusions (GCIs) are the most important hallmark of the disease. GCIs are argyrophilic intracellular aggregates, mainly composed of alpha-synuclein, which are located in oligodendrocytes. (Jellinger, 2014; Jellinger and Lantos, 2010; Papp et al., 1989; Papp and Lantos, 1992; Papp and Lantos, 1994; Lantos and Papp, 1994) The presence of alpha-synuclein aggregates in patients is the rationale for the inclusion of MSA, together with Parkinson's disease (PD) and Dementia with Lewy bodies (DLB), in the group of alpha-synucleinopathies. However, the selectivity of these aggregates for oligodendroglia differentiates MSA from PD and DLB, where alpha-synuclein aggregates are mainly found in neurons. Although GCIs are widely distributed in the nervous system, a region-specific selectivity can be observed. Pons, medulla, putamen, substantia nigra pars compacta, cerebellum and preganglionic autonomic structures are the most affected areas. Furthermore, even inside these specific regions of the nervous system, a further selectivity of GCIs for specific cellular subpopulations can be observed. For example, in the putamen only calcineurin-positive medium spiny neurons degenerate, whereas ChAT-positive neurons are relatively spared. (Sato et al., 2007)

As already stated, alpha-synuclein is the main constituent of GCIs. However, alpha-synuclein is not usually found in its basal form, but often undergoes modifications. The phosphorylation of serine 129 residue is a common finding, as well as protein nitration. Furthermore, not only the monomeric

form of the protein, but also granular and filamentous structures are found in aggregates.

In addition to alpha-synuclein, many other proteins can be detected in GCIs. p25alpha/TPPP (involved in myelination and supposed to trigger alpha-synuclein aggregation), ubiquitin, microtubule-associated tau protein, prion disease-linked 14-3-3 protein, heat shock proteins Hsc70 and Hsp70, alpha and beta tubulin, microtubule associated proteins, cdk5, DARRP-32, HtrA2/Omi, metallothionein-III, LRRK2 and Parkin are some examples.

Although glial protein inclusions are the main hallmark of the disease, alpha-synuclein aggregates can be observed also in neurons, both in cytoplasm (neuronal cytoplasmic inclusions or NCIs) and in nuclei (neuronal nuclear inclusions or NNIs). NCIs and NNIs can usually be found in pontine nuclei, inferior olives, putamen, substantia nigra, locus coeruleus, cortical pyramidal neurons, lower motor neurons and intermediolateral column of thoracic spinal cord. Pontine basis and inferior olives are the most affected regions.

Astrogliosis and microglial activation are other important neuropathological findings of MSA.

Concerning the localization of neuropathological lesions, some differences exist between MSA-P and MSA-C. In MSA-P the most affected areas are dorsolateral caudal putamen, caudate nucleus, globus pallidus and subthalamic nucleus, whereas thalamic nuclei are spared.

In MSA-C neuronal degeneration can be observed in pontine basis, cerebellopontine fibers, cerebellar vermis, cerebellar hemispheres, dentate nucleus. Striatum, substantia nigra and locus coeruleus are affected too, although not as heavily as in MSA-P. Pontine gray, paracerebellar nuclei and inferior olivary complex can display neuronal inclusions. Cerebellar

Purkinje's cells, although found to degenerate, do not contain GCIs, but accumulate glial cell line derived neurotrophic factor (GDNF).

Intermediolateral column of spinal cord, dorsal nucleus of vagus and Onufrowicz nucleus are affected both in MSA-P and in MSA-C.

## Available models

The development of reliable models of MSA is particularly challenging because of the complexity of the clinical and pathological features. (Ubhi et al., 2011; Fernagut et al., 2012; Stefanova et al., 2015)

The first models were obtained through the administration of toxins to animals. As the main pathological features of MSA are characterized by the involvement of striatum and substantia nigra, it was initially proposed to administer toxins able to damage these specific areas. The first attempt was based on the injection of 6-hydroxydopamine (6-ODA) in medial forebrain and quinolinic acid (QA) in striatum. Although this approach effectively led to striatal and dopaminergic loss, it proved to be too destructive, impeding a correct evaluation of pathogenic mechanisms. (Ghorayeb et al., 2001)

An alternative toxin-mediated approach was based on the intraperitoneal injection of 3-nitroproprionic acid (3NP) in mice. Motor dysfunction and a variable degree of striatal and dopaminergic degeneration was observed. (Fernagut et al., 2002)

Also the effect of the concomitant administration of 3NP and MPTP was assessed. This approach was used also in mokeys, leading to a clinical and pathological phenotype which included an impaired motor behavior and the degeneration of putamen and caudate nucleus. However, the remarkable

methodological limitations strongly affected the actual application of this method. (Stefanova et al., 2003; Ghorayeb et al., 2000)

The following step in modeling MSA was represented by the generation of transgenic animals. As the main pathological feature of the disease is the finding of alpha-synuclein aggregates in oligodendrocytes, the main efforts were devoted to recapitulate this specific phenotype. Therefore, the majority of transgenic animal models are represented by mice overexpressing human alpha-synuclein under the promoter of genes specifically expressed in oligodendrocytes (Ubhi et al., 2011).

The PLP-tg-mouse-model has been generated overexpressing human alpha-synuclein under the promoter of proteolipid protein (PLP). These mice display a selective localization of the protein in oligodendrocytes and the pattern of protein aggregates resembles that of GCIs. The typical pathological feature of alpha-synuclein hyperphosphorylation at S129 can be observed too. (Kahle et al., 2002) Furthermore, in addition to classicaly affected brain regions, also other areas of the nervous system are involved. In particular, the degeneration of Onuf's nucleus, peduncolopontine tegmental nucleus, laterodorsal tegmental nucleus, cholinergic neurons of nucleus ambiguus and other areas which are connected to autonomic failure and other non motor symptoms has been described. (Sternberger et al., 2010) The administration of 3-nitroproprionic acid to PLP-hasyn-tg-mice leads to a worsening of both clinical and pathological features. In particular, an exasperation of motor symptoms, striatonigral and cerebellar degeneration, microglial activation and astrogliosis has been observed. (Stefanova et al., 2005) Furthermore, PLP-mice have also been used to assess the effect of the MAO-B inhibitor rasagiline. This compound has been administered to animals which had previously been treated with 3-NP acid. An improvement in motor behhavior and in the degeneration of substantia

nigra, striatum, cerebellum, pons and inferior olives has been observed. (Stefanova et al., 2008)

Another transgenic mouse model has been generated overexpressing human alpha-synuclein under the promoter of myelin basic protein (MBP). These mice display a strong pathological phenotype. Human alpha-synuclein can be detected in oligodendrocytes of brainstem, cerebellum, basal ganglia, neocortex and corpus callosum. S129-phosphorylated alpha-synuclein and ubiquitin can be found in intracellular inclusions as well. Astrogliosis, myelin pallor and degeneration of dopaminergic fibers in basal ganglia are other feaures of these animals. (Shults et al., 2005) The effect of 3-NP acid has been assessed also in this model, showing a worsening of neurodegeneration and clinical phenotype. Moreover, an alteration of the levels of nitrated and oxidized alpha-synuclein (but not of the total and phosphorylated forms of the protein) has been detected. (Ubhi et al., 2009) The levels of brain-derived neurotrophic factor (BDNF), insulin like growth factor 1 (IGF1) and glial cell line derived neurotrophic factor (GDNF) have proven to be reduced in MBP-mice and the intracerebroventricular infusion of GDNF has been associated with an improvement of both clinical and pathological features. (Ubhi et al., 2010)

A third transgenic model has been generated overexpressing human alpha-synuclein under the promoter of 2'-3'cyclic-nucleotide-3'-phosphodiesterase (CNP). A motor involvement and a neurodegenerative pattern has been observed in these animals. (Yazawa et al., 2005)

Finally, an atypical model has been generated overexpressing the alpha-1B adrenergic receptor in mice. A parkinsonian syndrome with autonomic dysfunction associated with the finding of alpha-synuclein aggregates in oligodendrocytes has been observed, although the precise mechanism at the basis of this phenotype is unclear. (Zuscic et al., 2000)

So far, very few studies have been performed to generate in vitro models of MSA.

The forced expression of alpha-synuclein (both wild-type and C-terminal truncated forms) in glial cell coltures has been associated with a reduction of cell survival and an increased vulnerability to external stress. (Stefanova et al., 2005)

A recent study has described the generation of iPSC-derived oligodendrocytes from 1 MSA-P and 1 MSA-C patients. A reduction of alpha-synuclein expressing cells has been observed during differentition, but a pathological phenotype has not been detected in these cells. (Djelloul et al., 2015)

## Pathogenesis

### Genetics

Differently from Parkinson's disease, where a remarkable percentage of cases are due to genetic mutations (dominant or recessive, with various degrees of penetrance) (Bonifati, 2014), MSA is generally considered as a sporadic disease. However, familial aggregations have been reported showing autosomal dominant and autosomal recessive inheritance. (Multiple System Atrophy Research Collaboration, 2013; Wullner et al., 2004; Hara et al., 2007)

Several studies have been carried out to explore the role of genetics in MSA. A possible role has been postulated for mutations in *COQ2*, a gene encoding an enzyne involved in the syntjesis of CoenzymeQ10 (Multiple System Atrophy Research Collaboration, 2013). Whole genome sequencing of a

japanese patient affected with autopsy-confirmed familial MSA displayed a functionally relevant mutation in *COQ2*. Furthermore, one common *COQ2* variant and various rare *COQ2* variants have been associated with increased MSA risk in Japan. However, these results have not been confirmed by other independent studies. (Sharma et al., 2014; Schottlaender et al., 2014, Ronchi et al., 2016)

An increased risk of MSA has been associated with variants in SNCA gene. (Scholz et al., 2009; Al-Chalabi et al., 2009) However this result was not confirmed by a genome wide association study (GWAS) involving 918 MSA patients and 3864 controls (Sailer et al., 2016).

Environmental factors

The role of environmental factors in the onset of the disease has been assessed by several studies.

MSA has been associated with occupational exposure to organic solvents, plastic monomers and additives, pesticides and metals. (Nee et al., 1991)

A European study involving 73 MSA patients, 146 hospital controls and 73 population controls has showed an increased incidence of MSA in agriculture workers. (Vanacore et al., 2005). However, this observation has not been replicated by other studies (Cho et al., 2008; Seo et al., 2010; Vidal et al., 2008).

Smoking has been associated with a reduced incidence of the disease. (Vanacore et al. 2000)

Alpha synuclein

Intracellular alpha-synuclein accumulation in oligodendrocytes is the main pathological hallmark of MSA and it is reasonable to speculate that this

protein has a key role in the still almost completely unknown mechanisms of the disease.

Alpha-synuclein is phisiologically expressed in neurons and in developing oligodendrocytes, whereas it is not expressed in mature oligodendrocytes. Therefore, the finding of the protein in these cells is difficultly comprehensible and many hypotheses have been formulated to explain the phenomenon.

The first hypothesis suggests a reactivation of the expression of alpha-synuclein gene (*SNCA*) in patients' cells. In situ hybridization technique performed on brain samples of MSA patients and controls has not succeeded in detecting *SNCA* mRNA (Miller et al., 2005). Differently, a more recent study (Asi et al., 2014), based on qPCR, has found an increased expression of the gene in patients.

A second plausible hypothesis is that alpha-synuclein is not directly translated in oligodendrocytes, but that it is taken up by these cells from surrounding neurons or from the extracellular environment. Interestingly, the possible transfer of alpha-synuclein both from-neuron-to-neuron (Desplats et al., 2009) and from-neuron-to-oligodendrocyte (Reyes et al., 2014) has been observed in vitro. In particular, oligodendrocytes have been treated with the monomeric, oligomeric and fibrillar forms of the protein and a concentration- and time-dependent cellular uptake has been observed. Furthermore, the injection of alpha-synuclein into mouse cortex has been found to be followed by in vivo oligodendroglial internalization.

A third recent hypothesis suggests a prion-like behavior of alpha-synuclein in MSA (Woerman et al., 2015; Prusiner et al., 2015).

An important issue related to alpha-synuclein pathology is to understand the cause which leads to accumulation specifically in oligodendrocytes. It has been proposed that the accumulation is triggered by specific oligodendroglial

proteins, with a particular focus on p25alpha/TPPP. As demonstrated co-expressing TPPP and alpha-synuclein in rat oligodendrocytes, TPPP enhances alpha-synuclein aggregation. (Hasegawa et al., 2010) This observation is particularly interesting because TPPP has been demonstrated to be implicated in the early phase of MSA pathogenesis. In particular, TPPP relocation from myelin sheath to oligodendrocyte's soma is the earliest pathological finding which has been observed in the progression of the disease. Only later, the accumulation of other proteins, including alpha-synuclein, is observed in oligodendrocytes' cytoplasm, followed by oligodendroglial and, finally, neuronal degeneration. (Jellinger, 2014)

The relationship between anomalous protein accumulation and cellular degeneration is another important issue correlated with the pathogenic mechanisms of MSA.

A role of both extrinsic and intrinsic apoptotic pathways has been postulated. As proposed in studies involving PLP-hasyn-tg-mice and MSA brain extracts, alpha-synuclein/TPPP co-expression leads to Fas receptor stimulation and Caspase 8 activation. (Kragh et al., 2013) Instead, the finding of the mitochondrial pro-apoptotic protein Omi/HtrA2 in GCIs, NCIs and dystrophic neurites is consistent with a possible involvement of the intrinsic apoptotic pathway. (Kawamoto et al., 2008)

The relationship between oligodendroglial and neuronal degeneration is not clear yet. Although neuronal death usually follows oligodendroglial degeneration, it has not been demonstrated that the pathology starts from the glia and subsequently spreads to neurons. However, a suggestive hypothesis is that oligodendroglial degeneration triggers or at least facilitates neuronal damage. This hypothesis is supported by the fact that neurons need oligodendrocytes not only for the formation of the myelin sheath but also for their trophic support. It has been shown that oligodendroglial precursors and

mature oligodendrocytes release factors which support neuronal survival and axonal length. GDNF has been found to be reduced in the MBP-hasyn-tg-mouse-model. Furthermore, intracerebroventricular GDNF infusion improves neurodegenerative pathology and behavioral deficit in these mice. (Wilkins et al., 2003; Ubhi et al., 2010)

Inflammation

Inflammation seems to play a crucial role in the pathogenesis of MSA.

Microglial activtion is a common finding in MSA autoptic brain tissues. Microgliosis, together with an increase of iNOS (inducible nitric oxide synthase) expression can be detected also in MSA mouse models. It is possible that alpha-synuclein overexpression in oligodendrocytes induces nitrosative stress-related inflammation. Furthermore, also the expression of toll-like receptor 4 is increased both in tg-mouse models and in autoptic brains. (Stefanova et a., 2005; Stefanova et al., 2007)

A possible role of alpha-synuclein in activating microglia through a toll-like receptor mediated pathway is supported by various studies. (Su et al., 2008; Su et al., 2009; Beraud et al., 2011; Beraud et al., 2013) Furthermore it has been shown that misfolded alpha-synuclein activates microglia inducing the production of the pro-inflammatory cytokine TNF-alpha and enhancing the expression of antioxidant enzymes.

A possible role of myeloperoxidase is supported by the finding that the inhibition of this enzyme in MSA mouse models reduces microglial activation, rescues vulnerable neurons, reduces alpha-synuclein aggregates and reduces motor impairment. (Stefanova et al., 2012)

Mitochondrial dysfunction

Mitochondrial dysfunction plays an important role in many neurodegenerative disorders, both as potential causative mechanism and as secondary effect.

Mitochondrial involvement in alpha-synucleinopathies has been widely studied, mainly in Parkinson's disease. (Schapira, 2008) Defect in complex I activity has been found in substantia nigra and other tissues of PD patients. (Schapira et al., 1989) Moreover, the administration of complex I inhibitors, namely MPTP and rotenone, to humans and animal models has been associated with striatonigral degeneration and/or parkinsonism. (Singer et al., 1986; Betarbet et al., 2000) Furthermore, an increased amount of mtDNA deletions has been observed in PD (Bender et al., 2006) and many of the genes involved in familial PD cases are directly or indirectly linked to mitochondrial functioning (e.g. *Parkin*, *PINK1*, *DJ-1*).

However, some studies have been carried out also in MSA. An old study, aimed to assess the activity of respiratory chain complexes in substantia nigra and platelets of patients and controls, has not found significant differences between groups. (Gu et al., 1997) Instead, great interest has been raised by the recent description of mutatons of *COQ2* gene (encoding an enzyme involved in CoQ10 biosynthesis) in sporadic and familial cases of MSA. (Multiple System Atrophy Research Collaboration, 2013) However, this finding has not been confirmed by other studies. (Sharma et al., 2014; Schottlaender et al., 2014; Ronchi et al., 2016) Moreover two independent groups have recently described a reduction of CoQ10 levels selectively in the cerebellum of MSA patients, but not in striatum, frontal cortex and occipital cortex. (Schottlaender et al., 2016; Barca et al., 2016) Furthermore, the amount of PDSS1 and COQ5, two enzymes involved in the synthesis of CoQ10 have been found to be reduced in MSA brains.

## Induced pluripotent stem cells (iPSCs)

"Stemness" is a relatively broad-spectrum concept referrable to a wide group of cellular subtypes which share two important abilities: self-replicating and differentiating.

Several classes of stem cells can be found in the human organism and can be distinguished on the basis of their residual differentiative potential and of their location. In adult human tissues stem cells maintain a restricted differentiative potential, being able to differentiate only towards a certain class of mature cellular subtypes. For example, hematopoietic stem cells, routinarely used in clinical practice, have a differentiative potential almost restricted to blood cells and, similarly, epidermis basal layer cells are aimed to provide new precursors for the generation of mature keratinocytes. Although the nervous system is mainly composed of non-replicating cells, adult stem cells have been detected also in this area, but little is known about them (Alvarez-Buylla et al., 2002).

Differently, in the first phase of embryonal development, it is possible to find cells which are able to differentiate towards all the cellular subtypes of the organism and, for this reason, are named pluripotent stem cells (PSCs).

Embryonal stem cells (ESCs) have been the only available form of PSCs until a decade ago, when the generation of induced pluripotent stem cells (iPSCs) has been described (Takahashi and Yamanaka, 2006).

iPSCs are not phisiologically present in the human organism but they are artificially produced in laboratory through the forced expression of specific factors, namely Sox2, Oct4, Klf4 and c-Myc. The expression of these factors reconducts adult somatic cells (e.g. skin fibroblasts) to a condition of pluripotency. The responsible mechanism has not been completely elucidated yet. Oct4 and Sox2 upregulate stemness genes and suppress

differentiation associated genes, acting synergistically (Boyer et al. 2005), whereas the role of Klf4 and c-Myc is less clear. However, it has been proposed that Oct4 and Sox2 cannot bind their target genes because of DNA methylation and histone modifications and it is possible that Klf4 and c-Myc modify chromatine structure, allowing the binding of Oct4 and Sox2.

Although iPSCs' generation has been described only a decade ago, they have already been used in a large number of studies and are promising for many reasons. iPSCs offer the potential to generate any kind of cellular population (even those which are hardly accessible in the human body, such as neurons and glia) just starting from a skin biopsy or a blood withdrawal. As these cells share the same genetic background of the subjects from whom they are derived, they can be useful to model genetic diseases or diseases in which a genetic predisposition is involved. Furthermore, iPSCs display a high potential in the field of therapeutics. Indeed, although much research is still needed, the advantage of replacing degenerated or damaged tissues with new cells directly derived from the patient is obvious and could potentially eliminate the problem of immunological reject. (Shi et al., 2017)

## Differentiation of pluripotent stem cells to different cellular subtypes

Pluripotent stem cells can be differentiated towards all the cellular subtypes of the organism, including neurons and glia.

Differentiation protocols are now available for many cell types of the nervous system: dopaminergic neurons, cortical and spinal motor neurons, GABAergic neurons (Purkinje cells, medium spiny neurons, interneurons), astrocytes, oligodendrocytes and others.

Methods are heterogeneous and can involve culturing cells in adhesion or in suspension. Also the generation of three-dimensional structures called organoids has been recently described.

Feasibilitty and efficiency are highly variable, too.

However, all the protocols share the same rationale, that is the administration of specific factors, called morphogens, at specific timing and concentration, which mimic the physiological development of the nervous system (Liu et al., 2011).

Nervous system starts developing when the inner mass begins to form the three germ layers (endoderm, mesoderm and ectoderm). The nervous system originates from the ectoderm. Activation of fibroblast growth factor (FGF) and inhibition of bone morphogenetic protein (BMP) and WNT leads to the specialization of neuroectoderm. Two main axis, rostro-caudal and dorso-ventral, are involved in the development of the nervous system.

All the central nervous system develops from primitive neuroepithelia, which carries a dorsal telencephalic identity.

Different areas can be found along the rostro-caudal axis. Forebrain, from which telencephalon and diencephalon differentiate, is the most rostral zone. Midbrain is located under the forebrain. Hindbrain, more caudal, can be divided into metencephalon and myelencephalon. Pons and cerebellum originate from metencephalon, medulla oblongata originates from myelencephalon. Spinal cord is the most caudal structure.

Also the dorso-ventral axis is important for cellular specification.

In forebrain, glutamatergic pyramidal neurons are the most dorsal population. GABAergic projection neurons (from which striatal medium spiny neurons develop) and basal forebrain cholinergic neurons originate more

ventrally, whereas GABAergic interneurons originate along the entire dorso-ventral axis.

On a different level, lower motor neurons originate from the ventral part of the spinal cord.

Being primitive neuroepithelia characterized by dorsal telencephalic features, the default fate of neural precursor cells is glutamatergic, leading to cells expressing cortical and dorsal markers like Pax6 and Tbr1.

Retinoic acid is the main factor involved in rostro-caudal differentiation, being a concentration-dependent caudalizing factor. The administration of retinoic acid leads to the loss of anterior markers like Otx2 and Foxg1 and to the expression of posterior markers like Hoxb4, Hoxc5 and Hoxc8.

Also the dorso-ventral axis is regulated by specific factors. WNT and sonic hedgehog (SHH) play an essential role, being WNT characterized by a dorsalizing activity and SHH by a ventralizing one. Indeed, SHH administration or WNT inhibition lead to the loss of the expression of the dorsal marker Pax6 and to the expression of ventral markers like Gsx2 and Nkx2.1. (Liu et al. 2011)

Glial differentiation is particularly long and complicated, in particular for oligodendrocytes. However, many protocols have been recently published, although with low efficiency rates.

Differentiation towards dopaminergic neurons, which are the main object of the present study, requires a specific paragraph.

**Dopaminergic differentiation and iPSC-based models of Parkinson's disease**

Substantia nigra dopaminergic neurons represent a peculiar cellular population.

PD has been widely modeled through iPSCs. The opportunity to assess not only sporadic but also genetic forms of the disease and the continuous improvement of dopaminergic neurons' differentiation protocols has further encouraged the application of this technique.

iPSC-based cellular models have been obtained from patients affected with sporadic forms of PD and from patients carrying mutations in *LRRK2*, *SNCA*, *GBA*, *Parkin* and *PINK1* genes (e.g. Nguyen et al., 2011; Sanchez-Danes et al., 2012; Byers et al., 2011; Woodard et al., 2014; Schöndorf et al., 2014; Seibler et al., 2011; Rakovic et al., 2013; Imaizumi et al., 2012).

The first protocols aimed to generate dopaminergic neurons were based on neural rosettes (Perrier et al., 2004) and were characterized by a relatively low efficiency.

However, a new method, based on dual SMAD inhibition has been described (Kriks et al., 2011). All the protocol is performed in adhesion and allows to obtain dopaminergic neurons with high efficiency.

The main rationale of the protocol is the observation that developing midbrain is characterized by the co-expression of the floor-plate marker FOXA2 and the roof plate marker LMX1A. Therefore, authors have developed a protocol leading to a balance of differentiation factors which allows to obtain this cellular identity. The procedure is based on different steps involving dual-SMAD inhibition (administration of LDN193189 and SB431542), administration of SHH agonists (purmorphamine + SHH), administration of FGF8 and administration of CHIR. The authors also demonstrate that the lack of any of these compounds leads to a lower efficiency of differentiation.

The protocol that has been applied in the present study (Zhang et al., 2014) is a slight modification of Kriks's protocol.

## AIM OF THE STUDY

The aim of the present study is the development and the analysis of new experimental models for the assessment of the pathogenic mechanisms of Multiple System Atrophy.

The lack of an exhaustive and reliable model of the disease is the rationale for the investigation of several tissues and cellular subtypes.

Both patient-derived fibroblasts, a cell type which is not directly affected in the disease but which can be easily withdrawn and expanded, and iPSC-derived dopaminergic neurons, strongly affected but difficult to generate in laboratory, will be used to investigate the molecular mechanisms of the disease. The availability of DNA extracted from peripheral blood cells and post-mortem brain tissue of large cohorts of patients and controls will be exploited for the same purpose.

The study will assess several topics, with a particular focus on three fields: alpha-synuclein, autophagy and mitochondrial functioning.

Alpha-synuclein expression, accumulation and regulation, basal autophagy and autophagic flux, mitochondrial mass, respiratory chain activity, mitochondrial DNA content and CoQ10 biosynthesis are the main themes which will be investigated in this project.

The present study will contribute to understand the molecular basis of the disease, so far widely unclear, and to lay the foundations for the future development of new therapeutic strategies.

## MATERIALS AND METHODS

### Ethical issues

All the phases of the present study were carried out in compliance with the principles of Helsinki Declaration. Informed consent was obtained from all the subjects and local ethical guidelines were observed.

### Diagnostic procedure

Diagnosis of probable MSA was performed according to widely accepted clinical criteria (Gilman's criteria).

### Skin biopsies and fibroblasts' expansion

Skin biopsies were obtained through a 3 mm punch from the ventral surface of the right arm after disinfection with lodopovidone and anesthesia with ice spray. Fibroblasts were isolated from biopsies and expanded in proper culture medium (Dulbecco's modified Eagle medium supplemented with fetal bovine serum 15%, amphotericin B 1% and penicillin/streptomycin 1 %).

The main details of all the subjects from whom skin biopsies were obtained are reported:

| | SEX | AGE |
|---|---|---|
| MSA-C1 | n/a | n/a |
| MSA-C2 | F | 59 |
| MSA-C3 | F | 60 |
| MSA-C4 | F | 68 |
| MSA-C5 | n/a | n/a |
| MSA-C6 | F | 70 |
| MSA-C7 | F | 66 |
| MSA-P1 | F | 80 |
| MSA-P2 | F | 66 |
| MSA-P3 | F | 61 |

| | | |
|---|---|---|
| MSA-P4 | F | 78 |
| MSA-P5 | M | 55 |
| MSA-P6 | n/a | n/a |
| MSA-P7 | F | 77 |
| CTR1 | F | 40 |
| CTR2 | M | 44 |
| CTR3 | F | 106 |
| CTR4 | M | 57 |
| CTR5 | M | 60 |
| CTR6 | M | 65 |

MSA-C1, MSA-C5 and MSA-P6 were obtained from a cell biobank and detailed information is lacking.

Reprogramming of fibroblasts towards iPSCs

Reprogramming of fibroblasts was obtained through the commercially available kit CytoTune®-iPS 2.0 Sendai Reprogramming Kit (Life technologies). This kit is based on a not-integrating viral method which allows the transfection of the factors Oct3/4, Sox2, Klf4 and c-Myc. After 1 week from reprogramming, fibroblasts were transferred to feeder-coated dishes. When iPSCs' colonies appeared, they were transferred to matrigel-coated dishes and expanded.

The main clinical features of all the subjects from whom iPSCs were generated are reported:

| | SEX | AGE | Corresponding fibroblast cell line |
|---|---|---|---|
| MSA-C1 (AT) | F | 59 | C2 |
| MSA-C2 | F | 60 | C3 |
| MSA-P1 | F | 78 | P4 |
| MSA-P2 | M | 55 | P5 |
| CTR 1 | M | 24 | / |
| CTR 2 | F | 60 | / |

| | | | |
|---|---|---|---|
| CTR 3 | M | 68 | / |
| CTR 4 | F | 80 | / |
| UT | F | 59 | / |

Differentiation of iPSCs towards dopaminergic neurons

An already described protocol was applied (with minor changes) for differentiation of iPSCs towards dopaminergic neurons (Zhang et al., 2014). The protocol is based on the administration of specific factors at proper timing and concentration - D0: KSR differentiation medium (DMEM 81%, KSR 15%, non-essential amino acids 1%, beta-mercaptoethanol 1%, penicillin(10000 units/ml)/streptomycin(10mg/ml) 1%, amphotericin 250 µg/ml 1%) supplemented with SB431542 10 µM and LDN-193189 100nM. - D1 and D2: KSR differentiation medium supplemented with SB431542 10 µM, LDN-193189 100nM, SAG 0.25 µM, purmorphamine 2 µM, FGF8b 50 ng/ml - D3 and D4: KSR differentiation medium supplemented with SB431542 10 µM, LDN-193189 100nM, SAG 0.25 µM, purmorphamine 2 µM, FGF8b 50 ng/ml, CHIR99021 3 µM - D5 and D6: 75% KSR differentiation medium and 25 % N2 differentiation medium (DMEM 97%, N2 supplement 1%, penicillin/streptomycin 1%, amphotericin 1%) supplemented with LDN-193189 100nM, SAG 0.25 µM, purmorphamine 2 µM, FGF8b 50 ng/ml, CHIR99021 3 µM - D7 and D8: 50% KSR differentiation medium and 50% N2 differentiation medium supplemented with LDN-193189 100nM and CHIR99021 3 µM - D9 and D10: 25% KSR differentiation medium and 75% N2 differentiation medium supplemented with LDN-193189 100nM and CHIR99021 3 µM - D11 and D12: B27 differentiation medium (Neurobasal medium 95%, B27 supplement 2%, glutamax 1%, penicillin/streptomycin 1%, amphotericin 1%) supplemented with CHIR99021 3 µM, BDNF 10 ng/ml, GDNF 10 ng/ml, TGFb3 1 ng/ml, ascorbic acid 0.2 mM, cAMP 0.1 mM - From D13 to the end of differentiation: B27 differentiation medium supplemented

with BDNF 10 ng/ml, GDNF 10 ng/ml, TGFb3 1 ng/ml, ascorbic acid 0.2 mM, cAMP 0.1 mM. At 20 DIV cells were splitted using accutase.

Immunocytochemistry

Slide-adherent cells were rinsed in PBS 1X (3 times), incubated in paraformaldehyde 4% for 10 minutes and rinsed in PBS 1X (3 times). Cells were then incubated in blocking solution (PBS 1X containing BSA 10% and triton 0.3%) for 1 hour and in saturation solution (PBS 1X containing BSA 3%) containing primary antibody at proper concentration overnight at 4 °C. Cells were then incubated in saturation solution containing secondary antibody and DAPI at proper concentration for 2 hours and rinsed in PBS 1 X (3 times). Finally, the slides were mounted. The confocal system Leica TCSSP2 (Leica Microsystems) was used for images acquisition.

Details about antibodies are indicated in the following table.

| Antibody | Manufacturer | Code | Dilution |
|---|---|---|---|
| Pluripotent Stem Cell 4-Marker Immunocytochemistry Kit | Thermo Fisher | A24881 | 1:100 |
| TUJ1 | Abcam | ab18207 | 1:250 |
| TH | R&D Systems | MAB7566 | 20 µg/ml |
| TH | Thermo Scientific | PA5-17800 | 1:100 |
| GIRK2 | Abcam | ab65096 | 1:100 |
| MAP2 | Sigma-Aldrich | M9942 | 1:100 |
| Alexa 488 anti-mouse | Life Technologies | A11001 | 1:500 |
| Alexa 488 anti-goat | Jackson ImmunoResearch | 705-545-003 | 1:500 |
| Alexa 488 anti-rabbit | Life Technologies | A11034 | 1:500 |
| Alexa 568 anti-mouse | Life Technologies | A11004 | 1:500 |
| Alexa 568 anti-rabbit | Life Technologies | A11011 | 1:500 |

Western Blot

Proteins were extracted in $H_2O$ + protease inhibitor cocktail (P2714, Sigma), sonicated 2 times for 15 seconds at 50 W and centrifuged for 10 minutes at 750 g. Proteins were quantified through the Lowry method. Samples were prepared in Novex Bolt LDS sample buffer and Novex Bolt Reducing Agent (Thermo Fisher) and boiled for 3 minutes. 5-30 µg of proteins were loaded in Precast Bolt® Bis-Tris Plus Gels 4-12 % and in Novex Bolt 1X MES/SDS Running buffer at 200 V for 30 minutes. Trans-Blot® Turbo™ system (BioRad) was used for transfer in nitrocellulose membrane. Membranes were blocked with milk 5% (BioRad) or BSA 1% + horse serum 10%. HRP secondary antibodies were used (Dako) and protein bands were visualized through ECL. ImageJ (NIH) was used for bands intensity quantification. Protein amount was normalized for Actin, GAPDH or Vinculin.

Details about antibodies are indicated in the following table.

| Antibody | Manufacturer | Code | Dilution |
|---|---|---|---|
| TUJ1 | Sigma | T8660 | 1:1000 |
| Alpha-synuclein | BD transduction laboratories | 610787 | 1:1000 |
| Bax | Cell Signaling | 2772 | 1:1000 |
| Bcl-2 | Abcam | ab32124 | 1:1000 |
| Cleaved Caspase 3 | Cell Signaling | 9661 | 1:1000 |
| LAMP1 | Abcam | ab25630 | 1:875 |
| P62 | Millipore | MABN130 | 1:1200 |
| Cathepsin D | Santa Cruz | SC-6486 | 1:1000 |
| LC3 | Cell Signaling | 2775 | 1:1000 |
| TOMM20 | Sigma | HPA011562 | 1:750 |
| OXPHOS (containing antibodies detecting NDUFB8, SDHB, UQCRC2, MTCO2 and ATP5A) | Abcam | ab110411 | 1:1000 |
| SDHA | Invitrogen | 459200 | 1:1000 |
| COX1 | Invitrogen | 459600 | 1:1000 |

| | | | |
|---|---|---|---|
| COX4 | Invitrogen | A21347 | 1:1000 |
| TH | Millipore | AB152 | 1:2000 |
| TAU | Cell Signaling | 4019 | 1:1000 |
| Synaptophysin | Synaptic System | 101011 | 1:5000 |
| Synapsin I | Synaptic System | 106103 | 1:2000 |
| Synapsin III | Synaptic System | 106303 | 1:2000 |
| ADCK3/CABC1 | Thermo Scientific | PA5-13906 | 1:1000 |
| PDSS1 | Sigma | AV46195 | 1:1000 |
| PDSS2 | Abcam | ab88817 | 1:1000 |
| COQ2 | Abnova | H00027235-M03 | 1:1000 |
| COQ4 | Abcam | ab167182 | 1:1000 |
| COQ5 | Thermo Scientific | PA5-26327 | 1:1000 |
| COQ6 | Abcam | ab128652 | 1:1000 |
| COQ7 | Thermo Scientific | PA5-25774 | 1:1000 |
| COQ9 | Thermo Scientific | PA5-24816 | 1:1000 |
| Actin | Sigma | A2066 | 1:1200 |
| Vinculin | Abcam | ab18058 | 1:5000 |
| GAPDH | Sigma-Aldrich | G8795 | 1:5000 |
| Secondary mouse HRP | Dako | P0260 | 1:3200 |
| Secondary rabbit HRP | Dako | P0217 | 1:2700 |
| Secondary goat HRP | Dako | P0160 | 1:4000 |
| Secondary mouse HRP | Sigma | A0545 | 1:2000 |
| Secondary rabbit HRP | Sigma | A9044 | 1:2000 |

## DNA and RNA extraction from cells and reverse transcription

DNA and RNA were extracted through commercially available kits (FlexiGene DNA Kit, Qiagen and RNeasy Mini Kit, Qiagen, respectively) according to the manufacturer's instructions. A Nanodrop spectrophotometer was used to measure DNA and RNA concentration.

cDNA was obtained through the commercially available kit “Ready-To-Go You-Prime First-Strand Beads” (GE Healthcare), using 1 µg of RNA for each sample.

qPCR

For each well, 25 µl were prepared as follows: - Taqman: 12.5 µl of TaqMan Universal PCR Master Mix (Thermo Fisher), 6.5 µl of $H_20$, 1 µl of primer/probe assay, 5 µl of 1:10 dilution of cDNA - SYBRgreen: 12.5 µl of Power SYBR® Green PCR Master Mix (Applied Biosystems), 5 µl of 1:10 dilution of cDNA, forward and reverse primers at proper concentration and $H_2O$ up to a total volume of 25 µl. *18S*, *ACTB* and *GAPDH* were used as housekeeping genes. Analyses were performed with the ΔΔCt method. A 7500 Real Time PCR System was used. For the mtDNA content evaluation genomic DNA was used, simultaneously detecting a mitochondrial gene and a nuclear reference gene (*ND4* vs *RNaseP*, *ND1* vs *RNaseP* or *CytB* vs *APP*). The ΔΔCt method was used for analyses.

Karyotype Analysis

After adding colchicine to culture, iPSCs were processed with a hypotonic solution (0.6% sodium citrate and 0.13% potassium chloride) and fixed with methanol/acetic acid solution at 3:1 ratio. Q-banding was obtained through a Quinacrine solution. Metaphases were acquired with a fluorescence microscope at 100X magnification and analyzed with MetaSystems-Ikaros analytical system.

Spectrophotometric analyses

Respiratory chain complexes activities were measured through a Lambda 2 Parkin Elmer spectrophotometer. Proteins were extracted at 4 °C by adding a buffer at pH 7.2 to cell pellets, sonicating 3 times at 50 W for 10 seconds, centrifuging at 750 g for 10 minutes and recovering the supernatant. Protein concentration was measured through the Lowry method. Complex I activity (NADH ubiq.1 red) was measured at 340 nm after preparing a solution containing: K-phosphate pH 7.5 0.1M (200 µl), sodium azide 100 mM (10 µl), albumin 1% (100 µl), NADH 2mM (70 µl), $H_2O$ (610 µl), homogenate (10 µl), CoQ1 6mM (5 µl); afterwards rotenone 1mM (5 µl) was added and the residue activity was subtracted from the total. Complex II activity (Succ. Coq. Red) was measured at 600 nm after preparing a solution containing: K-phosphate pH 7 0.1M (500 µl), succinic acid 400 mM (40 µl), 2,6 dichloroindophenol 0.5 mM (200 µl), KCN 30mM (50 µl), $H_2O$ (190 µl), homogenate (20 µl), CoQ1 15 mM (3 µl). Complexes I+III activity (NADH cit C red) was measured at 550 nm after preparing a solution containing: K-phosphate pH 7.5 0.1M (250 µl), KCN 30mM (20 µl), NADH 2 mM (120 µl), cytochromeC 1mM (100 µl), homogenate (20 µl), $H_2O$ (490 µl). Complexes II+III activity (Succ cit C red) was measured at 550 nm after preparing a solution containing: K-phosphate pH 7.5 0.1M (500 µl), KCN 30 mM (20 µl), succinate 400 mM (50 µl), cytochromeC 1 mM (100 µl), homogenate (30 µl), $H_2O$ (300 µl). Complex IV activity (Cytochrome ox) was measured at 550 nm after preparing a solution containing: K-phosphate pH 7 0.1M (200 µl), reduced cytochromeC 1% (100 µl), $H_2O$ (680 µl), homogenate (20 µl). Citrate synthase activity was measured at 412 nm after preparing a solution containing: DTNB 1 mM (100 µl), oxaloacetic acid 10 mM (50 µl), AcetylCoA 10 mM (30 µl), $H_2O$ (800 µl), homogenate (20 µl). All the experiments were performed at 30 °C. All the activities were normalized for the activity of citrate synthase.

Sphingolipids analyses

Neurons were incubated with $3\times10^{-8}$ M [1-3H]sphingosine for a 2 hours pulse followed by a 48 hours chase. After harvesting, cell lysates were lyophilized and lipids were extracted with chloroform/methanol/water 2:1:0.1. Total lipid extracts were subjected to a two-phase partitioning, resulting in the separation of an aqueous phase containing gangliosides and in an organic phase containing all other lipids. Organic phases were subjected to an alkaline treatment aimed to remove glycerophospholipids. High performance thin layer chromatography was used for lipid extraction using the solvent systems chloroform/methanol/water 110:40:6 and chloroform/methanol/calcium chloride 0.2% 50:42:11 for the alkali-stable organic and the aqueous phases respectively. Digital autoradiography was used to detect and quantify radioactive lipids (Beta-Imager 2000 instrument, BioSpace). Lipids were identified by co-migration with authentic standards. M3Vision software was used to determine the radioactivity associated with individual lipids. Liquid scintillation counting was used to determine the radioactivity associated with lipid extracts and aqueous or organic phases.

Lysosomal enzymatic activity assays

The fluorogenic substrates used to determine the activities of lysosomal enzymes were purchased by Glycosynth: 4-Methylumbelliferyl β-D-glucopyranoside (MUB-β-Gluc) for β-glucocerebrosidase GBA1, 4-Methylumbelliferyl β-D-galactopyranoside (MUB-β-Gal) for β-galactosidase, 4-Methylumbelliferyl N-acetyl-β-D-glucuronide (MUG) for β-hexosaminidase, 4-Methylumbelliferyl α-D-mannopyranoside (MUB-α-Man) for α-mannosidase, 4-Methylumbelliferyl β-D-mannopyranoside (MUB-β-Man) for β-mannosidase. 6-hexadecanoylamino 4-MU-phosphoryl-choline (HMU-PC) (Moscerdam Substrates) was used for measuring sphingomyelinase activity. iPSC-derived neurons were harvested and lysed in water containing

protease inhibitors. The activities of β-galactosidase, β-hexosaminidase, α-mannosidase, β-mannosidase and sphingomyelinase were measured in McIlvaine Buffer pH 5.2 using 0.5 mM MUB-β-Gal, 0.5 mM MUG, 0.5 mM MUB-α-Man, 0.5 mM MUB-β-Man and 0.25 mM HMU-PC, respectively. For GBA1 assay, the cells were pre-incubated for 30 min at room temperature in McIlvaine containing 5 nM AMP-DNM N-(5-adamantane-1-yl-methoxy-pentyl)-deoxynojirimycin), specific inhibitor of GBA2. After incubation with the inhibitor, MUB-β-Gluc was added at a final concentration of 6 mM. The reaction mixtures were incubated at 37 °C under gentle shaking. The fluorescence was recorded after transferring 10 µl of the reaction mixtures to a microplate and adding 190 µl of 0.25 M glycine, pH 10.7.

Electrophysiology

Currents and Action Potentials, recorded in whole-cell configuration, were measured using an Axopatch 200B Amplifier and pClamp 10.2 software (Molecular Devices). Traces were sampled at 10 KHz using a Digidata 1322A acquisition Interface (Molecular Devices) and filtered at 1 KHz. Borosilicate glass pipettes were filled with a solution containing K-gluconate 126 mM, NaCl 4 mM, HEPES 10 mM, Glucose 10 mM, $MgSO_4$ 1 mM, $CaCl_2$ 0.5 mM, EGTA 1 mM, ATP (magnesium salt) 3 mM, GTP (sodium salt) 0.1 mM, pH 7.2. External solution contained NaCl 140 mM, KCl 3 mM, $MgCl_2$ 1.2 mM, $CaCl_2$ 2 mM, HEPES 10 mM, Glucose 10 mM, pH 7.4. Action potentials were recorded in current-clamp mode, setting membrane potential at -65 mV and injecting 5 pulses of increasing intensity. Spontaneous action potentials were measured at resting membrane potential, without injecting currents. Voltage-dependent ionic currents were recorded clamping cell membrane potential at -70 mV and delivering voltage steps lasting 800 ms and ranging from -80 mV to 60 mV at 20 mV increments.

Methylation assay by mass array

Five-hundred ng of genomic DNA were treated with sodium bisulphite using the EZ - DNA Methylation-Gold™ Kit (Zymo-Research, Irvine, CA), following the manufacturer's instructions. The massARRAY EpiTYPER technology (Agena Bioscience, Hamburg, Germany) was used to measure the methylation status of 10 CpG units (i.e. regions containing one or multiple CpG sites), containing 17 CpG sites, within the SNCA promoter region (chr4: 90,757,297 – 90,757,684). 15 ng of bisulphite-treated DNA were PCR-amplified using the following primers: Fw: 5' – aggaagagagTAAGGGTTGAGAGATTAGGTTGTTT – 3'; Rev: T7R, cagtaatacgactcactatagggagaaggctCAAACAAACAACAAACCCAAATATAA. Primers were designed by the EpiDesigner software (Agena), with the reverse primer containing a T7 promoter tag. The PCR reaction conditions were: 94°C for 4 min, followed by 45 cycles at 94°C for 20 sec, 56°C for 30 sec, and 72°C for 1min. After shrimp alkaline phosphatase treatment, to discard unincorporated DNA nucleotides, the T7 tag added during PCR was used to transcribe the PCR product from the reverse strand, yielding a single stranded RNA product. This RNA product was cleaved with RNase A, resulting in a specific fragmentation of the RNA product. Finally, samples were loaded on a 96-pad SpectroCHIP (Agena Bioscience), spectra were acquired by the MassARRAY Analyzer and methylation data of individual units were generated by the EpiTyper v1.0.5 software (Agena Bioscience). A single experiment was performed for each cell line.

CoQ10 dosage

CoQ10 was extracted with the hexane/ethanol 5:2 extraction technique. The hexane extract was dried under slow $N_2$ gas flow and resuspended in 1-propanol. CoQ10 levels were assessed by HPLC on a reverse-phase

Symmetry® C18 3.5 mm, 4.6 × 150 mm column, using a mobile phase consisting of methanol, ethanol, 2-propanol, acetic acid (500:500:15:15), and 50mM sodium acetate at a flow rate of 0.9 ml/min. The electrochemical detection system consisted of an ESA Coulochem III with a guard cell (upstream of the injector) at +900 mV, conditioning cell at 600 mV (downstream of the column), followed by the analytical cell at +500 mV. Standard peaks were used to estimate CoQ10 concentration.

Oxygraph

A high-resolution respirometry Oxygraph-2k (Oroboros Instruments, Innsbruck, Austria) was used for respirometry analyses on fibroblasts. For each analysis, 800000 cells were resuspended in proper medium (MiRO5) and injected into the instrument's chambers. Oxygen flux was measured at basal level and after the progressive administration of several compounds: digitonine, malate + glutamate, ADP, succinate, FCCP, rotenone and antimycin A. The value obtained after Antimycin A administration was subtracted to all other values. This experimental procedure was applied to assess basal respiration, complex I-related respiration, complex II-related respiration, maximal respiration, complex II-dependent maximal respiration. Values are expressed as pmol/(s x mL).

Bafilomycin and CCCP treatment

Cells were treated with bafilomycin at 200 nM for 24 hours.

Cells were treated with CCCP at 40 µM for 6 and 14 hours.

Statistical analyses

A two-tail Student's T test was used for comparisons between two groups. A one way ANOVA test was used for comparisons involving more than two groups.

## RESULTS

### Analyses on fibroblasts

Several experiments were performed on 20 fibroblast cell lines (7 MSA-C, 7 MSA-P and 6 healthy controls) to assess cell survival, autophagy and mitochondrial functioning.

Apoptosis

To investigate whether patients' and controls' fibroblasts displayed a different survival rate, the amount of the apoptosis-related proteins Bax (pro-apoptotic), Bcl-2 (anti-apoptotic) and cleaved Caspase3 (pro-apoptotic) was assessed through western blot. No significant differences were detected between patients and controls.

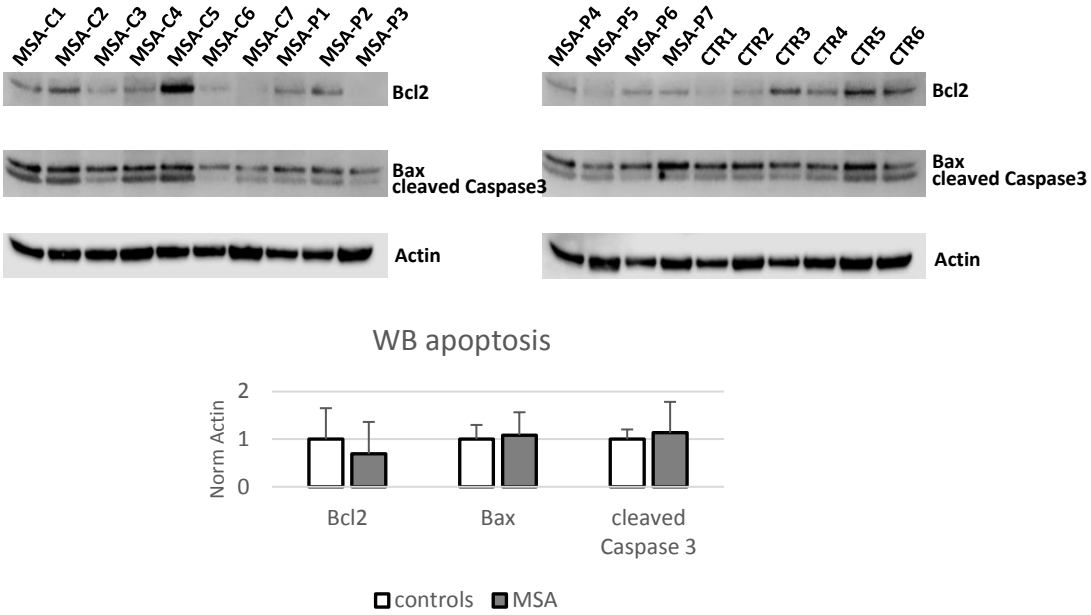


**Fig.1**
WB assessing the amount of the apoptosis-related markers Bcl2, Bax, cleaved Caspase 3 and Actin in MSA and control fibroblasts and related graph (values normalized for Actin).

Autophagy

As a defect in the autophagic flux has been described in all alpha-synucleinopathies, the amount of autophagy-related proteins LAMP1, Cathepsin D, p62 and LC3 was assessed through WB before and after the administration of bafilomycin, a V-ATPase inhibitor that causes the block of the fusion between the autophagosome and the lysosome. No significant differences were observed between patients and controls, neither at basal level, nor measuring the autophagic flux (bafilomycin-treated/basal ratio).

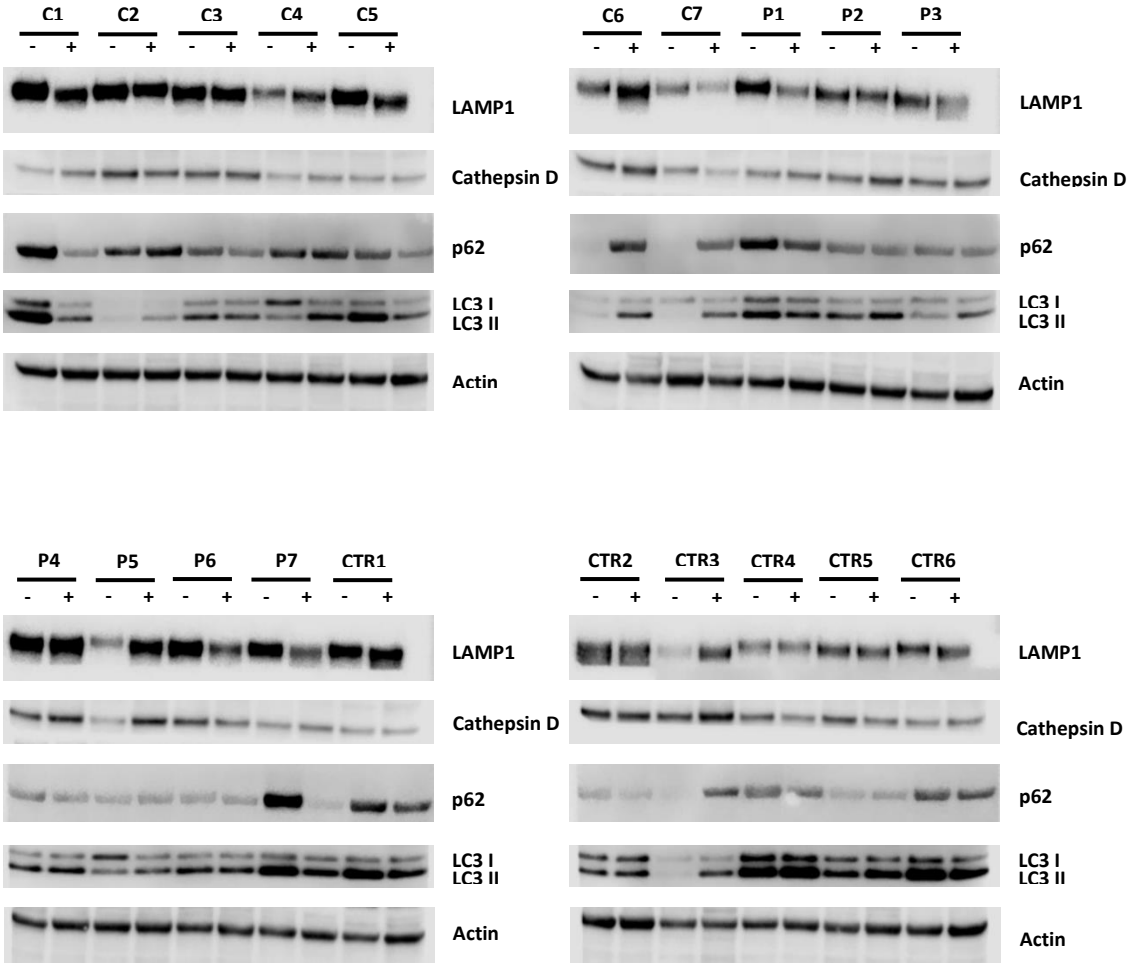


**Fig. 2**
Autophagy in fibroblasts. WB assessing the amount of LAMP1, Cathepsin D, p62, LC3 and Actin in MSA and control fibroblasts before (-) and after (+) the administration of bafilomycin (200 nM, 24 h).

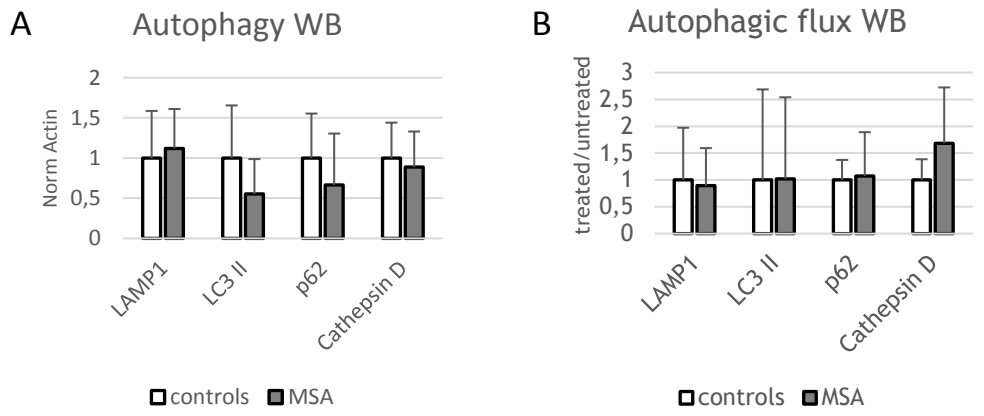


**Fig. 3**

Autophagy in fibroblasts. Graphs showing WB quantification. A) Basal amount of the autophagy-related proteins LAMP1, LC3 II, p62 and Cathpesin D (all normalized for Actin) in MSA and control fibroblasts. B) Autophagic flux measured as the ratio between the level of the autophagy-related proteins LAMP1, LC3 II, p62 and Cathepsin D after bafilomycin administration and their basal level.

## Mitochondrial functioning

Spectrophotometric analyses showed an impaired activity of respiratory chain complexes. In particular, the activity of complexes II and II+III were significantly reduced in patients compared to controls.

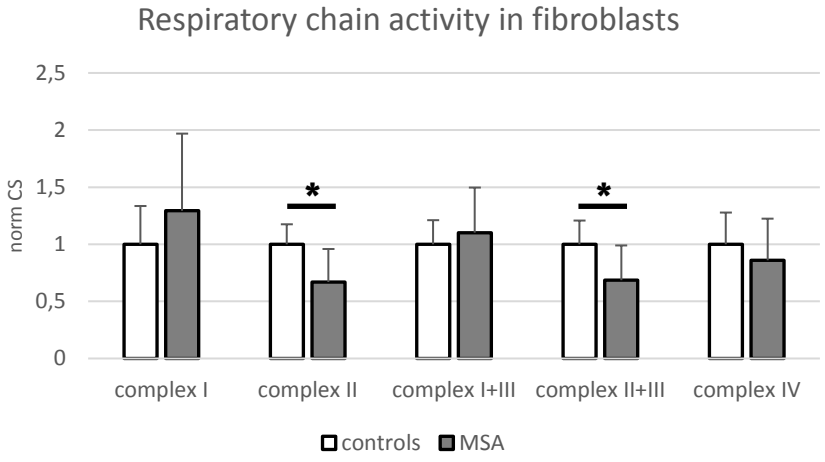


**Fig. 4**

Graph showing the activity level of respiratory chain complexes I, II, I+III, II+III and IV in MSA and control fibroblasts, measured through spectrophotometric analyses. Values are normalized for the activity of the mitochondrial matrix enzyme citrate synthase.

Western Blot analyses, aimed to assess the amount of respiratory chain complex I, complex II (SDHA and SDHB), complex III, complex IV and complex V, showed a trend of reduction in patients, significant for complex II.

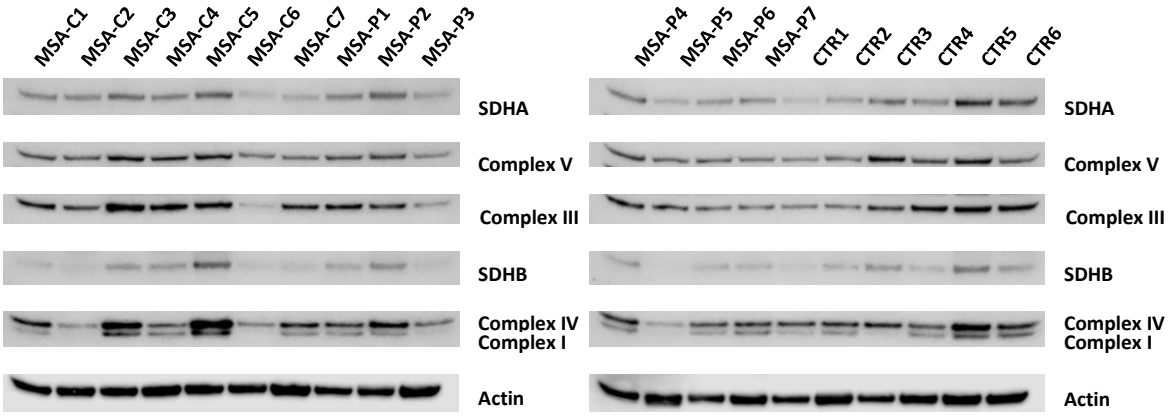


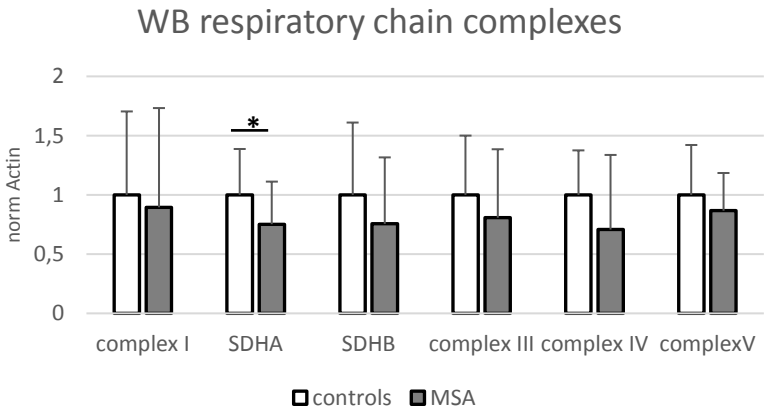


**Fig. 5**
Respiratory chain complexes in fibroblasts. WB assessing the amount of SDHA, complex V, complex III, SDHB, complex IV, complex I and Actin in MSA and control fibroblasts and related graph (values normalized for Actin).

qPCR, aimed to assess mtDNA content and performed through the simultaneous analysis of the mitochondrial gene *ND1* and the nuclear

reference gene *RNaseP*, did not show statistically significant differences between patients and controls.

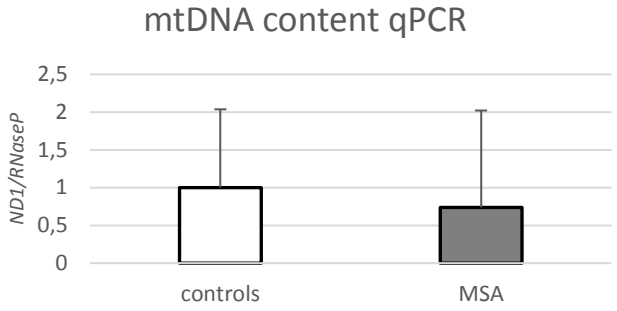


**Fig. 6**
Graphs showing mtDNA content in MSA and control fibroblasts measured by qPCR through the simultaneous detection of the mitochondrial gene *ND1* and the nuclear reference gene *RNaseP*.

Oxygen consumption, measured through high resolution respirometry (Oxygraph), was assessed at basal level and after the serial administratrion of specific compounds: digitonin, malate+glutamate, ADP, succinate, FCCP and rotenone. No significant differences were detected between patients and controls, although a trend of reduction was observed at maximal respiration rate in patients.

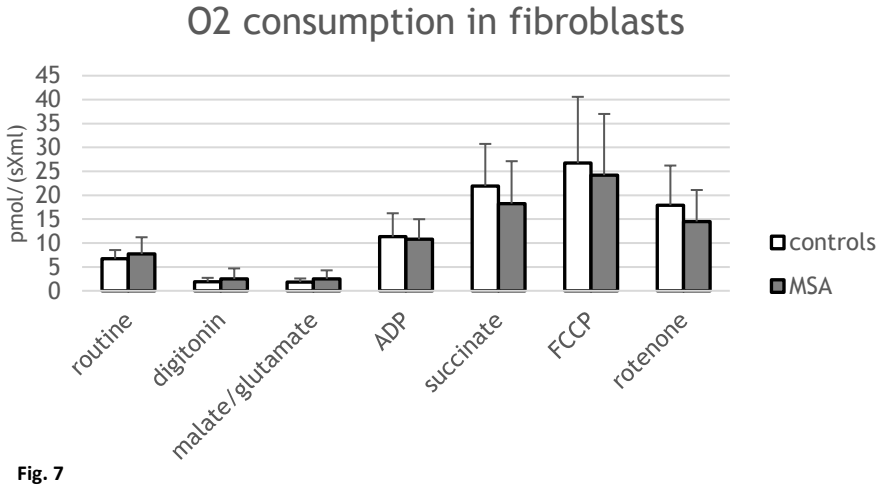


**Fig. 7**
Oxygen consumption in fibroblasts. Oxygen consumption in MSA and control fibroblasts measured through Oxygraph at basal level and after the administration of digitonin, malate+glutamate, ADP, succinate, FCCP and rotenone. Values are expressed in pmol/(s*ml)

To evaluate mitophagy, the amount of the mitochondrial proteins COX IV, TOMM20, SDHA and Porin was measured through WB at basal level and after 6 and 14 hours from the administration of the mitochondrial membrane uncoupler CCCP (40uM), which has been demonstrated to trigger the mitophagic pathway. A lower reduction of all the markers was observed in patients after 14 hours from CCCP administration, reaching significance for COX IV.

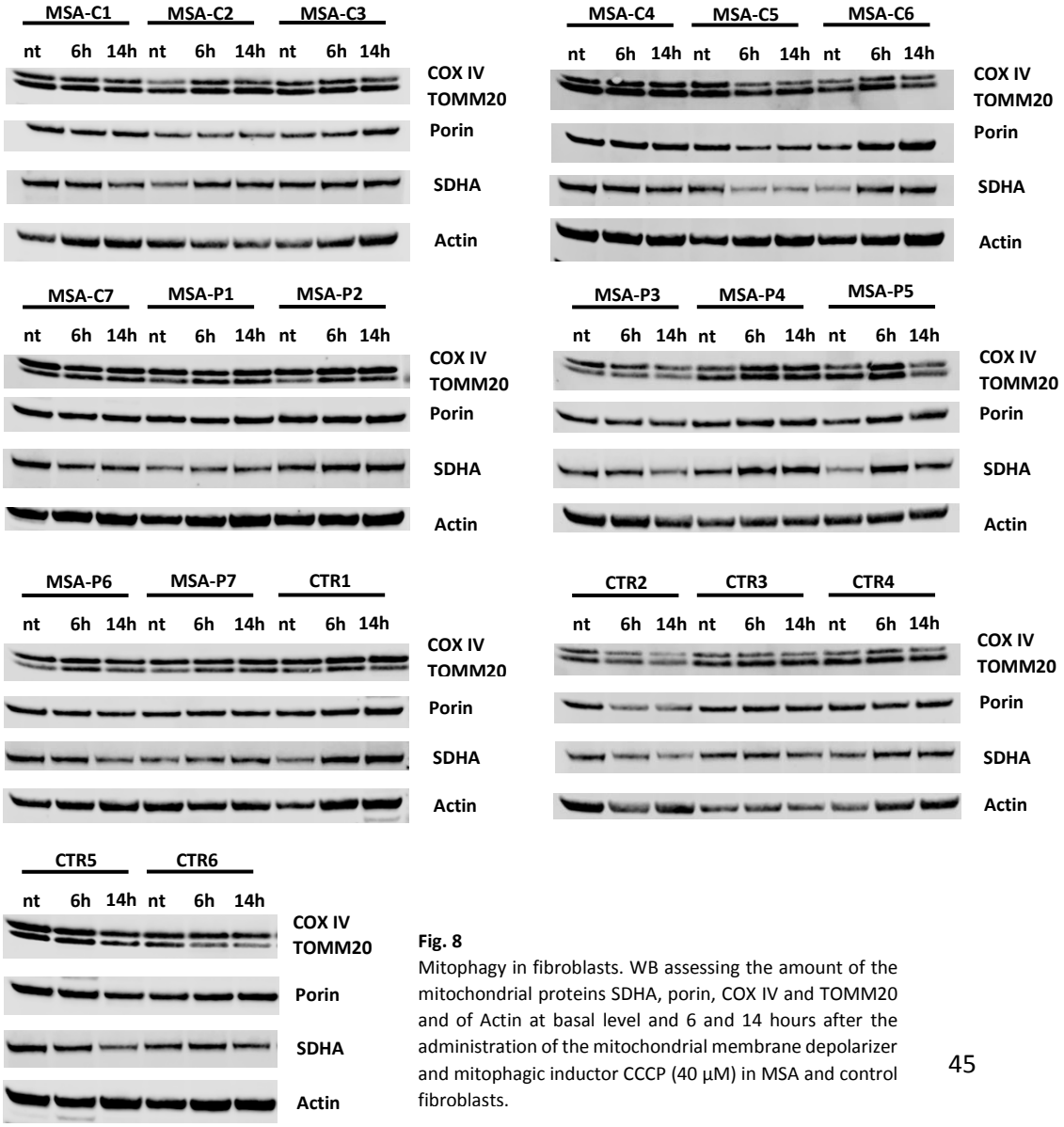


**Fig. 8**
Mitophagy in fibroblasts. WB assessing the amount of the mitochondrial proteins SDHA, porin, COX IV and TOMM20 and of Actin at basal level and 6 and 14 hours after the administration of the mitochondrial membrane depolarizer and mitophagic inductor CCCP (40 µM) in MSA and control fibroblasts.

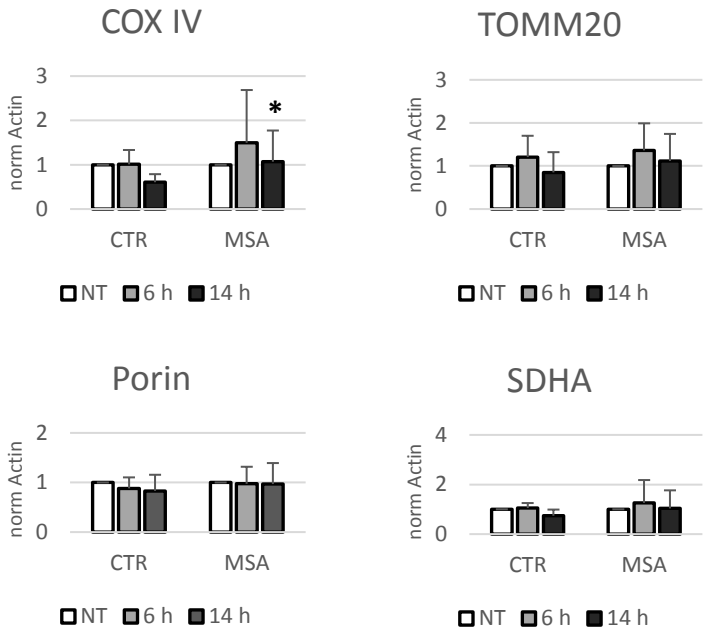


**Fig. 9**
Mitophagy in fibroblasts. Graphs showing quantification of WB assessing the amount of SDHA, Porin, COX IV and TOMM20 (normalized for Actin) at basal level and 6 and 14 hours after CCCP administration.

## Analyses on iPSC-derived neurons

### Generation and characterization of iPSCs

iPSCs were generated through a non-integrating viral protocol from fibroblasts of 2 MSA-C, 2 MSA-P, 4 healthy controls and the healthy monozygotic twin of one of the patients.

Phase contrast microscope showed typical pluripotent stem cell colonies.

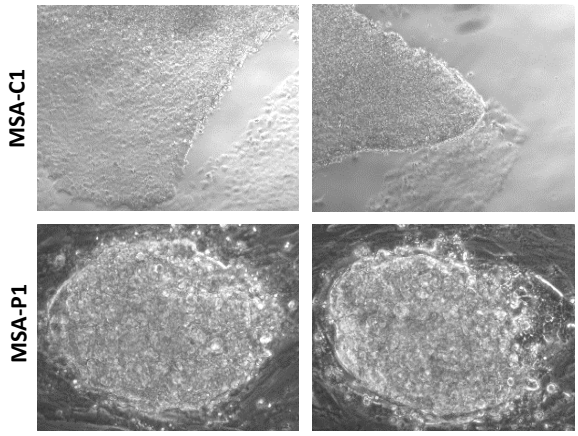


**Fig. 10**
Phase contrast microscope images showing the morphology of iPSC-colonies of two patients (MSA-C1 and MSA-P1).

The expression of specific markers was evaluated to assess the efficiency of the reprogramming process.

ICC analyses showed a high expression of the stemness markers TRA-1-60, SSEA-4, OCT4 and SOX2 in all iPSC-lines.

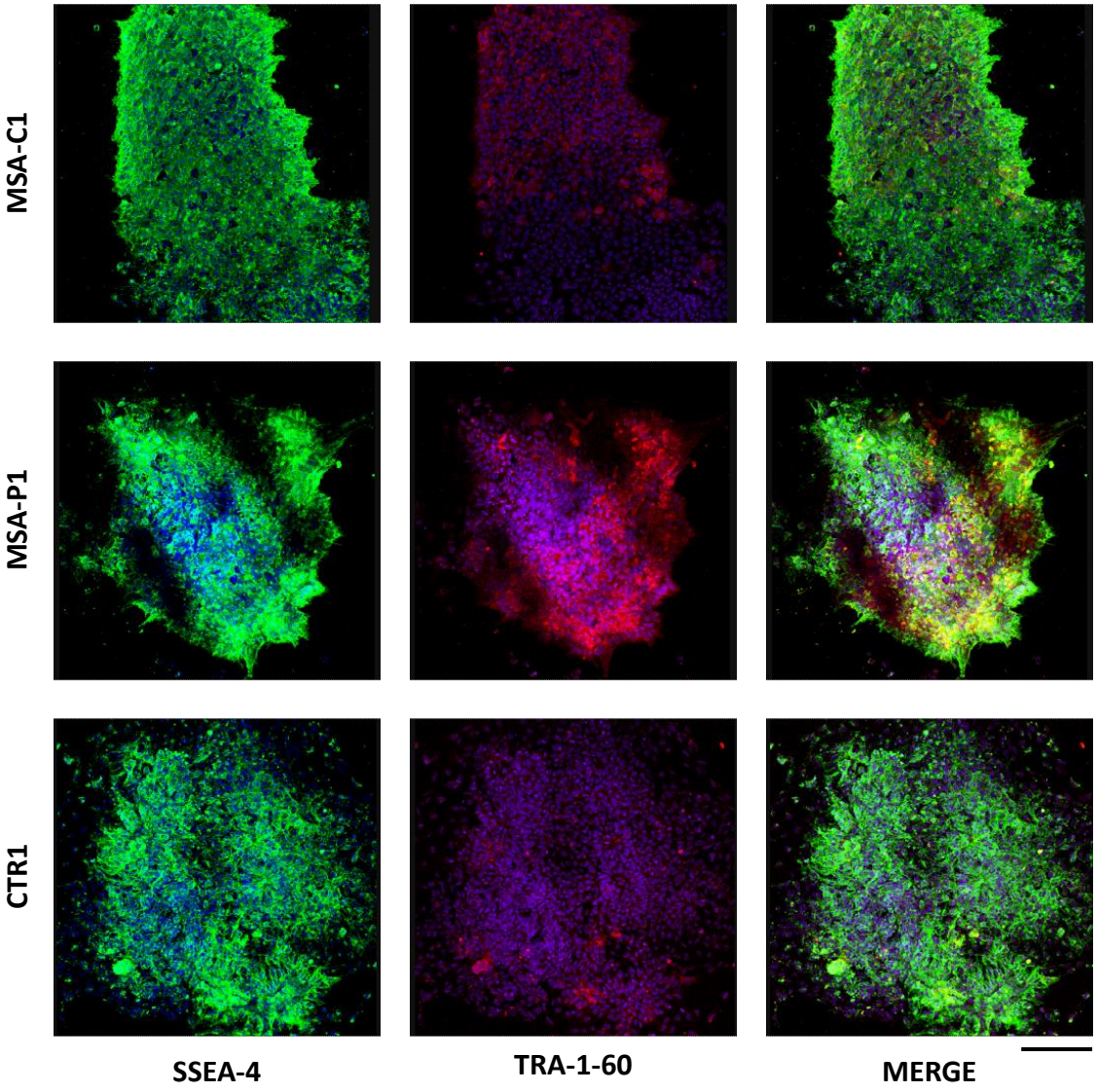


**Fig. 11**
ICC assessing the expression of the pluripotency markers SSEA-4 (green) and TRA-1-60 (red) in three iPSC-lines (MSA-C1, MSA-P1 and CTR1). Scalebar = 75 µm

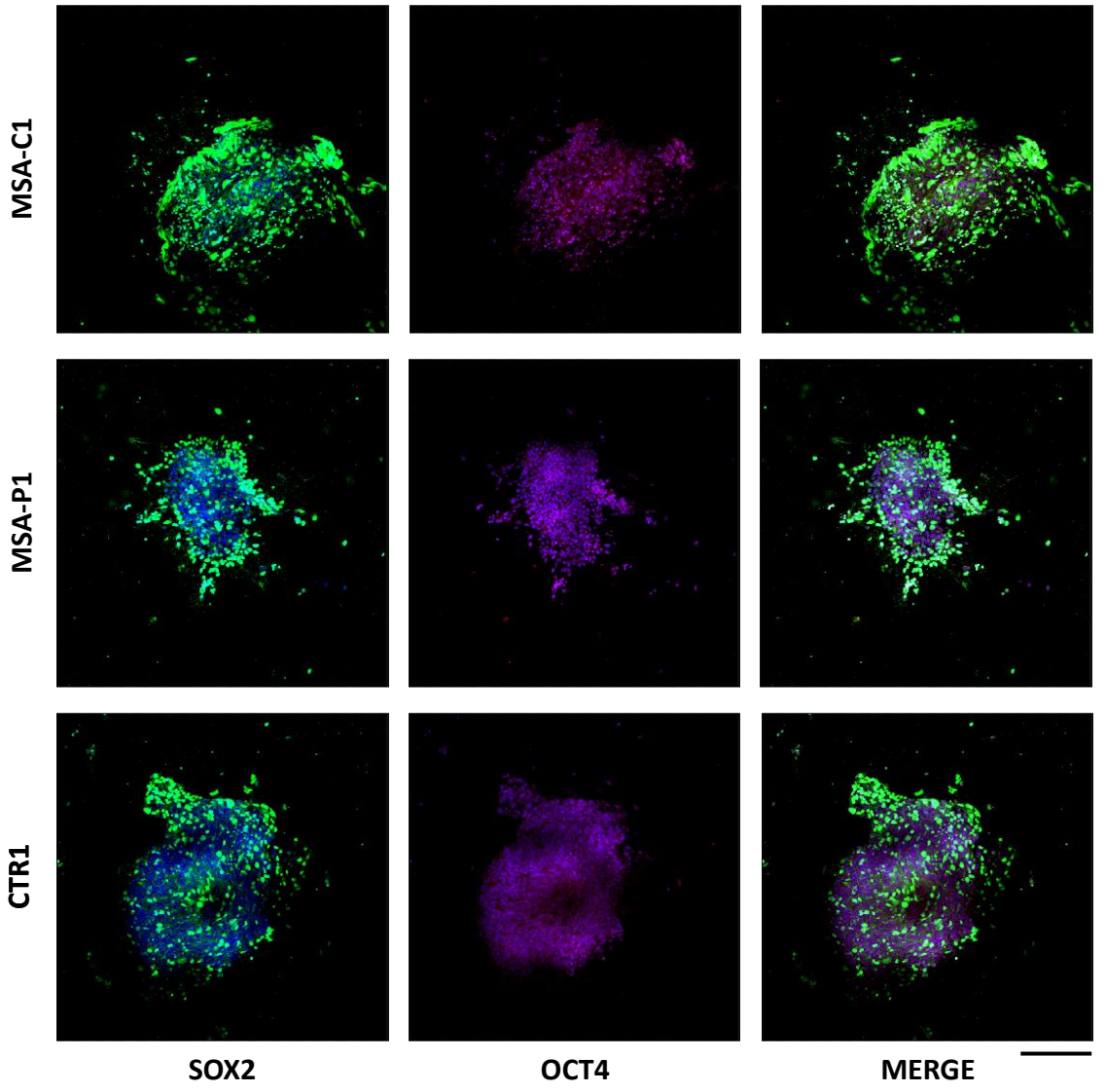


**Fig. 12**
ICC assessing the expression of the pluripotency markers SOX2 (green) and OCT4 (red) in three iPSC-lines (MSA-C1, MSA-P1 and CTR1). Scalebar = 75 µm

RT-PCR analyses confirmed high expression levels of the stemness-related genes *NANOG* and *OCT4* respect to fibroblasts.

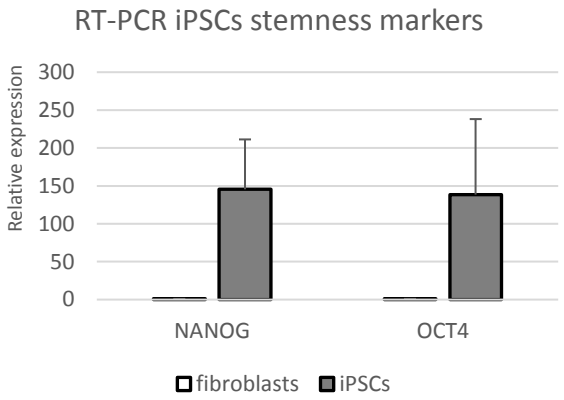


Fig. 13
iPSCs characterization. Graph showing high expression levels of the pluripotency markers *NANOG* and *OCT4* in iPSCs respect to fibroblasts measured through qPCR.

The presence of major genetic rearrangements due to the reprogramming process was ruled out through karyotype evaluation.

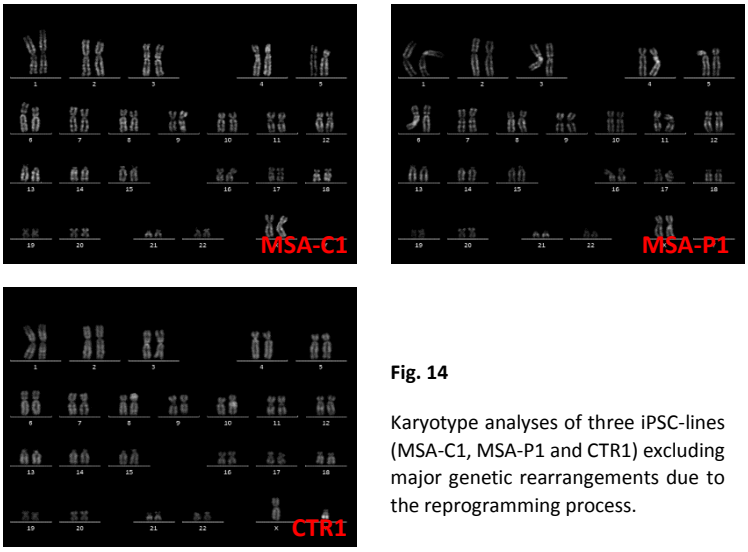


**Fig. 14**

Karyotype analyses of three iPSC-lines (MSA-C1, MSA-P1 and CTR1) excluding major genetic rearrangements due to the reprogramming process.

## Generation and characterization of iPSC-derived dopaminergic neurons

As dopaminergic neurons are strongly affected in MSA, all iPSC lines were differentiated towards this neuronal subtype, following an already described protocol (Zhang et al., 2014).

The effectiveness of the differentiation protocol was assessed through ICC by evaluating the expression of specific markers at different time-points.

At 35 days in vitro (DIV) more than 75 % of differentiating cells expressed the neuronal marker Tuj1 and at least 55 % of Tuj1-positive cells also expressed the catecholaminergic marker TH.

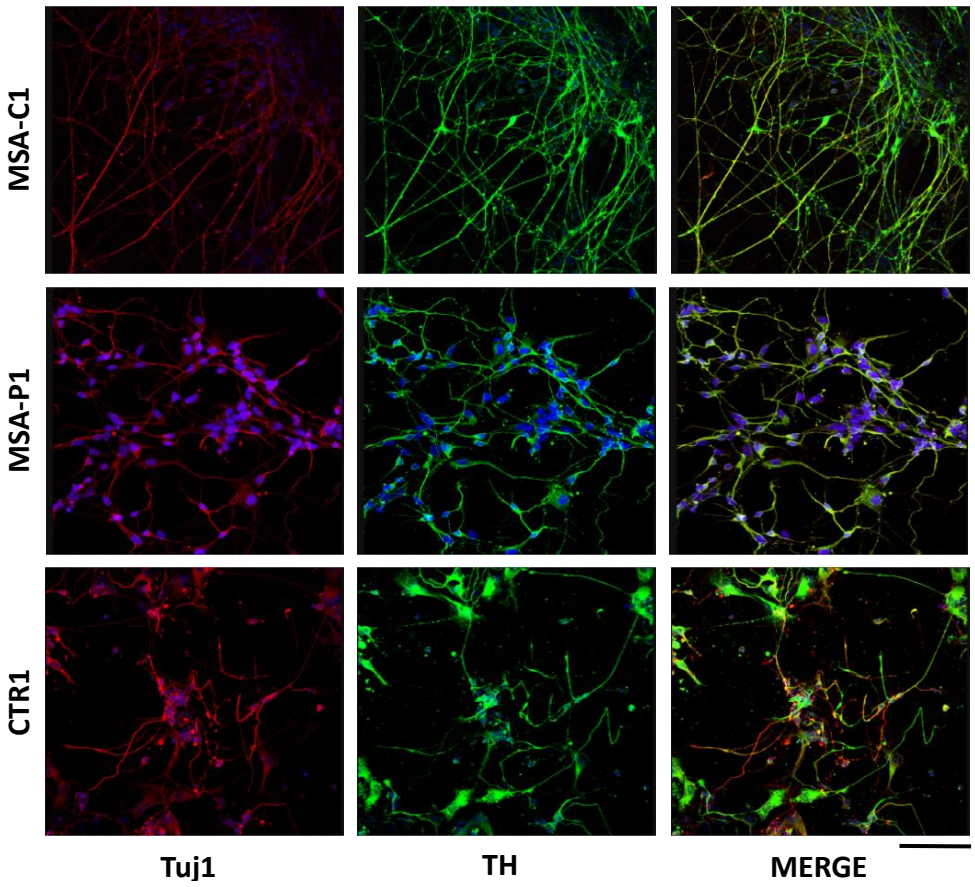


**Fig. 15**

ICC assessing the expression of the neuronal marker Tuj1 (red) and of the catecholaminergic marker TH (green) in three lines of iPSC-derived neurons (MSA-C1, MSA-P1 and CTR1) at 35 DIV. Scalebar = 50 µm

At 50 DIV the expression of the neuronal marker MAP2 was expressed in at least 75 % of differentiating cells

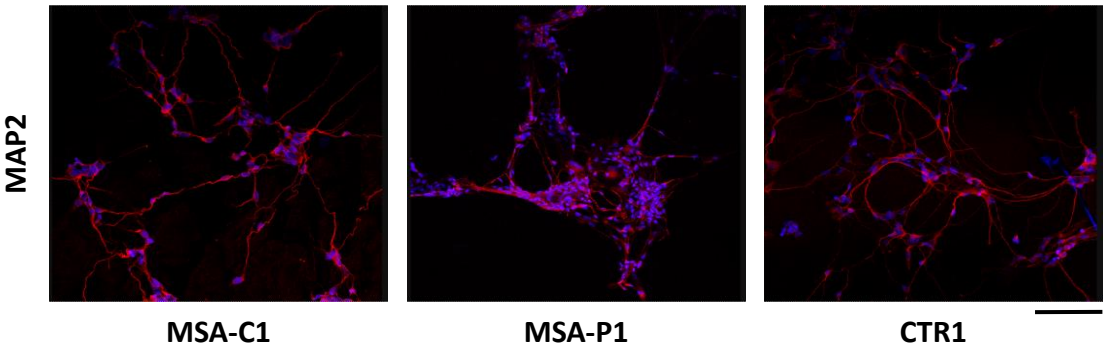


**Fig. 16**

ICC assessing the expression of the neuronal marker MAP2 in three lines of iPSC-derived neurons (MSA-C1, MSA-P1 and CTR1) at 50 DIV. Scalebar = 75 µm

Furthermore, at 70 DIV more than half of TH-positive cells also expressed the marker GIRK2 which identifies neurons of midbrain area A9, involved in the striatonigral pathway.

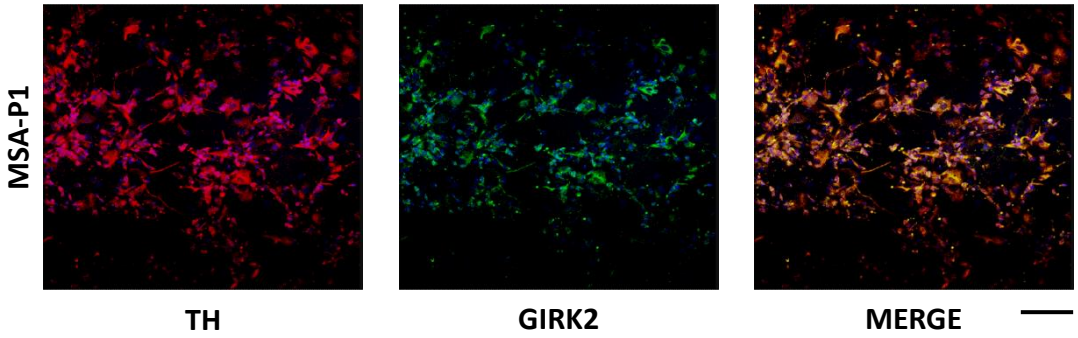


**Fig. 17**

ICC assessing the expression of the catecholaminergic marker TH (red) and of the midbrain area A9 marker GIRK2 (green) in one line (MSA-P1) of iPSC-derived neurons at 70 DIV. Scalebar = 75 µm

The expression of specific markers was also assessed through RT-PCR at 35 DIV. The neuronal markers *TUBB3* and *MAP2* and the catecholaminergic marker *TH* were highly expressed respect to fibroblasts and iPSCs.

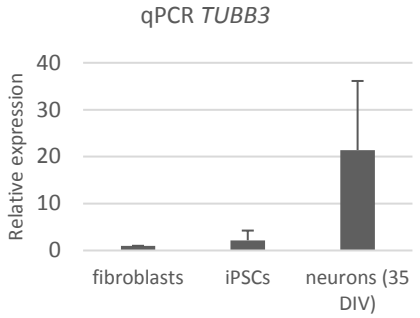


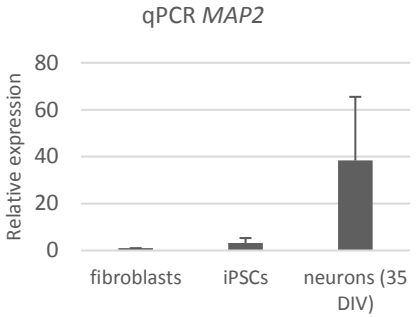


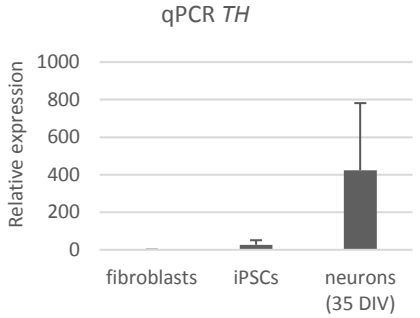


**Fig. 18**

Graphs showing high expression level of the neuronal markers *TUBB3* and *MAP2* and of the catecholaminergic marker *TH* in iPSC-derived neurons respect to fibroblasts and iPSCs measured through qPCR.

The expression of the neuronal marker Tuj1 at 35 DIV was also assessed through western blot, demonstrating a high protein amount respect to fibroblasts.

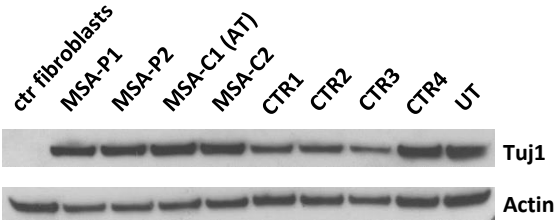


**Fig. 19**

WB assessing the amount of the neuronal marker Tuj1 and of Actin in iPSC-derived neurons and in one fibroblasts line.

As firing activity is an important feature of fully differentiated neurons electrophisiological analyses were performed.

Inward and outward currents were recorded at 56 DIV. Spontaneous firing activity and evoked action potentials were observed at the same differentiation step. Only a few spikes of low amplitude were observed when assessing post-synaptic potentials at 70 DIV.

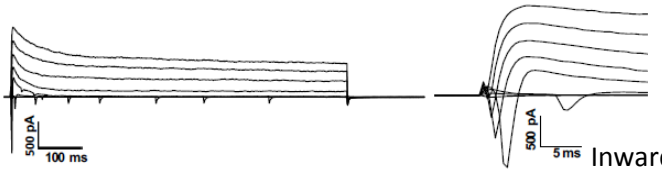


Inward and outward currents

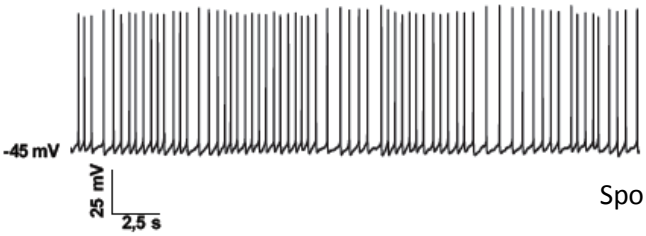


Spontaneous firing activity

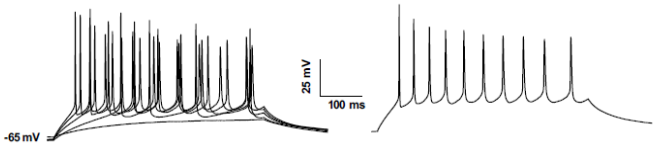


Evoked action potentials

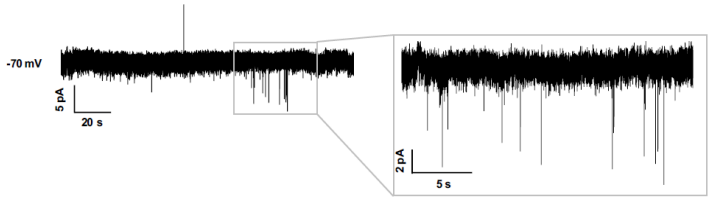


Post-synaptic potentials

**Fig. 20**

Electrophysiological analyses assessing the presence of inward and outward currents (56 DIV), spontaneous firing activity (56 DIV), evoked action potentials (56 DIV) and post-synaptic potentials (70 DIV) in iPSC-derived neurons.

To further characterize neurons, the lipidic pattern of three cell lines (MSA-C2, MSA-P2 and CTR1 was assessed at 35 and 70 DIV. Despite the presence of a certain amount of the simple gangliosides GM3 and GD3, differentiating lines displayed high levels of all the polysialogangliosides detectable in mature nervous system. Notably, patients' neurons displayed higher levels of GlcCeramide and LacCeramide and lower levels of Ceramide respect to control.

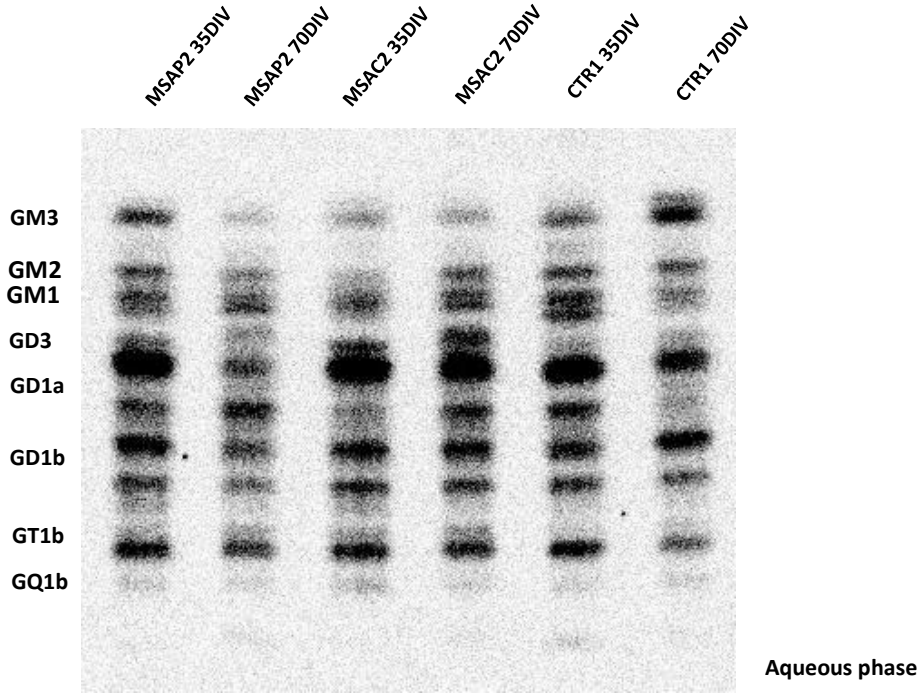


**Fig. 21**

Autoradiography assessing the amount of the lipids GM3, GM2, GM1, GD3, GD1a, GD1b, GT1b, GQ1b in three lines (MSA-P2, MSA-C2 and CTR1) of iPSC-derived neurons at 35 and 70 DIV.

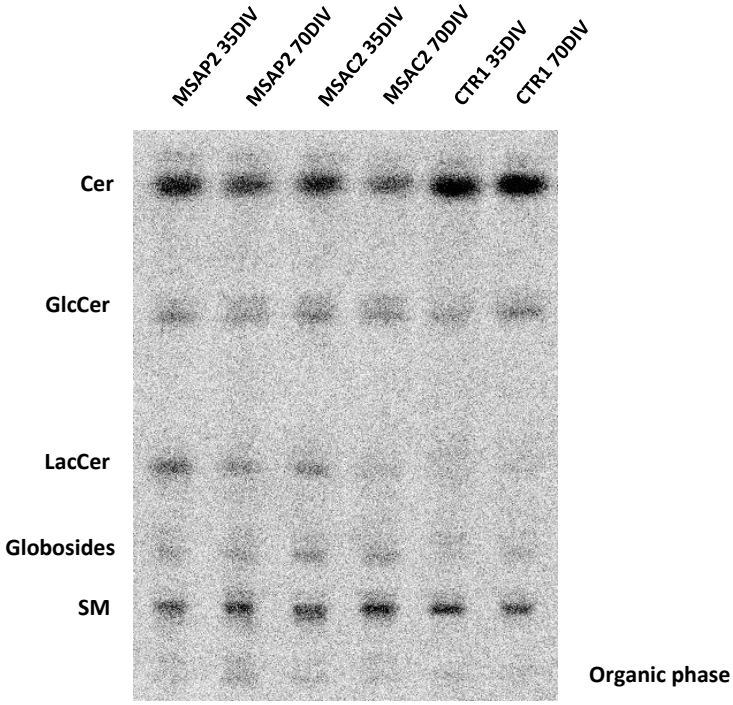


**Fig. 22**

Autoradiography assessing the amount of the lipids Ceramide, Glucosylceramide, Lactosylceramide, Globosides and Sphyngomyelin in three lines (MSA-P2, MSA-C2 and CTR1) of iPSC-derived neurons at 35 and 70 DIV.

## Apoptosis and neuronal survival

The amount of the apoptotic markers Bax (pro-apoptotic), Bcl2 (anti-apoptotic) and cleaved Caspase 3 (pro-apoptotic) was assessed through WB in neurons at 35 DIV. No significant differences were observed, although a trend of increase of cleaved Caspase 3 could be observed both in MSA group and in the affected twin.

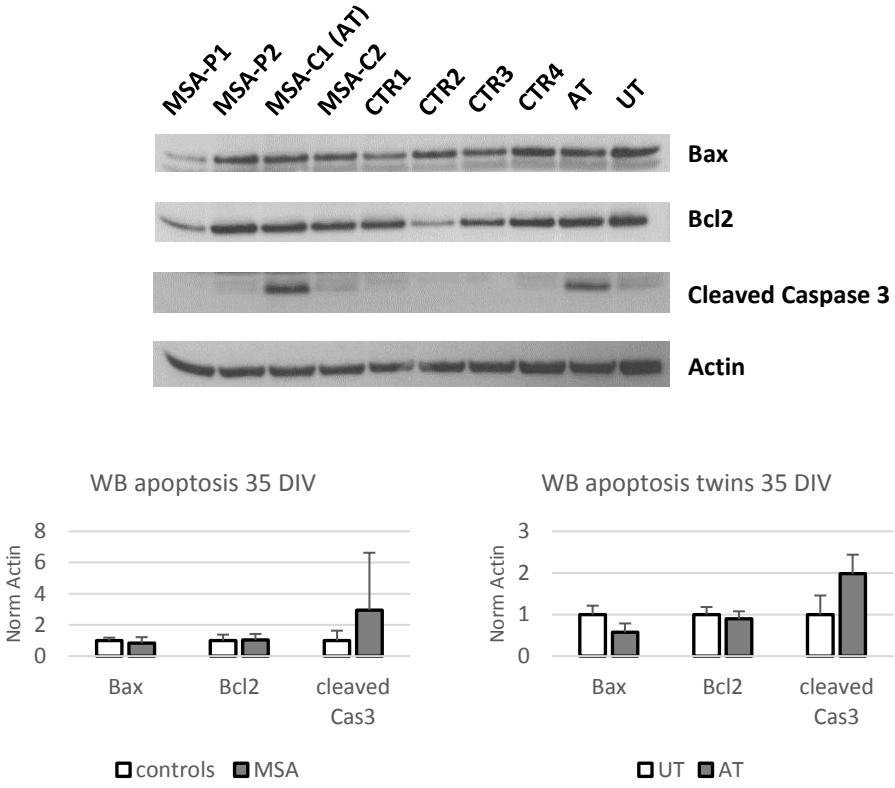


**Fig. 23**

Apoptosis in neurons. WB assessing the amount of the apoptosis-related markers Bax, Bcl2, cleaved Caspase 3 and of Actin in MSA and control iPSC-derived neurons at 35 DIV and related graphs (values normalized for Actin).

The amount of various neuronal, axonal and synaptic markers was assessed through WB at 35 and 70 DIV to evaluate neuronal survival and integrity during differentiation: TH (dopaminergic marker), tau and phospho-tau (axonal markers), synapsin I, synapsin III and synaptophysin (synaptic markers). No significant results were obtained at 35 DIV. At 70 DIV neuronal markers were more expressed than at 35 DIV; no major differences were observed between groups and between twins in the amount of phospho-tau, synapsin III and synaptophysin, whereas TH, tau and synapsin I proved to be strongly reduced both in MSA group and in the affected twin.

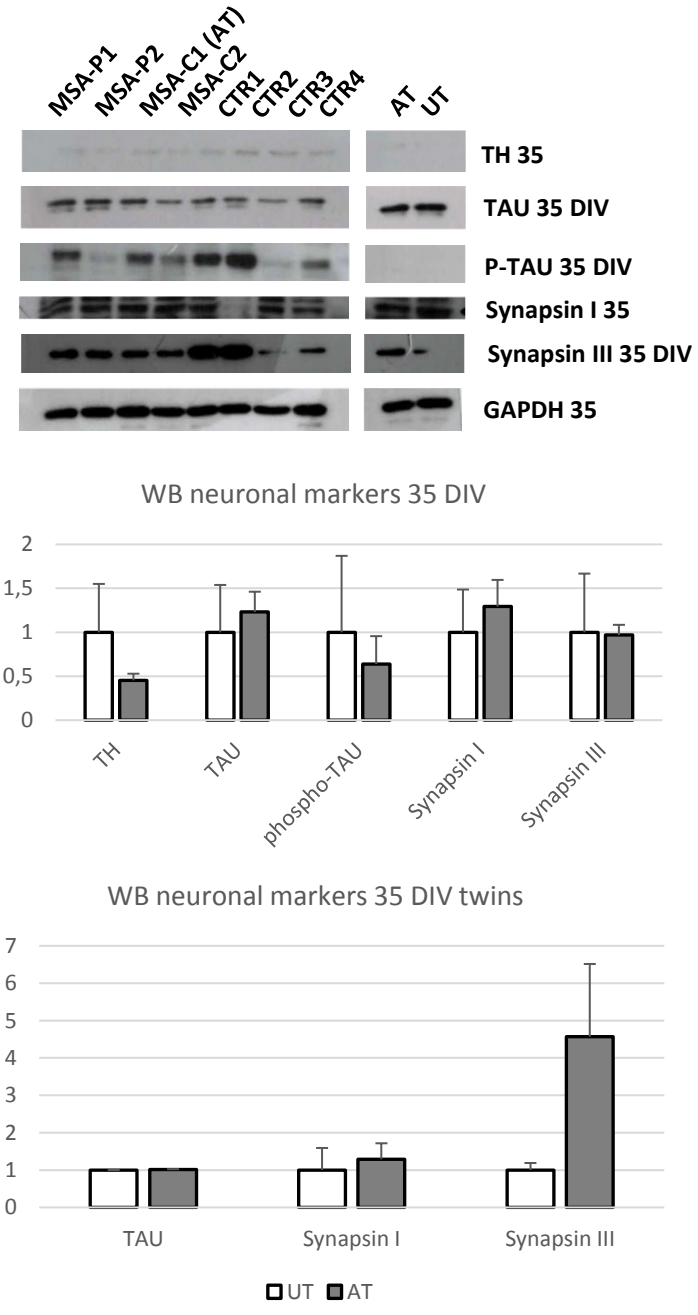


**Fig. 24**

WB assessing the amount of the proteins TH, TAU, phospho-TAU, Synapsin I, Synapsin III and GAPDH in MSA and control iPSC-derived neurons at 35 DIV and related graphs (values normalized for GAPDH)

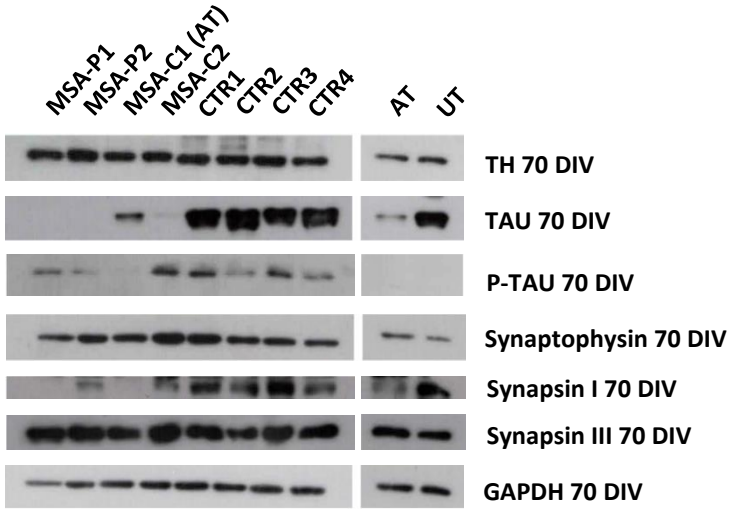


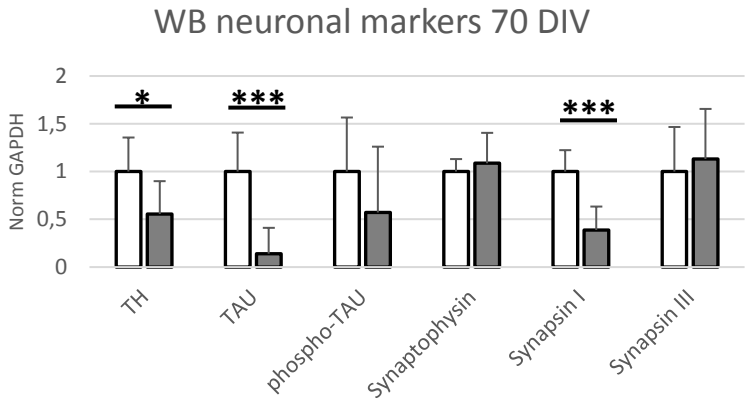


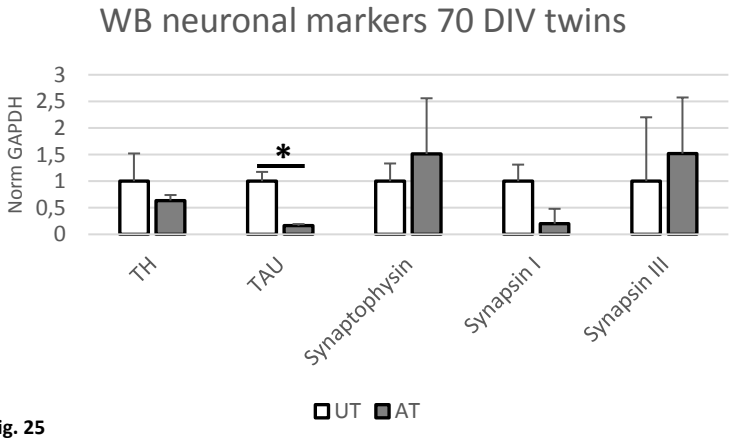


**Fig. 25**

WB assessing the amount of the proteins TH, TAU, phospho-TAU, Synaptophysin, Synapsin I, Synapsin III and GAPDH in MSA and control iPSC-derived neurons at 70 DIV and related graphs (values normalized for GAPDH).

qPCR showed that tau protein reduction in patients and in the affected twin was not due to a decreased gene expression level. Not only *MAPT* expression was not reduced, but it was even increased in patients and in the affected twin at both time-points.

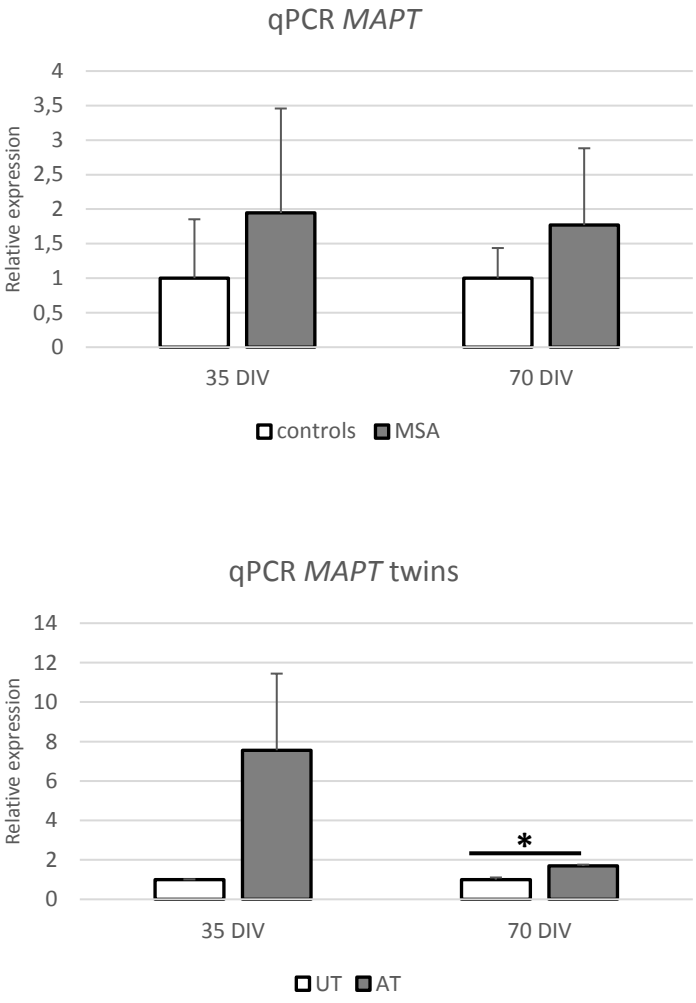


**Fig. 26**

Graphs showing *MAPT* gene expression level in MSA and control iPSC-derived neurons at 35 and 70 DIV measured through qPCR.

Alpha-synuclein

As alpha-synuclein accumulation is the most important neuropathological hallmark of MSA, several experiments were carried out to assess its expression.

WB, performed at 35 and 70 DIV, did not detect any difference neither between patients and controls, nor between the twins in the amount of the monomeric form of the protein.

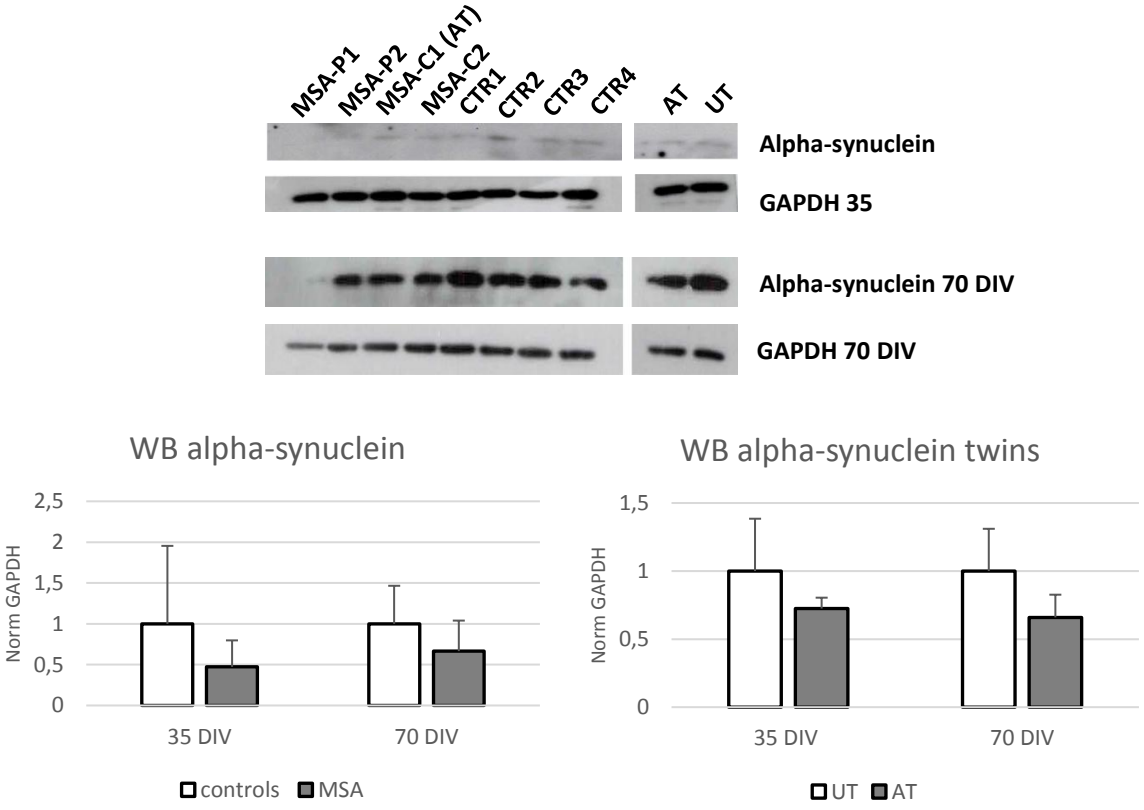


**Fig. 27**

Alpha-synuclein in neurons. WB assessing the amount of alpha-synuclein and Actin in MSA and control iPSC-derived neurons at 35 and 70 DIV and graphs showing related quantification (values normalized for GAPDH).

qPCR showed a higher level of *SNCA* transcript in controls at 35 DIV and in patients at 70 DIV. Twins showed a higher *SNCA* mRNA level in the unaffected at both time-points.

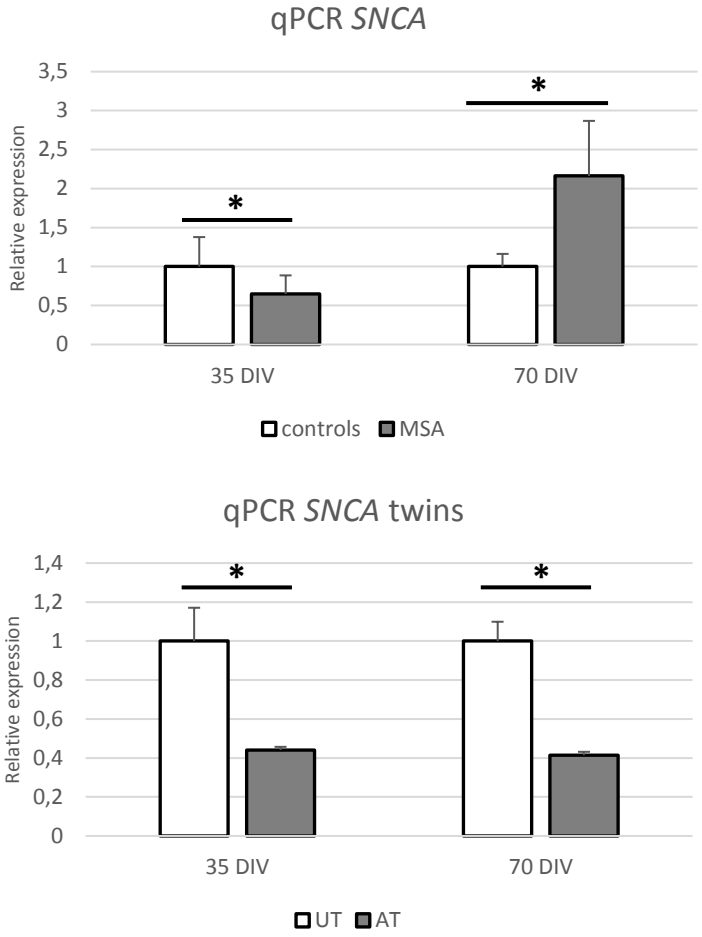


**Fig. 28**

Graphs showing *SNCA* gene expression level in MSA and control iPSC-derived neurons at 35 and 70 DIV.

To further assess alpha-synuclein expression, various mechanisms of gene expression regulation were evaluated: the expression level of the transcription factor GATA2 and the methylation pattern of *SNCA* intron 1.

qPCR demonstrated a higher expression level of *GATA2* both in controls and in the healthy twin at 35 DIV. Differently, at 70 DIV no differences were observed between MSA and control groups and a higher expression level was found in the affected twin respect to the unaffected.

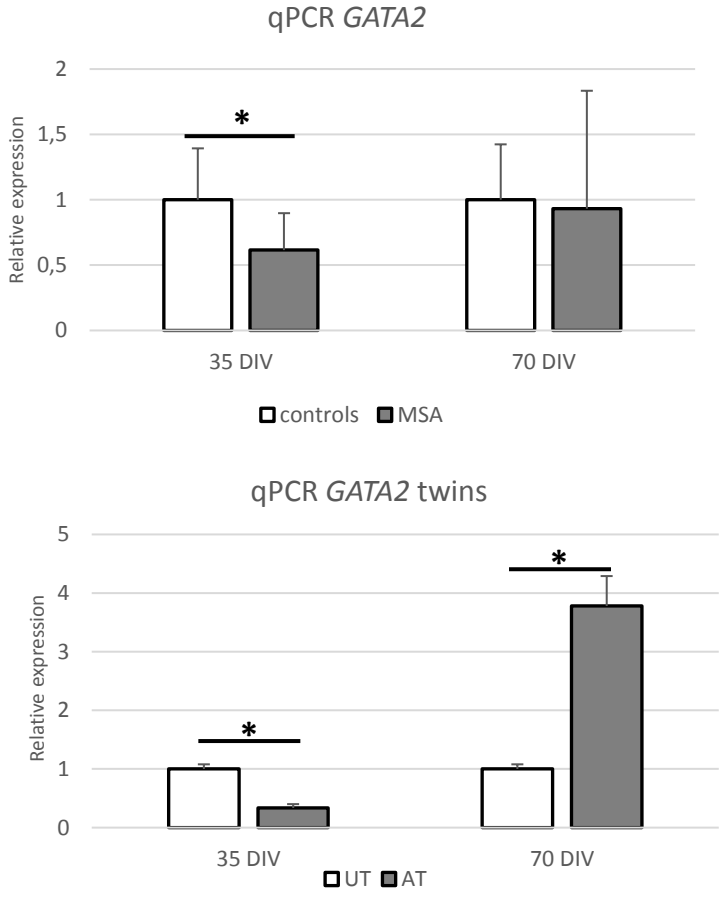


**Fig. 29**

Graphs showing *GATA2* gene expression level in MSA and control iPSC-derived neurons at 35 and 70 DIV.

Mass array technique allowed to investigate the methylation pattern of a CpG island located in *SNCA* intron 1. The patients' group displayed a generalized hypomethylation pattern, consistent with the increased gene expression levels at 70 DIV, which reached statistical significance in three sites. Also the

affected twin displayed a lower degree of methylation respect to the unaffected.

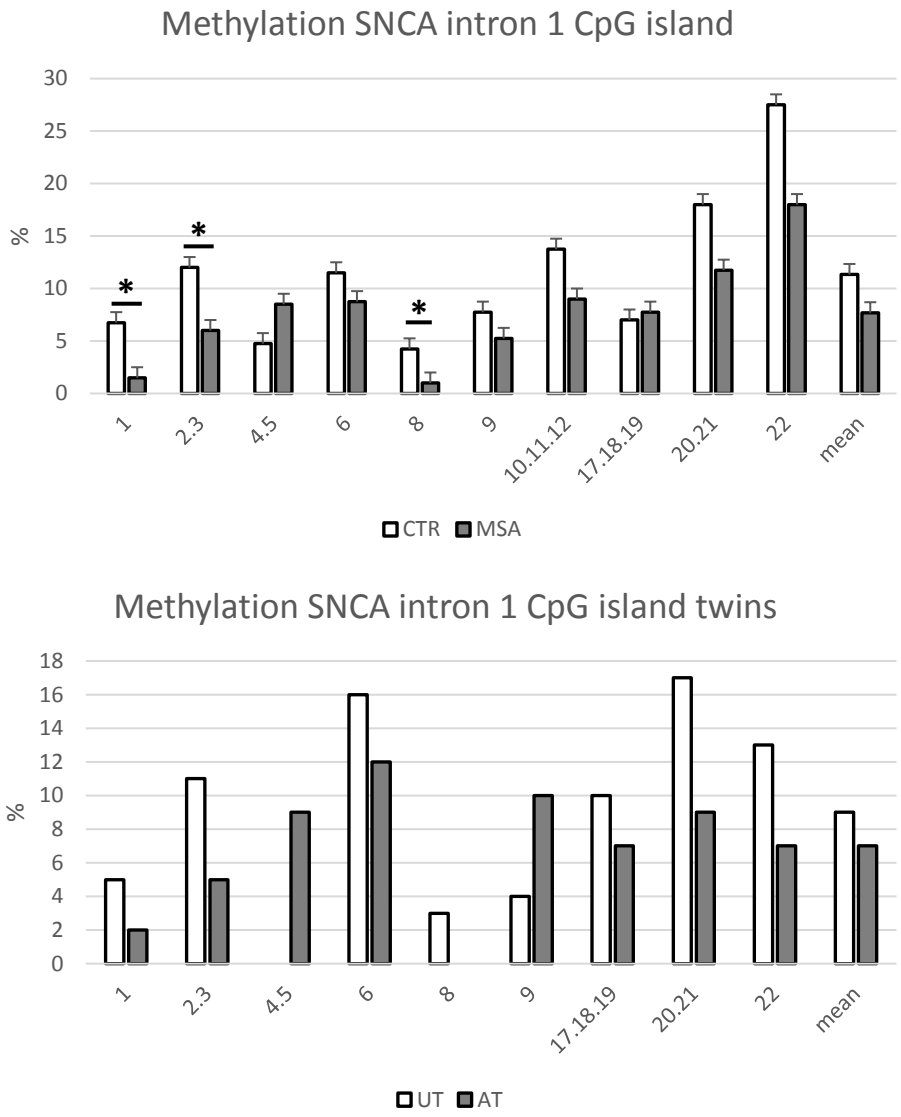


**Fig. 30**

Graphs showing the methylation pattern of a CpG island located in SNCA intron 1 in MSA and control iPSC-derived neurons at 35 DIV measured through mass array.

Autophagy

The amount of the autophagy-related proteins LAMP1, Cathepsin D, p62 and LC3 was assessed through WB at basal level and after bafilomycin administration at 35 DIV. No significant results were observed for LAMP1, Cathepsin D and p62, whereas LC3 analyses showed remarkable signs of autophagic impairment: an increased basal level of LC3II and a reduced autophagic flux, both in MSA group and in the affected twin.

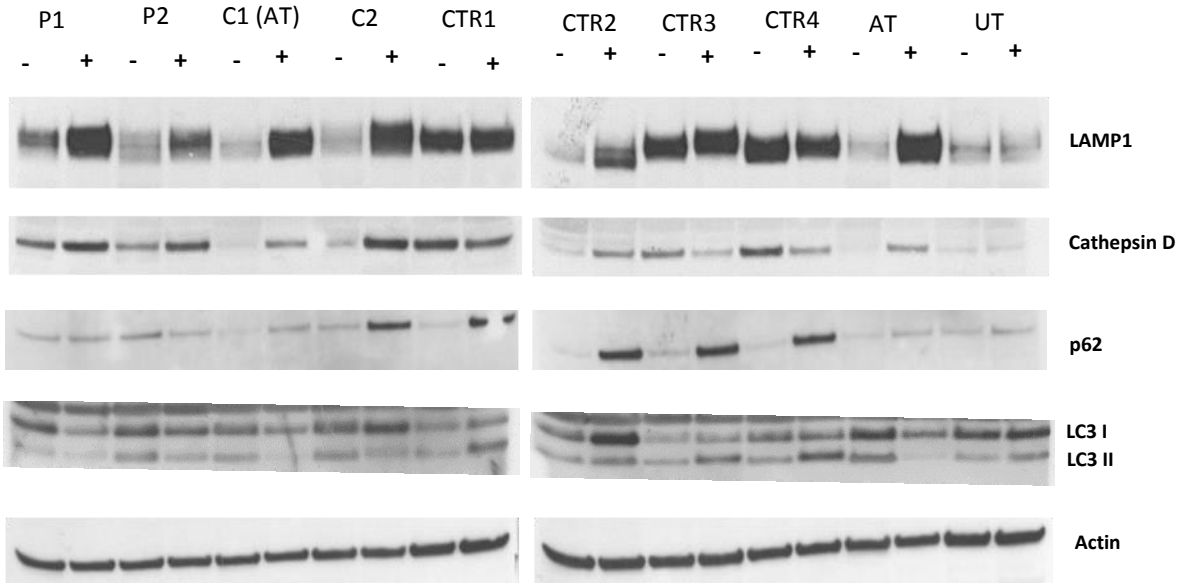


**Fig. 31**

Autophagy in neurons. WB assessing the amount of LAMP1, Cathepsin D, p62, LC3 and Actin in MSA and control iPSC-derived neurons at 35 DIV before (-) and after (+) the administration of bafilomycin (200 nM, 24 h).

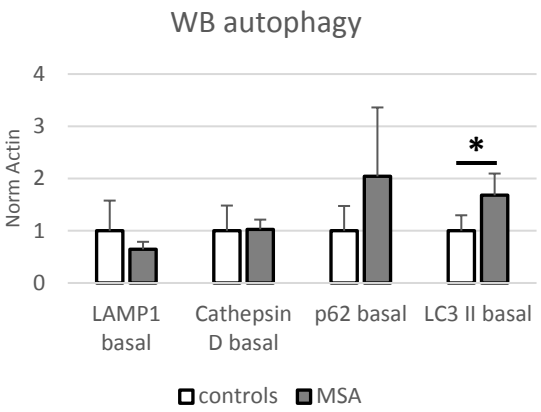


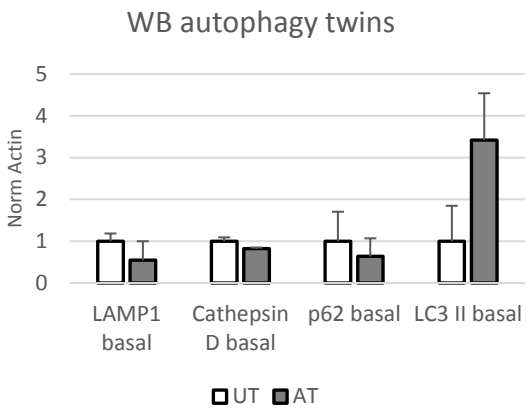


**Fig. 32**

Graphs showing quantification of basal amount of the autophagy-related proteins LAMP1, LC3 II, p62 and Cathpesin D (all normalized for Actin) in MSA and control neurons.

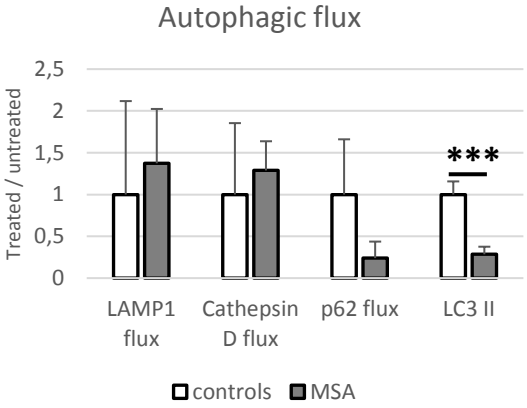


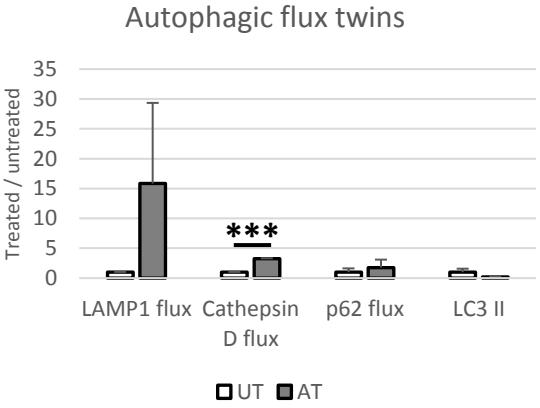


**Fig. 33**

Graphs showing quantification of the autophagic flux in neurons, measured as the ratio between the level of the autophagy-related proteins LAMP1, LC3 II, p62 and Cathepsin D after bafilomycin administration and their basal level.

To further assess autophagy, the activity of the lysosomal enzymes GBA, α-Mannosidase, β-Mannosidase, β-Hexosaminidase, β-Galactosidase and

Sphingomyelinase was measured at 35 DIV. α-Mannosidase and β-Mannosidase showed a significantly reduced activity level both in the MSA group and in the affected twin.

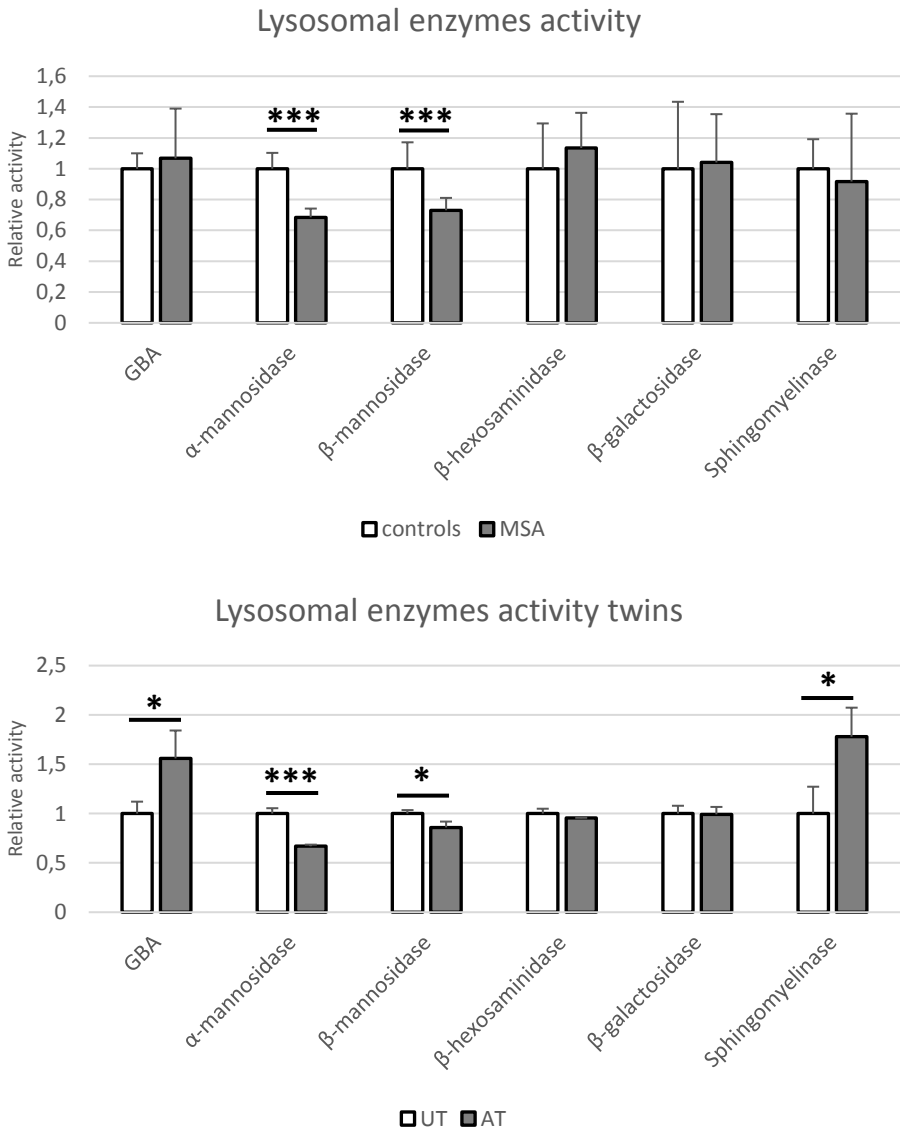


**Fig. 34**

Graphs showing the activity level of the lysosomal enzymes GBA1, α-Mannosidase, β-Mannosidase, β-Hexosaminidase, β-Galactosidase and Sphingomyelinase in MSA and control neurons at 35 DIV.

Mitochondrial functioning

Spectrophotometric analyses, performed at 35 DIV, showed a reduced activity of respiratory chain complexes in MSA group (significant for complexes II+III) and in the affected twin (significant for complexes II and II+III).

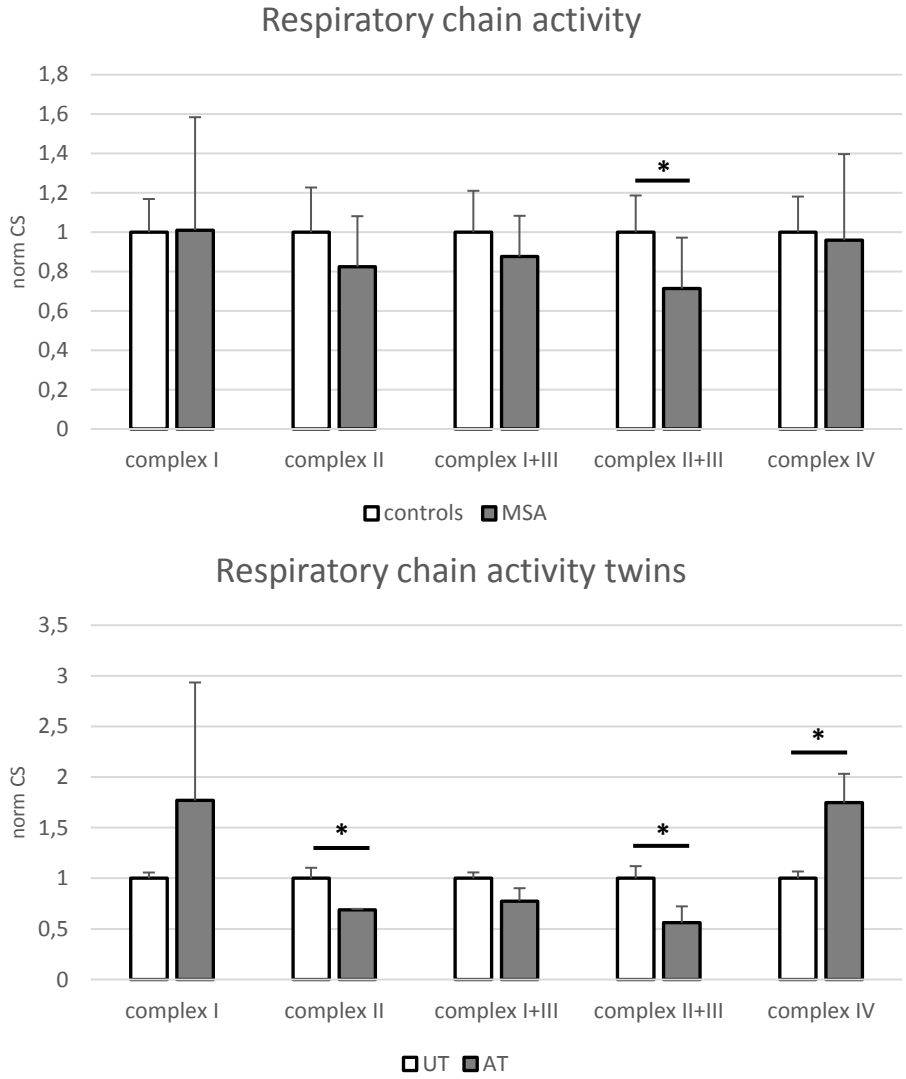


**Fig. 35**

Graphs showing the activity level of respiratory chain complexes I, II, I+III, II+III and IV in MSA and control iPSC-derived neurons at 35 DIV, measured through spectrophotometric analyses. Values are normalized for the activity of the mitochondrial matrix enzyme citrate synthase.

The amount of the structural mitochondrial protein TOMM20 was assessed through WB and normalized for Actin in order to estimate mitochondrial content in cells. TOMM20 was significantly increased in MSA group and a trend of increase was observed also in the affected twin.

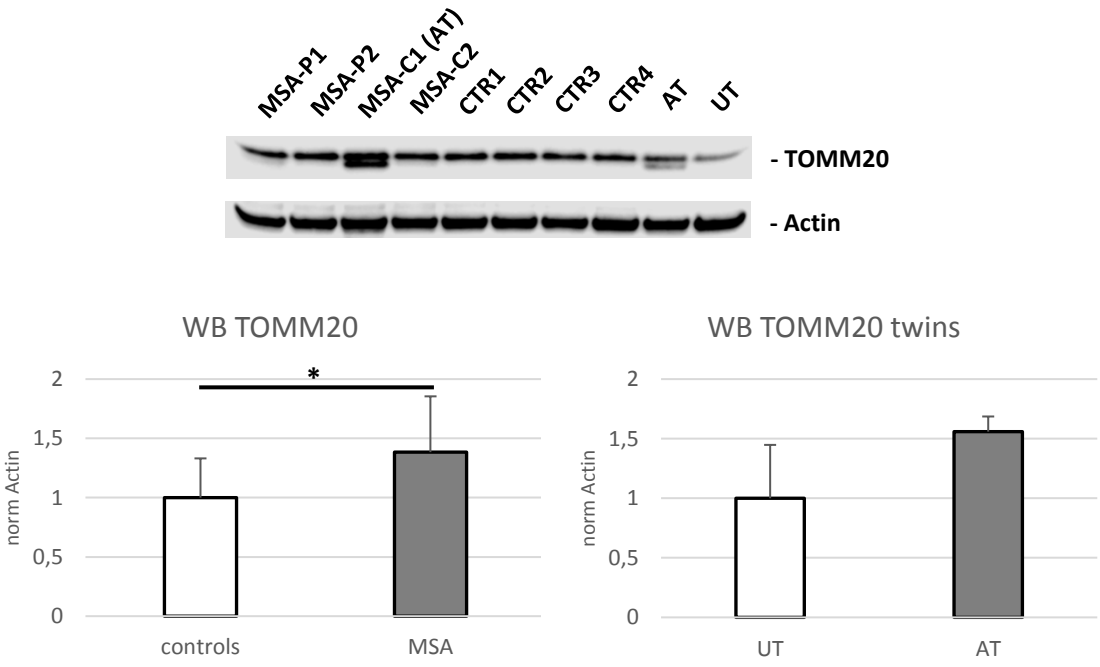


Fig. 36

WB assessing the amount of the mitochondrial protein TOMM20 and Actin in MSA and control iPSC-derived neurons at 35 DIV and graphs showing related quantification (values normalized for Actin).

The amount of all the complexes of respiratory chain was measured through WB and normalized for the mitochondrial structural protein TOMM20: complex I, complex II (SDHA and SDHB), complex III, complex IV and complex V. A significant increase in the amount of both SDHA and SDHB was observed in patients.

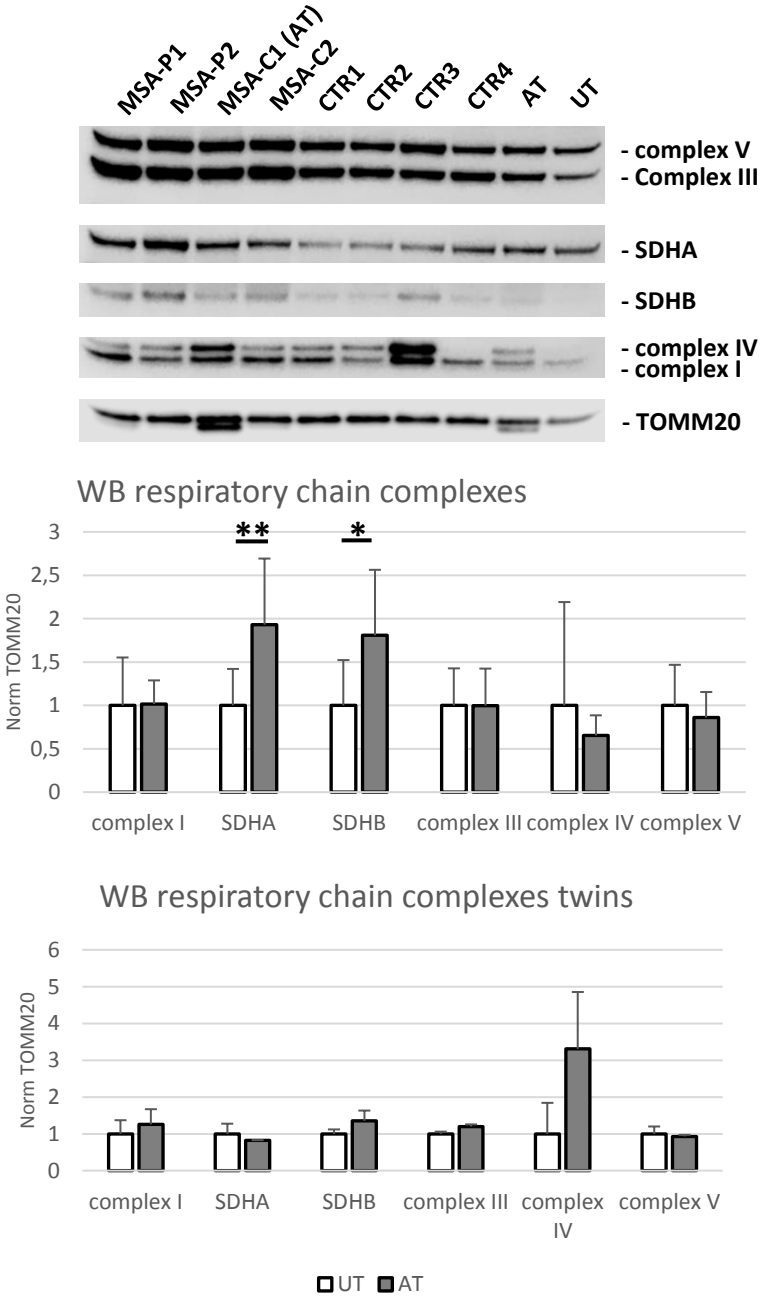


**Fig. 37**

WB assessing the amount of SDHA, complex V, complex III, SDHB, complex IV, complex I and Actin in MSA and control iPSC-derived neurons at 35 DIV and related graphs (values normalized for TOMM20).

The evaluation of mtDNA content, measured by qPCR through the simultaneous detection of the mitochondrial gene *CytB* and the nuclear gene *APP*, showed an increase in patients and in the affected twin.

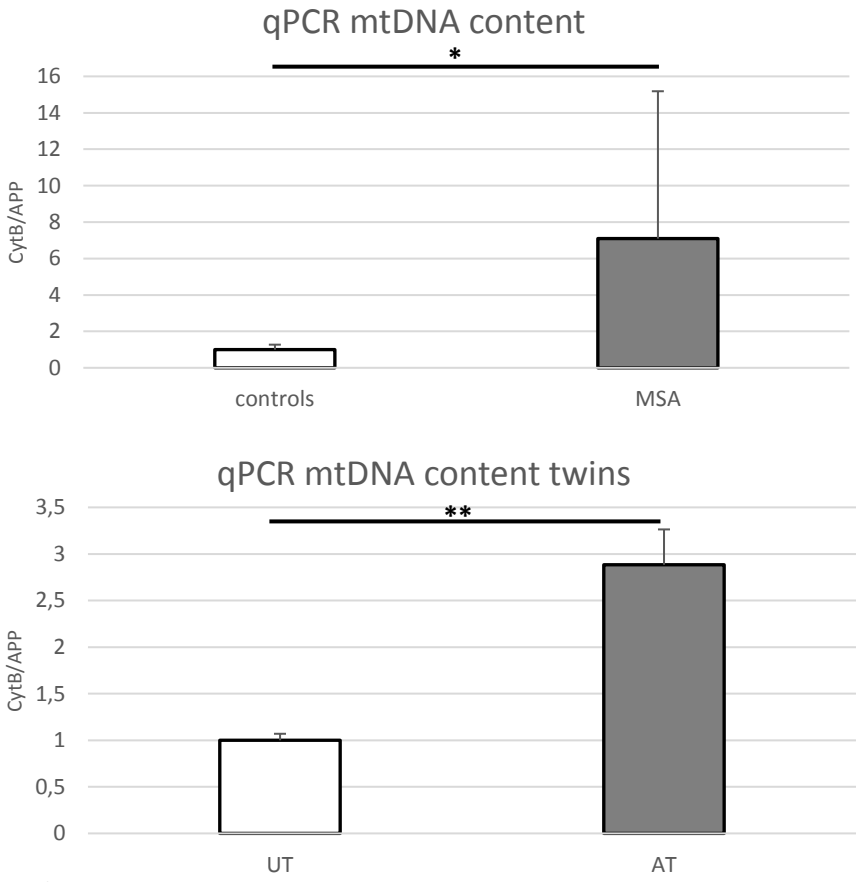


**Fig. 38**

Graphs showing mtDNA content in MSA and control iPSC-derived neurons measured by qPCR through the simultaneous detection of the mitochondrial gene *CytB* and the nuclear reference gene *APP*.

The expression level of 5 genes involved in the synthesis of respiratory chain complexes (the mitochondrial-encoded *MT-ND1* and *MT-CO1* and the nuclear-encoded *NDUFA2*, *NDUFA11*, *NDUFB4*) was assessed through qPCR. A higher expression level was observed in patients respect to controls

for all the genes, reaching statistical significance for *NDUFA2*. Twins displayed a more heterogeneous behaviour.

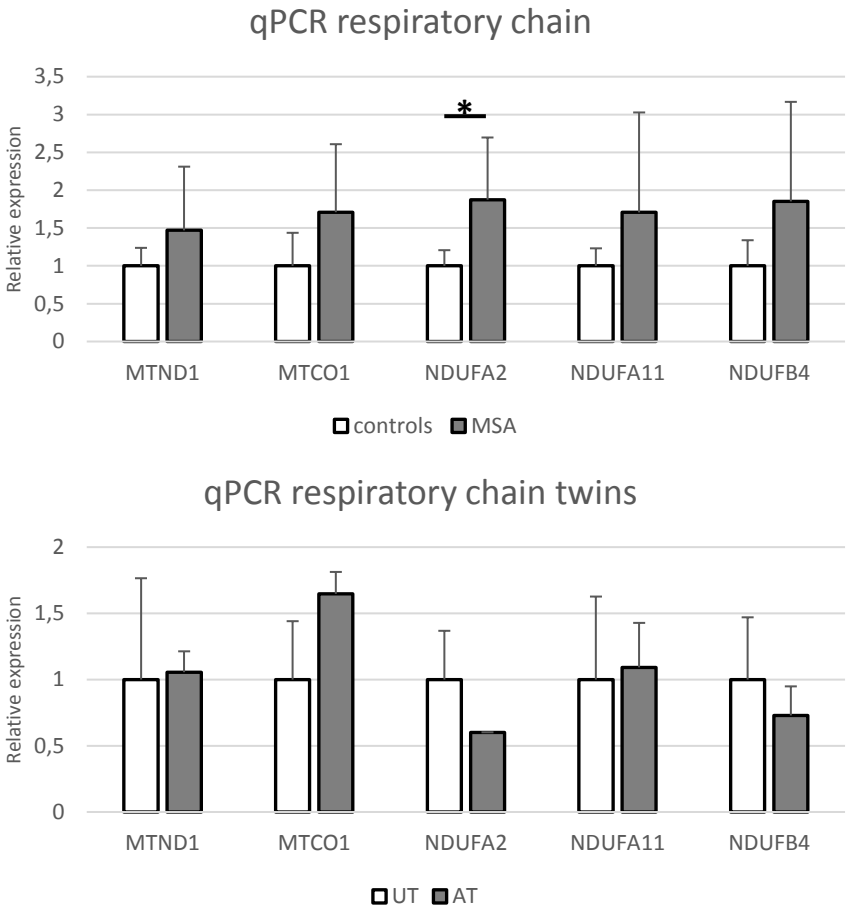


**Fig. 39**

Graphs showing the expression level of the genes *MT-ND1, MT-CO1, NDUFA2, NDUFA11* and *NDUFB4* in MSA and control neurons measured by qPCR.

To evaluate the possible presence of an unbalance between the translation of mitochondrial- and nuclear-encoded proteins, the amount of the complex IV subunits COXI (mitochondrial-encoded) and COXIV (nuclear-encoded) was assessed through WB. The COXI/COXIV ratio did not show significant differences between patients and controls and between the twins.

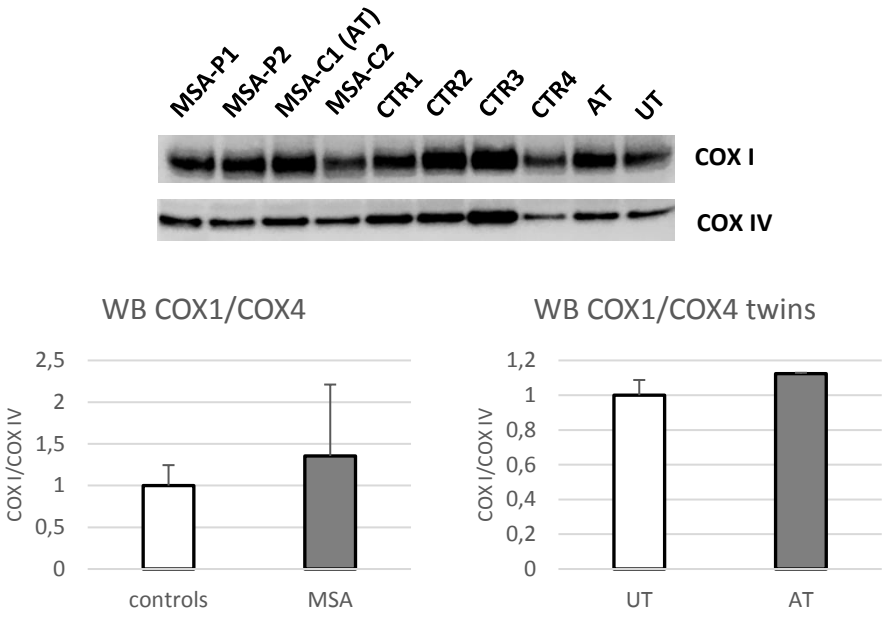


**Fig. 40**

WB assessing the amount of the two subunits of respiratory chain complex IV COX I (mitochondrial-encoded) and COX IV (nuclear-encoded) in MSA and control iPSC-derived neurons and graphs showing quantification of COX I / COX IV ratio.

The assessment of CoQ10 levels through HPLC did not reveal statistically significant differences between groups, although a trend of increase could be observed in patients' group.

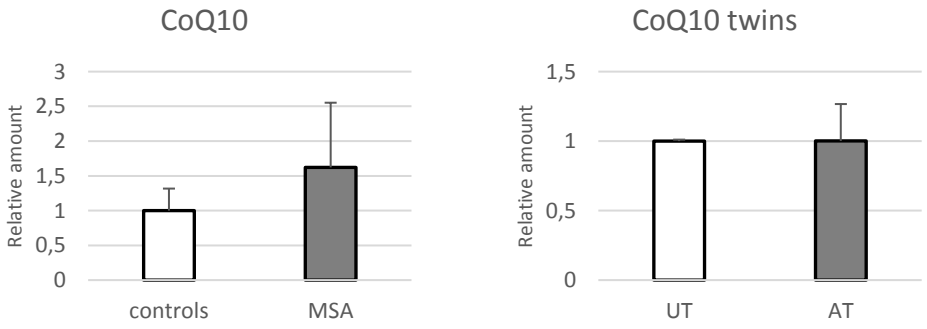


**Fig. 41**

Graphs showing CoQ10 amount in MSA and control iPSC-derived neurons measured through HPLC.

The amount of 9 enzymes involved in CoQ10 synthesis (PDSS1, PDSS2, COQ2, COQ4, COQ5, COQ6, COQ7, ADCK3/COQ8A, COQ9) was assessed through WB. A generalized upregulation of these enzymes was observed in patients, reaching statistical significance for PDSS1, PDSS2, COQ4, ADCK3/COQ8A. The affected twin displayed the same trend of increase, although without reaching statistical significance.

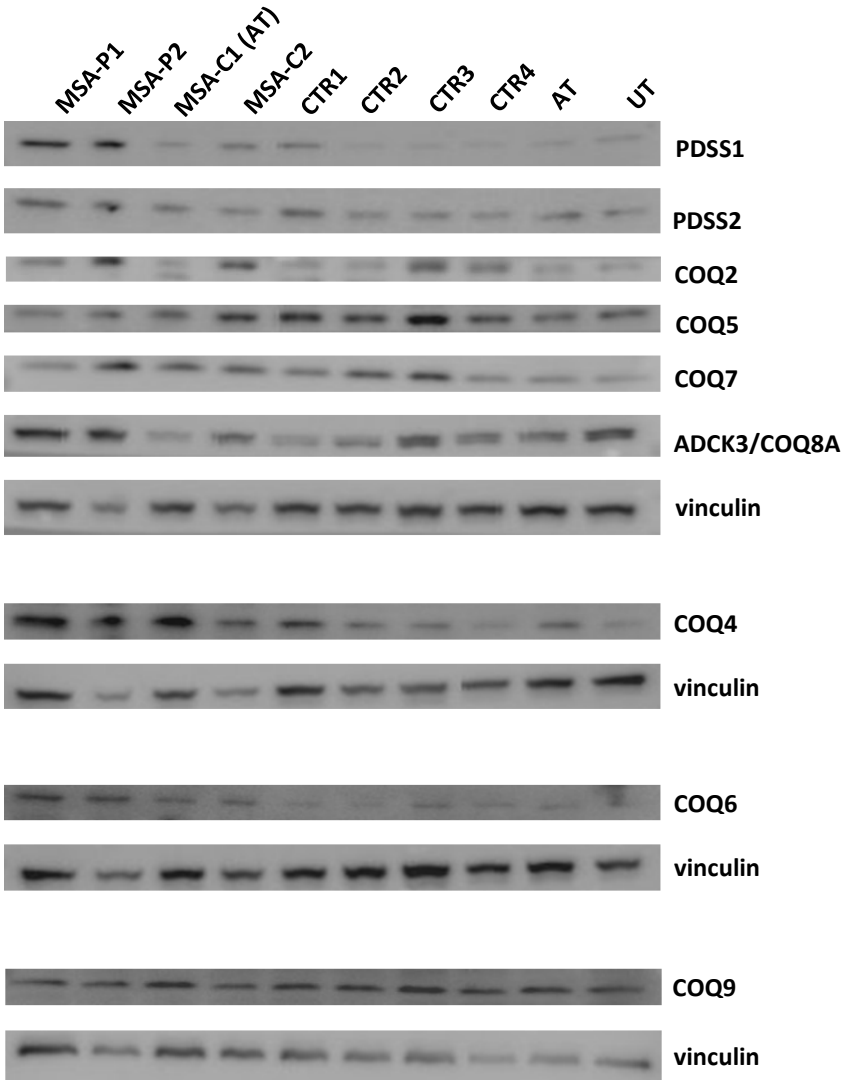


**Fig. 42**

WB assessing the amount of CoQ10 biosynthesis enzymes PDSS1, PDSS2, COQ2, COQ4, COQ5, COQ6, COQ7, ADCK3/COQ8A, COQ9 and Vinculin in MSA and control iPSC-derived neurons.

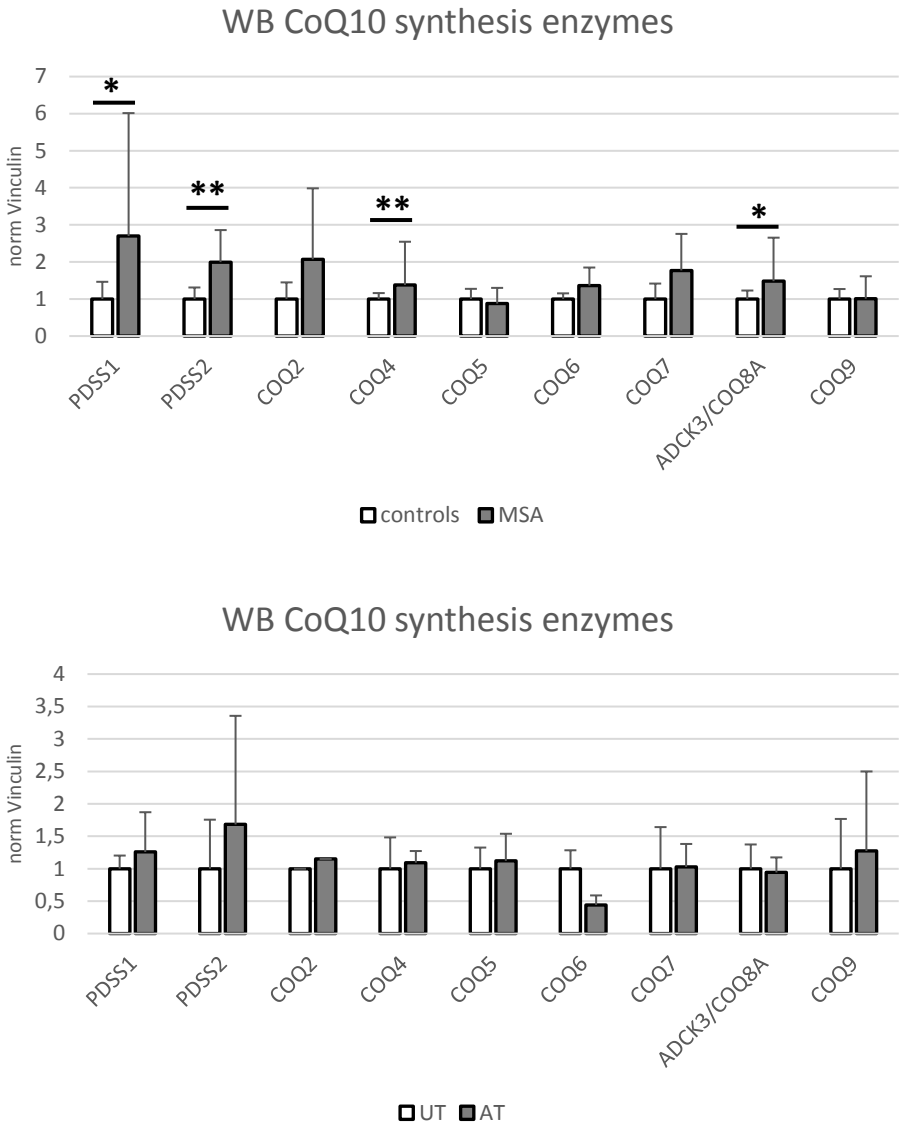


**Fig. 43**

Graphs showing quantification of WB assessing the amount of CoQ10 biosynthesis enzymes PDSS1, PDSS2, COQ2, COQ4, COQ5, COQ6, COQ7, ADCK3/COQ8A and COQ9 (values normalized for Vinculin).

**Analyses on peripheral blood cells (PBCs) and brain tissue**

To further characterize mitochondrial functioning, analyses were performed also on PBCs and post-mortem brain tissue of patients affected with MSA and healthy controls.

PBCs of 125 MSA patients (73 MSA-P and 52 MSA-C), 90 PD and 177 age-matched healthy controls and post-mortem brain tissue of 58 MSA patients (21 MSA-P, 12 MSA-C and 25 undefined MSA), 25 PD and 99 age-matched healthy controls were analyzed.

In all these samples mtDNA content was measured by qPCR through the simultaneous detection of a mitochondrial gene and a nuclear gene and analyzed through the ΔΔCt method. PBCs were analyzed through two independent combinations of mitochondrial and nuclear probes: *CytB* vs *APP* and *ND4* vs *RNaseP*. Brain tissue was analyzed with a single probe combination (*ND4* vs *RNaseP*).

Analyses on PBCs showed a significantly increased mtDNA content in MSA respect to controls with both probe combinations, which was exclusively driven by MSA-C. Indeed, mtDNA content proved to be significantly increased in MSA-C respect to controls but not in MSA-P respect to controls. The analysis with the *ND4*/*RNaseP* probes combination also showed a significant increase of mtDNA in MSA-C respect to MSA-P.

Analyses on post-mortem brain tissue confirmed most of the results observed in PBCs, showing a significant increase of mtDNA in MSA-C respect to controls, in MSA-C respect to all MSA samples and in MSA-C respect to MSA-P.

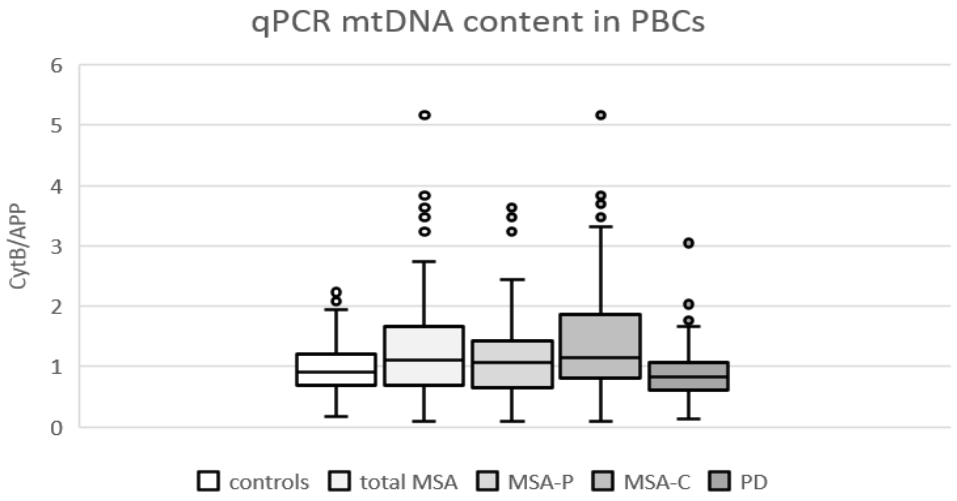


**Fig. 44**

Box plot showing mtDNA content in peripheral blood cells of MSA patients and healthy controls measured by qPCR through the simultaneous detection of the mitochondrial gene *CytB* and the nuclear reference gene *APP*. Significant values: ctr vs MSA p<0.01; controls vs MSA-C p< 0,001; MSA vs PD p<0,001; MSA-C vs PD p<0,001.

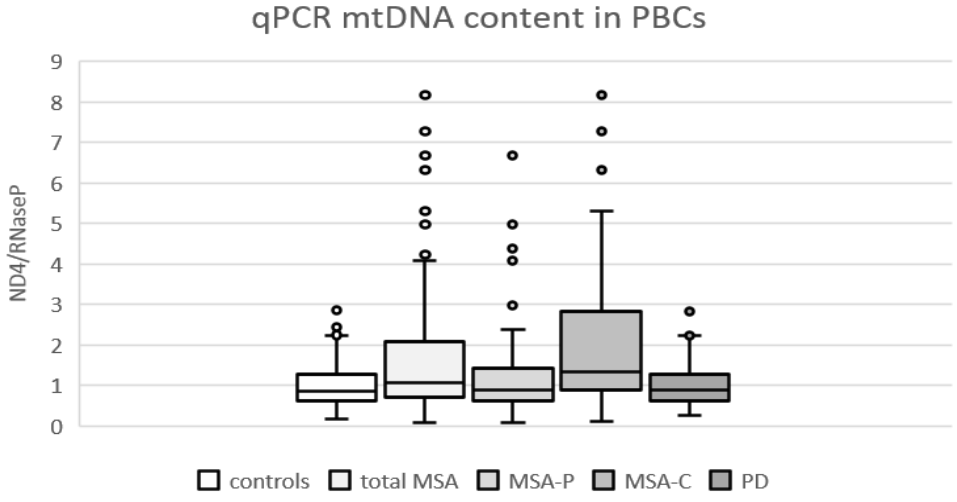


**Fig. 45**

Box plot showing mtDNA content in peripheral blood cells of MSA patients and healthy controls measured by qPCR through the simultaneous detection of the mitochondrial gene *ND4* and the nuclear reference gene *RNaseP*. Significant values: controls vs MSA p<0,001; controls vs MSA-C p<0,001; MSA-P vs MSA-C p<0,05; MSA vs PD p<0,001; MSA-C vs PD p<0,001.

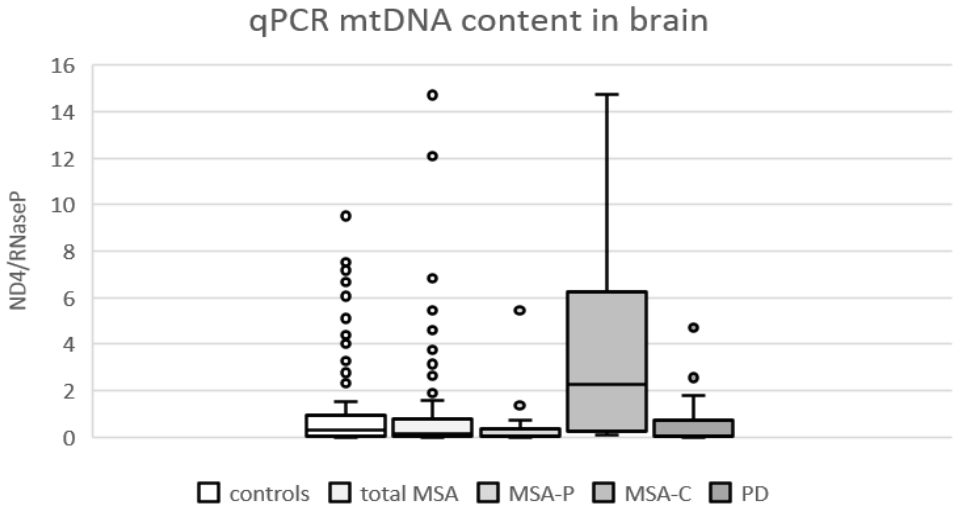


**Fig. 46**

Box plot showing mtDNA content in brain tissue of MSA patients and healthy controls measured by qPCR through the simultaneous detection of the mitochondrial gene *ND4* and the nuclear reference gene *RNaseP*. Significant values: controls vs MSA p<0,001; MSA vs MSA-C p<0,05; MSA-P vs MSA-C p<0,05; MSA-C vs PD p<0,05.

## DISCUSSION

The present study aimed to contribute to the comprehension of the still widely unknown pathogenic mechanisms of MSA and to lay the foundations for the development of new therapeutic approaches.

The study has taken advantage from various techniques and has been based on different models: peripheral blood cells, fibroblasts and iPSC-derived neurons. Remarkably, this work represents the first comprehensive iPSC-based model of MSA.

As the pathogenic mechanisms of MSA are still elusive, many fields have been investigated, ranging from mitochondrial functioning to autophagy, alpha-synuclein accumulation and cell survival.

### Alpha-synuclein

The role of alpha-synuclein in pathology is highly debated in the scientific community. Its heterogeous behavior raises many doubts about the causes which lead to its accumulation and aggregation and about the pernicious effect which is caused by the protein itself. Not only different subclasses of alpha-synucleinopathies are characterized by the involvement of different cellular subtypes (namely neurons or oligodendrocytes) or different brain areas, but many different protein conformations can be observed in disease. The evaluation of intracellular alpha-synuclein is particularly difficult because the exact description of the physiological and pathological conformations of the protein is still a matter of debate. On the one hand, some laboratories argue that alpha-synuclein native form is a folded tetramer of 58-60 kDa (Bartels et al., 2011; Wang et al., 2011). On the other hand, other investigators assert that the native form of alpha-synuclein is an unfolded monomer and that the higher molecular weight which can be observed in

native gel is due to an extended conformation of the protein (Fauvet et al., 2012; Lashuel et al., 2013). Furthermore, the pathogenesis of alpha-synucleinopathies has been associated with more complex forms of alpha-synuclein, in particular oligomers and fibrils (Lashuel et al., 2013). However, investigating these specific mechanisms was beyond the aim of the present study, which was only focused on the monomeric form of the protein, which did not show significant differences between patients and controls at WB. More interesting results have been found evaluating the methylation pattern of *SNCA* CpG islands (CGIs). CGIs are short interspersed DNA sequences rich in CpG dinucleotides. Most CGIs are located at the sites of transcription initiation and are predominantly non-methylated. Silencing of CGI promoters can be achieved through epigenetic modifications, namely CpG methylation. (Deaton and Bird, 2011). Previous studies (Jowaed et al., 2010; Matsumoto et al., 2010) evaluated the *SNCA* sequence and identified two CpG-rich regions at the 5' of the gene: the first including the promoter and the second located within intron 1 (-1074 to -26 from ATG) (Jowaed et al., 2010). The methylation of this latter region has been proven to be correlated with *SNCA* transcription regulation. Additional studies of the *SNCA* gene methylation pattern found that the CpG island within intron 1 was hypomethylated in brains of PD patients respect to healthy controls (Jowaed et al., 2010; Matsumoto et al., 2010). Furthermore, intron 1 is the same region which has been supposed to be involved in GATA-mediated *SNCA* regulatory mechanisms. In particular, in neuroblastoma cells, the silencing of the transcription factor GATA2 leads to a reduction of *SNCA* mRNA level and of alpha-synuclein amount (Scherzer et al., 2008). The finding that the CGI is less methylated in patients compared to controls and in the affected twin compared to the unaffected one opens new perspectives for the comprehension of MSA. Indeed, this epigenetic pattern may contribute to the onset of the disease by promoting the expression of the gene and,

subsequently, the synthesis of the protein. This finding is only partially consistent with qPCR data, which show an increased level of *SNCA* expression in patients only at 70 DIV. However, it is tempting to speculate that alternative regulatory mechanisms act in the early phase of differentiation to counterbalance the effect of hypomethylation, restoring the equilibrium between patients and controls. The assessment of *GATA2* expression levels seems to confirm this hypothesis, showing a reduced *GATA2* expression in patients at 35 DIV, which may be sufficient to normalize the otherwise altered levels of *SNCA* transcript. However, further investigation is needed to confirm this hypothesis. In particular, it will be important to explore the involvement of all the pre- and post-transcriptional regulatory mechanisms which have been described so far for *SNCA* gene (transcription factors (Scherzer et al., 2008; Clough et al., 2009; Dermentzaki et al., 2016), lncRNAs (Mizuta et al., 2013) and miRNAs (Junn et al., 2009; Doxakis 2010)) and to evaluate the presence of alpha-synuclein oligomers and fibrils through proper techniques (e.g. thioflavin staining).

As alpha-synuclein pathology in MSA mainly affects oligodendrocytes, this study would strongly benefit from the generation of iPSC-derived oligodendroglia and from the establishment of neurons-oligodendrocytes co-coltures. This achievement would allow to investigate alpha-synuclein expression in glial cells and to assess protein cell-to-cell transfer.

However, the available differentiation protocols (Douvaras and Fossati, 2015) for oligodendroglia are still characterized by low efficiency and have to be improved before being used in an extensive project which requires a high amount of mature and well differentiated cells.

**Apoptosis and cellular survival**

To investigate whether patients' fibroblasts and iPSC-derived neurons displayed a different survival rate or signs of cellular suffering, many experiments have been carried out. The assessment of the apoptosis-related markers Bax (pro-apoptotic), Bcl2 (anti-apoptotic) and cleaved Caspase 3 (pro-apoptotic) did not provide significant results. Differently, the assessment of the amount of various neuronal markers in iPSC-derived neurons at two different time-points showed a clear pattern of neuronal suffering which proved to be related to the progression of differentiation. In particular the finding of a remarkable reduction of the catecholaminergic marker TH, the axonal marker tau and the synaptic marker synapsin I in patients' neurons at 70 DIV is indicative of neurites' damage and of a reduced dopaminergic neurons' survival rate. This is further confirmed by the observation that only synapsin I, specifically located at synapses, is reduced, whereas synapsin III, which has been identified also in other cellular compartments, has not shown significant differences between patients and controls. (Porton et al., 2011) The finding of the same behavior in twins further supports the hypothesis. Furthermore, it is important to notice that these signs of cellular suffering can be observed only at 70 DIV and not at 35 DIV, demonstrating that neuronal damage is correlated with the progression of differentiation and, more in general, with aging.

**Autophagy**

Autophagy has been widely studied in alpha-synucleinopathies and an impairment in this pathway has been described. (Xilouri et al., 2016)

An autophagic defect has been detected in PD, both in autoptic samples and in animal models. (Klucken et al., 2012; Yu et al., 2009, Crews et al., 2010) Remarkably, the most important risk factor for the development of PD and DLB is represented by mutations in *GBA*, the gene encoding the lysosomal

enzyme glucocerebrosidase. Furthermore, glucocerebrosidase dysfunction and alpha-synuclein accumulation seem to be strictly correlated, enhancing each other in a self-propagating fashion. (Aflaki et al., 2017; Mazzulli et al., 2011)

An activation of the autophagic pathway has been observed also in MSA brain samples. (Schwarz et al. 2012; Tanji et al., 2012)

The present study has assessed autophagy from many points of view and has demonstrated a strong impairment in MSA.

Data on fibroblasts have not provided major hints, probably because these cells are not affected in the disease.

Differently, iPSC-derived neurons, evaluated only at 35 DIV, have shown a strong activation of autophagy accompanied by an impairment of the same pathway. This observation is particularly supported by the findings observed with LC3 II, both at basal level and after the administration of bafilomycin A1, a V-ATPase inhibitor which causes the block of the fusion between the autophagosome and the lysosome (Klionsky et al., 2012).

LC3 is commonly used to monitor the autophagic pathway. Two forms of LC3 can be detected: LC3-I and LC3-II. LC3-I is the cytosolic form of the protein and can be converted to LC3-II through conjugation with phosphatidylethanolamine. LC3-II is associated with autophagosomes and is degraded after fusion with lysosomes. The basal level of LC3-II can be considered as a good marker of autophagic activity, whereas the change in protein amount after treatment with autophagy inhibitors is a reliable marker of the effectiveness of the autophagic flux.

In this study LC3-II basal level was found to be increased and autophagic flux (measured as LC3-II treated/untreated) was found to be reduced both in patients and in the affected twin.

Other investigations further supported the impairment of autophagy in patients. In particular, the activity level of some lysosomal enzymes, namely α- and β-Mannosidase, proved to be significantly reduced in MSA.

Furthermore, lipid analyses, although only preliminar and performed on a limited number of subjects, provided some interesting hints consistent with the hypothesis of an autophagic dysfunction which also affects lipidic turnover. In particular, the finding of an increased level of GlucosylCeramide and LactosylCeramide and of a reduced level of Ceramide in patients is intriguing, although further analyses are required to confirm the hypothesis and to understand why the finding is not accompanied by a reduction of GBA activity.

## Mitochondrial dysfunction

Mitochondrial dysfunction has proved to play an essential role in alpha-synucleinopathies.

The present study further supports this hypothesis, suggesting a strong alteration of several mitochondrial mechanisms.

In particular, two main findings have emerged from the study: a mitochondrial dysfunction and an up-regulation of mitochondria-related pathways.

Mitochondrial dysfunction is confirmed by the results of spectrophotometric analyses, which show a reduction of respiratory chain activity in patients, both in fibroblasts and in neurons. Patients' fibroblasts also display a trend of reduction of maximal respiration rate, although the high variability among cell lines does not allow to reach statistical significance.

Differently, the mitochondrial up-regulation, detectable mainly in neurons, is suggested by many findings. Total mitochondrial mass (assessed through

WB and qPCR) is increased, as well as the amount of SDHA and SDHB, the expression levels of various genes involved in the synthesis of respiratory chain complexes' subunits and the amount of several enzymes involved in CoQ10 biosynthesis.

These two findings may be closely related to each other, being the up-regulation of mitochondrial pathways a possible compensatory mechanism to an underlying mitochondrial dysfunction.

An intriguing comprehensive hypothesis is that mitochondrial dysfunction may be closely related to the autophagic impairment. A dysregulation in autophagy, which impairs also the mitophagic machinery, would lead to a defect in mitochondrial degradation and to the accumulation of damaged senescent organelles, which do not work properly and further trigger mitochondrial biogenesis in a self-propagating fashion.

The results related to mtDNA are particularly interesting, showing a significant increase of mtDNA content in MSA-C both in peripheral blood cells and in brain tissue. The reliability of the finding is supported by the high number of patients and controls involved in the analyses and by the replication of the analyses with two different experimental methods (i.e. with two different combinations of mitochondrial and nuclear probes). Data obtained on fibroblasts and neurons are not so striking, but they have been performed on a far smaller cohort of subjects.

The finding of a selective alteration of mtDNA content in the cerebellar subtype of MSA is particularly noticeable because MSA-P and MSA-C are usually considered as different manifestations of the same disease and the reported finding may shed light on the different pathogenic mechanisms at the basis of these two forms. In this view, it is important to observe that mitochondrial dysfunction is a common finding of cerebellar diseases, both as a causative mechanism and as a secondary clinical manifestation. The

close relationship between mitochondrial dysfunction and cerebellar diseases is indicative of the fact that the result observed in MSA may be the consequence of the early and massive cerebellar involvement which can be observed in this subtype of the disease. The recent description of a selective depletion of CoQ10 in the cerebella of MSA patients (Schottlaender et al., 2016; Barca et al., 2016) further supports this hypothesis, providing evidence for the strict relationship between cerebellar degeneration and mitochondrial dysfunction.

The finding of mtDNA alteration in MSA-C does not only provide an interesting hint to further understand the pathogenic mechanisms at the basis of the disease but may also be useful in clinical practice. Indeed, mtDNA content in peripheral blood cells may be a useful tool for the differential diagnosis of alpha-synucleinopathies, although further investigation is needed to confirm this finding and to assess sensitivity and specificity of the test.

mtDNA content has been assessed also in a cohort of PD patients (both PBCs and brain tissue), without significant results (respect to controls).

However, mtDNA content in PD patients has already been investigated in previous studies, although with conflicting observations. In particular, one study (Pyle et al., 2016) has detected a reduction of mtDNA in PD PBCs and brain samples, while another one (Wei et al., 2017) has not found significant differences in brain samples.

## CONCLUSIONS

The present study aimed to investigate the pathogenic mechanisms of MSA, a disease whose etiology is still widely unknown but which causes a remarkable burden for patients and still lacks an effective treatment.

The study provides a comprehensive description of various experimental models of MSA involving fibroblasts, iPSC-derived dopaminergic neurons, peripheral blood cells and brain tissue.

As an univocal hypothesis about MSA pathogenesis is absent, various potentially causative molecular mechanisms have been taken into consideration, ranging from alpha-synuclein expression to autophagy and mitochondrial functioning.

The opportunity to rely on various models has further strengthened the robustness of the observations.

The development of the iPSC-based neuronal model is remarkable because this technique has almost never been used in this disease so far.

The results of the study outline an impairment of specific pathways: alpha-synuclein gene expression regulation, autophagy and mitochondrial functioning.

All these pathways may be related to one another and it is intriguing to hypothesize that a single link connects all of them. A comprehensive hypothesis could be that autophagic impairment also affects mitophagy, leading to the formation of senescent damaged mitochondria which, in turn, up-regulate the pathways involved in their own maintenance (e.g. CoQ10 biosynthesis). Malfunctioning mitochondria may then contribute to cellular suffering and, eventually, death. The role of alpha-synuclein dysregulation in this context may be found in the already described link between alpha-

synuclein aggregation and lysosomal impairment, deeply investigated in Parkinson's disease. However, further investigation is needed to clearly understand the whole pathogenic network.

In the future, it will be important to unravel the role of alpha-synuclein in more detail, assessing the presence of oligomeric and fibrillar forms of the protein, evaluating the presence of protein and/or mRNA in the extracellular environment or in exosomes and assessing the possible transfer of the protein to oligodendroglia establishing co-coltures of iPSC-derived neurons and oligodendrocytes.

It will be important to further investigate the impairment of autophagy, extending lipid analyses to a proper number of patients and controls and assessing the precise connection between autophagic dysfunction and alpha-synuclein accumulation.

It will be crucial to perform other experiments for the dissection of the mitophagic machinery, which could represent a potential connection between autophagic and mitochondrial defects.

Finally, it is important to remark that the establishment of a human neuronal model of the disease may be of great usefulness for the assessment of the therapeutic effect of novel pharmacological compounds and for regenerative medicine techniques.

## REFERENCES


1. Aflaki E, Westbroek W, Sidransky E. The Complicated Relationship between Gaucher Disease and Parkinsonism: Insights from a Rare Disease. Neuron. 2017 Feb 22;93(4):737-746.
2. Al-Chalabi A, Dürr A, Wood NW, Parkinson MH, Camuzat A, Hulot JS, Morrison KE, Renton A, Sussmuth SD et al. Genetic variants of the alphasynuclein gene SNCA are associated with multiple system atrophy. PLoS One 2009 Sep 22;4(9):e7114.
3. Alvarez-Buylla A, Garcia-Verdugo JM. Neurogenesis in adult subventricular zone. J Neurosci, 2002. 22(3): p. 629-34
4. Asi YT, Simpson JE, Heath PR, Wharton SB, Lees AJ, Revesz T, Houlden H, Holton JL. Alpha-synuclein mRNA expression in oligodendrocytes in MSA. Glia. 2014 Jun;62(6):964-70.
5. Barca E, Kleiner G, Tang G, Ziosi M, Tadesse S, Masliah E, Louis ED, Faust P, Kang UJ, Torres J et al. Decreased Coenzyme Q10 Levels in Multiple System Atrophy Cerebellum. J Neuropathol Exp Neurol. 2016 Jul;75(7):663-72.
6. Bartels T, Choi JG, Selkoe DJ. α-Synuclein occurs physiologically as a helically folded tetramer that resists aggregation. Nature. 2011 Aug 14;477(7362):107-10.
7. Bender A, Krishnan KJ, Morris CM, Taylor GA, Reeve AK, Perry RH, Jaros E, Hersheson JS, Betts J, Klopstock T et al. High levels of mitochondrial DNA deletions in substantia nigra neurons in aging and Parkinson disease. Nat Genet. 2006 May;38(5):515-7. Epub 2006 Apr 9.
8. Bensimon G, Ludolph A, Agid Y, Vidailhet, Payan C, Leigh PN, NNIPPS Study Group. Riluzole treatment, survival and diagnostic

criteria in Parkinson plus disorders: the NNIPPS study. Brain, 2009. 132(Pt 1): p. 156-71.

9. Beraud D, Hathaway HA, Trecki J, Chasovskikh S, Johnson DA, Johnson JA, Federoff HJ, Shimoji M, Mhyre TR, Maguire-Zeiss KA. Microglial activation and antioxidant responses induced by the Parkinson's disease protein alpha-synuclein.J Neuroimmune Pharmacol, 2013. 8(1): p. 94-117.
10. Beraud D, Twomey M, Bloom M, Mittereder A, Ton V, Neitzke K, Chasovskikh S, MhyreTR, Maguire-Zeiss KA. alphaSynuclein Alters Toll-Like Receptor Expression.Front Neurosci, 2011. 5: p. 80.
11. Betarbet R, Sherer TB, MacKenzie G, Garcia-Osuna M, Panov AV, Greenamyre JT. Chronic systemic pesticide exposure reproduces features of Parkinson's disease. Nat Neurosci. 2000 Dec;3(12):1301-6.
12. Bonifati, V. Genetics of Parkinson's disease--state of the art, 2013.Parkinsonism Relat Disord, 2014. 20 Suppl 1: p. S23-8.
13. Boyer LA, Lee TI, Cole MF, Johnstone SE, Levine SS, Zucker JP, Guenther MG, Kumar RM, Murray HL, Jenner RG et al.. Core transcriptional regulatory circuitry in human embryonic stem cells. Cell, 2005. 122(6): p. 947-56.
14. Brooks DJ, Seppi K. Proposed neuroimaging criteria for the diagnosis of multiple system atrophy. Mov. Disord. 24, 949–964 (2009)
15. Byers B, Cord B, Nguyen HN, Schüle B, Fenno L, Lee PC, Deisseroth K, Langston JW, Pera RR, Palmer TD. SNCA triplication Parkinson's patient's iPSC-derived DA neurons accumulate α-synuclein and are susceptible to oxidative stress. PLoS One. 2011;6(11):e26159

16. Cho JW, Jeon BS, Jeong D, Choi YJ, Lee JY, Lee HS, Hong SY. Association between parkinsonism and participation in agriculture in Korea. J Clin Neurol. 2008 Mar;4(1):23-8.
17. Clough RL, Dermentzaki G, Stefanis L. Functional dissection of the alpha-synuclein promoter: transcriptional regulation by ZSCAN21 and ZNF219. J Neurochem. 2009 Sep;110(5):1479-90.
18. Crews L, Spencer B, Desplats P, Patrick C, Paulino A, Rockenstein E, Hansen L, Adame A, Galasko D, Masliah E. Selective molecular alterations in the autophagy pathway in patients with Lewy body disease and in models of alpha-synucleinopathy. PLoS One. 2010 Feb 19;5(2):e9313.
19. Deaton AM, Bird A. CpG islands and the regulation of transcription. Genes & Dev. 2011. 25: 1010-1022
20. Dermentzaki G, Paschalidis N, Politis PK, Stefanis L. Complex Effects of the ZSCAN21 Transcription Factor on Transcriptional Regulation of α-Synuclein in Primary Neuronal Cultures and in Vivo. J Biol Chem. 2016 Apr 15;291(16):8756-72.
21. Desplats P, Lee HJ, Bae EJ, Patrick C, Rockenstein E, Crews L, Spencer B, Masliah E, Lee SJ. Inclusion formation and neuronal cell death through neuron-to-neuron transmission of alpha-synuclein. Proc Natl Acad Sci U S A. 2009 Aug 4;106(31):13010-5.
22. Dodel R, Spottke A, Gerhard A, Reuss A, Reinecker S, Schimke N, Trenkwalder C, Sixel-Döring F, Herting B, Kamm C et al. Minocycline 1-year therapy in multiple-system-atrophy: effect on clinical symptoms and [(11)C] (R)-PK11195 PET (MEMSA-trial).Mov Disord, 2010. 25(1): p. 97-107.
23. Douvaras P, Fossati V. Generation and isolation of oligodendrocyte progenitor cells from human pluripotent stem cells. Nat Protoc. 2015 Aug;10(8):1143-54.

24. Djelloul M, Holmqvist S, Boza-Serrano A, Azevedo C, Yeung MS, Goldwurm S, Frisén J, Deierborg T, Roybon L. Alpha-Synuclein Expression in the Oligodendrocyte Lineage: an In Vitro and In Vivo Study Using Rodent and Human Models. Stem Cell Reports. 2015 Aug 11;5(2):174-8.
25. Doxakis Post-transcriptional regulation of alpha-synuclein expression by mir-7 and mir-153. E J Biol Chem. 2010 Apr 23;285(17):12726-34.
26. Fanciulli A, Wenning GK. Multiple-system atrophy. N Engl J Med 2015 Jan 15;372(3):249-63.
27. Fauvet B, Mbefo MK, Fares MB, Desobry C, Michael S, Ardah MT, Tsika E, Coune P, Prudent M, Lion N et al. α-Synuclein in central nervous system and from erythrocytes, mammalian cells, and Escherichia coli exists predominantly as disordered monomer J Biol Chem. 2012 May 4;287(19):15345-64.
28. Fernagut PO, Diguet E, Stefanova N, Biran M, Wenning GK, Canioni P, Bioulac B, Tison F. Subacute systemic 3-nitropropionic acid intoxication induces a distinct motor disorder in adult C57Bl/6 mice: behavioural and histopathological characterisation. Neuroscience. 2002;114(4):1005-17.
29. Fernagut PO, Tison F. Animal models of multiple system atrophy. Neuroscience. 2012 Jun 1;211:77-82.
30. Ghorayeb I, Fernagut PO, Aubert I, Bezard E, Poewe W, Wenning GK, Tison F. Toward a primate model of L-dopa-unresponsive parkinsonism mimicking striatonigral degeneration. Mov Disord. 2000 May;15(3):531-6.
31. Ghorayeb I, Puschban Z, Fernagut PO, Scherfler C, Rouland R, Wenning GK, Tison F. Simultaneous intrastriatal 6-hydroxydopamine and quinolinic acid injection: a model of early-

stage striatonigral degeneration. Exp Neurol. 2001 Jan;167(1):133-47.

32. Gilman S, Wenning GK, Low PA, Brooks DJ, Mathias CJ, Trojanowski JQ, Wood NW, Colosimo C, Dürr A, Fowler CJ et al. Second consensus statement on the diagnosis of multiple system atrophy. Neurology, 2008. 71(9): p. 670-6.
33. Gu M, Gash MT, Cooper JM, Wenning GK, Daniel SE, Quinn NP, Marsden CD, Schapira AH. Mitochondrial respiratory chain function in multiple system atrophy. Mov Disord. 1997 May;12(3):418-22.
34. Hara K, Momose Y, Tokiguchi S, Shimohata M, Terajima K, Onodera O, Kakita A, Yamada M, Takahashi H, Hirasawa M et al. Multiplex families with multiple system atrophy. Arch Neurol. 2007 Apr;64(4):545-51.
35. Hasegawa T, Baba T, Kobayashi M, Konno M, Sugeno N, Kikuchi A, Itoyama Y, Takeda A. Role of TPPP/p25 on alpha-synuclein-mediated oligodendroglial degeneration and the protective effect of SIRT2 inhibition in a cellular model of multiple system atrophy.Neurochem Int, 2010. 57(8): p. 857-66.
36. Holmberg B, Johansson JO, Poewe W, Wenning G, Quinn NP, Mathias C Tolosa E, Cardozo A, Dizdar N, Rascol O et al. Safety and tolerability of growth hormone therapy in multiple system atrophy: a doubleblind, placebo-controlled study. Mov Disord, 2007. 22(8): p. 1138-44.
37. Imaizumi Y, Okada Y, Akamatsu W, Koike M, Kuzumaki N, Hayakawa H, Nihira T, Kobayashi T, Ohyama M, Sato S et al. Mitochondrial dysfunction associated with increased oxidative stress and α-synuclein accumulation in PARK2 iPSC-derived neurons and postmortem brain tissue. Mol Brain. 2012 Oct 6;5:35.

38. Jellinger, KA. Neuropathology of multiple system atrophy: new thoughts about pathogenesis. Mov Disord, 2014. 29(14): p. 1720-41.
39. Jellinger KA, Lantos PL. Papp-Lantos inclusions and the pathogenesis of multiple system atrophy: an update. Acta Neuropathol, 2010. 119(6): p. 657-67.
40. Jowaed A, Schmitt I, Kaut O, Wüllner U. Methylation regulates alpha-synuclein expression and is decreased in Parkinson's disease patients' brains. J Neurosci. 2010 May 5;30(18):6355-9.
41. Junn E, Lee KW, Jeong BS, Chan TW, Im JY, Mouradian MM. Repression of alpha-synuclein expression and toxicity by microRNA-7. Proc Natl Acad Sci U S A. 2009 Aug 4;106(31):13052-7.
42. Kahle PJ, Neumann M, Ozmen L, Muller V, Jacobsen H, Spooren W, Fuss B, Mallon B, Macklin WB, Fujiwara H et al. Hyperphosphorylation and insolubility of alpha-synuclein in transgenic mouse oligodendrocytes. EMBO Rep. 2002 Jun;3(6):583-8. Epub 2002 May 24.
43. Kawamoto Y, Kobayashi Y, Suzuki Y, Inoue H, Tomimoto H, Akiguchi I, Budka H, Martins LM, Downward J, Takahashi R. Accumulation of HtrA2/Omi in neuronal and glial inclusions in brains with alphasynucleinopathies. J Neuropathol Exp Neurol, 2008. 67(10): p. 984-93.
44. Klionsky DJ, Abdelmohsen K, Abe A, Abedin MJ, Abeliovich H, Acevedo Arozena A, Adachi H, Adams CM, Adams PD, Adeli K et al Guidelines for the use and interpretation of assays for monitoring autophagy. Autophagy. 2012 Apr;8(4):445-544.
45. Klucken J, Poehler AM, Ebrahimi-Fakhari D, Schneider J, Nuber S, Rockenstein E, Schlötzer-Schrehardt U, Hyman BT, McLean PJ,

Masliah E, Winkler J. Alpha-synuclein aggregation involves a bafilomycin A 1-sensitive autophagy pathway. Autophagy. 2012 May 1;8(5):754-66.

46. Kragh CL, Fillon G, Gysbers A, Hansen HD, Neumann M, Richter-Landsberg C, Haass C, Zalc B, Lubetzki C, Gai WP et al. FAS-dependent cell death in alpha-synuclein transgenic oligodendrocyte models of multiple system atrophy. PLoS One, 2013. 8(1): p. e55243.
47. Kriks S, Shim JW, Piao J, Ganat YM, Wakeman DR, Xie Z, Carrillo-Reid L, Auyeung G, Antonacci C, Buch A, et al. Dopamine neurons derived from human ES cells efficiently engraft in animal models of Parkinson's disease. Nature. 2011 Nov 6;480(7378):547-51.
48. Krismer F, Wenning GK. Multiple system atrophy: insights into a rare and debilitating movement disorder. Nat Rev Neurol. 2017 Apr;13(4):232-243.
49. Lantos PL, Papp MI. Cellular pathology of multiple system atrophy: a review. J Neurol Neurosurg Psychiatry, 1994. 57(2): p. 129-33.
50. Lashuel HA, Overk CR, Oueslati A, Masliah E. The many faces of α-synuclein: from structure and toxicity to therapeutic target. Nat Rev Neurosci. 2013 Jan;14(1):38-48.
51. Lee PH, Lee JE, Kim HS, Song SK, Lee HS, Nam HS, Cheong JW, Jeong Y, Park HJ, Kim DJ et al. A randomized trial of mesenchymal stem cells in multiple system atrophy. Ann Neurol, 2012. 72(1): p. 32-40.
52. Liu H, Zhang SC. Specification of neuronal and glial subtypes from human pluripotent stem cells. Cell Mol Life Sci. 2011 Dec;68(24):3995-4008.
53. Lorenzen N, Nielsen SB, Yoshimura Y, Vad BS, Andersen CB, Betzer C, Kaspersen JD, Christiansen G, Pedersen JS, Jensen PH

et al. How epigallocatechin gallate can inhibit alpha-synuclein oligomer toxicity in vitro. J Biol Chem. 2014; 289:21299–310.

54. Low PA, Robertson D, Gilman S, Kaufmann H, Singer W, Biaggioni I, Freeman R, Perlman S, Hauser RA, Cheshire W et al. Efficacy and safety of rifampicin for multiple system atrophy: a randomised, double-blind, placebocontrolled trial. Lancet Neurol, 2014. 13(3): p. 268-75.
55. Mandler M, Valera E, Rockenstein E, Mante M, Weninger H, Patrick C, Adame A, Schmidhuber S, Santic R, Schneeberger A, et al. Active immunization against alpha-synuclein ameliorates the degenerative pathology and prevents demyelination in a model of multiple system atrophy. Mol Neurodegener. 2015; 10:10.
56. Mandler M, Valera E, Rockenstein E, Weninger H, Patrick C, Adame A, Santic R, Meindl S, Vigl B, Smrzka O et al. Next-generation active immunization approach for synucleinopathies: implications for Parkinson's disease clinical trials. Acta neuropathologica. 2014; 127:861–79.
57. Masliah E, Rockenstein E, Mante M, Crews L, Spencer B, Adame A, Patrick C, Trejo M, Ubhi K, Rohn TT et al. Passive immunization reduces behavioral and neuropathological deficits in an alpha-synuclein transgenic model of Lewy body disease. PloS one. 2011; 6:e19338.
58. Matsumoto L, Takuma H, Tamaoka A, Kurisaki H, Date H, Tsuji S, Iwata A. CpG demethylation enhances alpha-synuclein expression and affects the pathogenesis of Parkinson's disease. PLoS One. 2010 Nov 24;5(11):e15522.
59. Mazzulli JR, Xu YH, Sun Y, Knight AL, McLean PJ, Caldwell GA, Sidransky E, Grabowski GA, Krainc D. Gaucher disease

glucocerebrosidase and α-synuclein form a bidirectional pathogenic loop in synucleinopathies. Cell. 2011 Jul 8;146(1):37-52.
60. Miller DW, Johnson JM, Solano SM, Hollingsworth ZR, Standaert DG, Young AB. Absence of alpha-synuclein mRNA expression in normal and multiple system atrophy oligodendroglia. J Neural Transm (Vienna). 2005 Dec;112(12):1613-24.
61. Mizuta I, Takafuji K, Ando Y, Satake W, Kanagawa M, Kobayashi K, Nagamori S, Shinohara T, Ito C, Yamamoto M et al. YY1 binds to α-synuclein 3'-flanking region SNP and stimulates antisense noncoding RNA expression. J Hum Genet. 2013 Nov;58(11):711-9.
62. Multiple-System Atrophy Research Collaboration. Mutations in COQ2 in familial and sporadic multiple-system atrophy. N Engl J Med. 2013 Jul 18;369(3):233-44.
63. Nee LE, Gomez MR, Dambrosia J, Bale S, Eldridge R, Polinsky RJ. Environmental-occupational risk factors and familial associations in multiple system atrophy: a preliminary investigation. Clin Auton Res. 1991 Mar;1(1):9-13.
64. Nguyen HN, Byers B, Cord B, Shcheglovitov A, Byrne J, Gujar P, Kee K, Schüle B, Dolmetsch RE, Langston W et al. LRRK2 mutant iPSC-derived DA neurons demonstrate increased susceptibility to oxidative stress. Cell Stem Cell. 2011 Mar 4;8(3):267-80.
65. Papp MI, Kahn JE, Lantos PL. Glial cytoplasmic inclusions in the CNS of patients with multiple system atrophy (striatonigral degeneration, olivopontocerebellar atrophy and Shy-Drager syndrome). J Neurol Sci, 1989. 94(1-3): p. 79-100.
66. Papp MI, Lantos PL, Accumulation of tubular structures in oligodendroglial and neuronal cells as the basic alteration in multiple system atrophy. J Neurol Sci, 1992. 107(2): p. 172-82.

67. Papp MI, Lantos PL. The distribution of oligodendroglial inclusions in multiple system atrophy and its relevance to clinical symptomatology. Brain, 1994. 117 (Pt 2): p. 235-43.
68. Park SM, Kim KS. Proteolytic clearance of extracellular α-synuclein as a new therapeutic approach against Parkinson disease. Prion. 2013:121–6.
69. Perrier AL, Tabar V, Barberi T, Rubio ME, Bruses J, Topf N, Harrison NL, Studer L. Derivation of midbrain dopamine neurons from human embryonic stem cells. Proc Natl Acad Sci U S A. 2004 Aug 24;101(34):12543-8.
70. Poewe W, Seppi K, Fitzer-Attas CJ, Wenning GK, Gilman S, Low PA, Giladi N, Barone P, Sampaio C, Eyal E et al., Efficacy of rasagiline in patients with the parkinsonian variant of multiple system atrophy: a randomised, placebo-controlled trial. Lancet Neurol, 2015. 14(2): p. 145-52.
71. Porton B, Wetsel WC, Kao HT. Synapsin III: role in neuronal plasticity and disease. Semin Cell Dev Biol. 2011 Jun;22(4):416-24.
72. Poston KL, Tang CC, Eckert T, Dhawan V, Frucht S, Vonsattel JP, Fahn S, Eidelberg D. Network correlates of disease severity in multiple system atrophy. Neurology. 2010 Apr 17;78(16):1237-44.
73. Poston KL, Eidelberg D. Functional brain networks and abnormal connectivity in the movement disorders. Neuroimage. 2012 Oct 1;62(4):2261-70.
74. Prusiner SB, Woerman AL, Mordes DA, Watts JC, Rampersaud R, Berry DB, Patel S, Oehler A, Lowe JK, Kravitz SN et al. Evidence for α-synuclein prions causing multiple system atrophy in humans with parkinsonism. Proc Natl Acad Sci U S A. 2015 Sep 22;112(38):E5308-17.

75. Pyle A, Anugrha H, Kurzawa-Akanbi M, Yarnall A, Burn D, Hudson G. Reduced mitochondrial DNA copy number is a biomarker of Parkinson's disease. Neurobiol Aging. 2016 Feb;38:216.e7-10.
76. Rakovic A, Shurkewitsch K, Seibler P, Grünewald A, Zanon A, Hagenah J, Krainc D, Klein C. Phosphatase and tensin homolog (PTEN)-induced putative kinase 1 (PINK1)-dependent ubiquitination of endogenous Parkin attenuates mitophagy: study in human primary fibroblasts and induced pluripotent stem cell-derived neurons. J Biol Chem. 2013 Jan 25;288(4):2223-37.
77. Reyes JF, Rey NL, Bousset L, Melki R, Brundin P, Angot E. Alpha-synuclein transfers from neurons to oligodendrocytes. Glia. 2014 Mar;62(3):387-98.
78. Ronchi D, Di Biase E, Franco G, Melzi V, Del Sorbo F, Elia A, Barzaghi C, Garavaglia B, Bergamini C, Fato R et al. Mutational analysis of COQ2 in patients with MSA in Italy. Neurobiol Aging. 2016 Sep;45:213.e1-2.
79. Sacca F, Marsili A, Quarantelli M, Brescia Morra V, Brunetti A, Carbone R, Pane C, Puorro G, Russo CV, Salvatore E et al. A randomized clinical trial of lithium in multiple system atrophy. J. Neurol. 2013 Feb;260(2):458-61.
80. Sailer A, Scholz SW, Nalls MA, Schulte C, Federoff M, Price TR, Lees A, Ross OA, Dickson DW, Mok K et al. A genome-wide association study in multiple system atrophy. Neurology. 2016 Oct 11;87(15):1591-1598.
81. Sánchez-Danés A, Richaud-Patin Y, Carballo-Carbajal I, Jiménez-Delgado S, Caig C, Mora S, Di Guglielmo C, Ezquerra M, Patel B, Giralt A et al. Disease-specific phenotypes in dopamine neurons from human iPS-based models of genetic and sporadic Parkinson's disease. EMBO Mol Med. 2012 May;4(5):380-95.

82. Sato K, Kaji R, Matsumoto S, Goto S. Cell type-specific neuronal loss in the putamen of patients with multiple system atrophy. Mov Disord, 2007. 22(5): p. 738-42.
83. Schapira AH. Mitochondria in the aetiology and pathogenesis of Parkinson's disease. Lancet Neurol. 2008 Jan;7(1):97-109.
84. Schapira AH, Cooper JM, Dexter D, Jenner P, Clark JB, Marsden CD. Mitochondrial complex I deficiency in Parkinson's disease. Lancet. 1989 Jun 3;1(8649):1269.
85. Scherzer CR, Grass JA, Liao Z, Pepivani I, Zheng B, Eklund AC, Ney PA, Ng J, McGoldrick M, Mollenhauer B et al. GATA transcription factors directly regulate the Parkinson's disease-linked gene alpha-synuclein. Proc Natl Acad Sci U S A. 2008 Aug 5;105(31):10907-12.
86. Scholz SW, Houlden H, Schulte C, Sharma M, Li A, Berg D, Melchers A, Paudel R, Gibbs JR, Simon-Sanchez J et al. SNCA variants are associated with increased risk for multiple system atrophy. Ann. Neurol. 2009 May;65(5):610-4.
87. Schöndorf DC, Aureli M, McAllister FE, Hindley CJ, Mayer F, Schmid B, Sardi SP, Valsecchi M, Hoffmann S, Schwarz LK et al. iPSC-derived neurons from GBA1-associated Parkinson's disease patients show autophagic defects and impaired calcium homeostasis. Nat Commun. 2014 Jun 6;5:4028.
88. Schottlaender LV, Bettencourt C, Kiely AP, Chalasani A, Neergheen V, Holton JL, Hargreaves I, Houlden H. Coenzyme Q10 Levels Are Decreased in the Cerebellum of Multiple-System Atrophy Patients. PLoS One. 2016 Feb 19;11(2):e0149557.
89. Schottlaender LV, Houlden H; Multiple-System Atrophy (MSA) Brain Bank Collaboration. Mutant COQ2 in multiple-system atrophy. N Engl J Med. 2014 Jul 3;371(1):81.

90. Schwarz L, Goldbaum O, Bergmann M, Probst-Cousin S, Richter-Landsberg C. Involvement of macroautophagy in multiple system atrophy and protein aggregate formation in oligodendrocytes. J Mol Neurosci. 2012 Jun;47(2):256-66.
91. Seibler P, Graziotto J, Jeong H, Simunovic F, Klein C, Krainc D. Mitochondrial Parkin recruitment is impaired in neurons derived from mutant PINK1 induced pluripotent stem cells. J Neurosci. 2011 Apr 20;31(16):5970-6.
92. Seo JH, Yong SW, Song SK, Lee JE, Sohn YH, Lee PH. A case-control study of multiple system atrophy in Korean patients. Mov Disord. 2010 Sep 15;25(12):1953-9.
93. Sharma M, Wenning G, Krüger R; European Multiple-System Atrophy Study Group. Mutant COQ2 in multiple-system atrophy. N Engl J Med. 2014 Jul 3;371(1):80-1.
94. Shi Y, Inoue H, Wu JC, Yamanaka S. Induced pluripotent stem cell technology: a decade of progress. Nat Rev Drug Discov. 2017 Feb;16(2):115-130.
95. Shults CW, Rockenstein E, Crews L, Adame A, Mante M, Larrea G, Hashimoto M, Song D, Iwatsubo T, Tsuboi K, Masliah E. Neurological and neurodegenerative alterations in a transgenic mouse model expressing human alpha-synuclein under oligodendrocyte promoter: implications for multiple system atrophy. J Neurosci. 2005 Nov 16;25(46):10689-99.
96. Singer TP, Salach JI, Castagnoli N Jr, Trevor A. Interactions of the neurotoxic amine 1-methyl-4-phenyl-1,2,3,6-tetrahydropyridine with monoamine oxidases. Biochem J. 1986 May 1;235(3):785-9
97. Spencer B, Michael S, Shen J, Kosberg K, Rockenstein E, Patrick C, Adame A, Masliah E. Lentivirus mediated delivery of neurosin promotes clearance of wild-type alpha-synuclein and reduces the

pathology in an alpha-synuclein model of LBD. Mol Ther. 2013; 21:31–41.

98. Spencer B, Valera E, Rockenstein E, Trejo-Morales M, Adame A, Masliah E. A brain-targeted, modified neurosin (kallikrein-6) reduces alpha-synuclein accumulation in a mouse model of multiple system atrophy. Mol Neurodegener. 2015; 10:48.
99. Stefanova N, Georgievska B, Eriksson H, Poewe W, Wenning GK. Myeloperoxidase inhibition ameliorates multiple system atrophy-like degeneration in a transgenic mouse model. Neurotox Res. 2012; 21:393–404.
100. Stefanova N, Poewe W, Wenning GK. Rasagiline is neuroprotective in a transgenic model of multiple system atrophy. Exp Neurol. 2008 Apr;210(2):421-7.
101. Stefanova N, Puschban Z, Fernagut PO, Brouillet E, Tison F, Reindl M, Jellinger KA, Poewe W, Wenning GK. Neuropathological and behavioral changes induced by various treatment paradigms with MPTP and 3-nitropropionic acid in mice: towards a model of striatonigral degeneration (multiple system atrophy). Acta Neuropathol. 2003 Aug;106(2):157-66. Epub 2003 May 23.
102. Stefanova N, Reindl M, Neumann M, Haass C, Poewe W, Kahle PJ, Wenning JK. Oxidative stress in transgenic mice with oligodendroglial alpha-synuclein overexpression replicates the characteristic neuropathology of multiple system atrophy.Am J Pathol. 2005 Mar;166(3):869-76.
103. Stefanova N, Reindl M, Neumann M, Kahle PJ, Poewe W, Wenning GK. Microglial activation mediates neurodegeneration related to oligodendroglial alphasynucleinopathy: implications for multiple system atrophy. Mov Disord, 2007. 22(15): p. 2196-203.

104. Stefanova N, Reindl M, Neumann M, Haass C, Poewe W, Kahle PJ, Wenning GK. Oxidative stress in transgenic mice with oligodendroglial alpha-synuclein overexpression replicates the characteristic neuropathology of multiple system atrophy. Am J Pathol. 2005 Mar;166(3):869-76

105. Stefanova N, Reindl M, Poewe W, Wenning GK. In vitro models of multiple system atrophy. Mov Disord. 2005 Aug;20 Suppl 12:S53-6.

106. Stefanova N, Wenning GK. Animal models of multiple system atrophy. Clin Auton Res. 2015 Feb;25(1):9-17.

107. Stemberger S, Poewe W, Wenning GK, Stefanova N. Targeted overexpression of human alpha-synuclein in oligodendroglia induces lesions linked to MSA-like progressive autonomic failure. Exp Neurol. 2010 Aug;224(2):459-64.

108. Su X, Federoff HJ, Maguire-Zeiss KA. Mutant alpha-synuclein overexpression mediates early proinflammatory activity. Neurotox Res, 2009. 16(3): p. 238-54.

109. Su X, Maguire-Zeiss KA, Giuliano R, Prifti L, Venkatesh K, Federoff HJ. Synuclein activates microglia in a model of Parkinson's disease. Neurobiol Aging, 2008. 29(11): p. 1690-701.

110. Takahashi M, Suzuki M, Fukuoka M, Fujikake N, Watanabe S, Murata M, Wada K, Nagai Y, Hohjoh H. Normalization of overexpressed alpha-Synuclein Causing Parkinson's Disease By a Moderate Gene Silencing With RNA Interference. Molecular therapy Nucleic acids. 2015; 4:e241.

111. Takahashi K, Yamanaka S. Induction of pluripotent stem cells from mouse embryonic and adult fibroblast cultures by defined factors. Cell, 2006. 126(4): p. 663-76

112. Tang CC, Poston KL, Eckert T, Feigin A, Frucht S, Gudesblatt M, Dhawan V, Lesser M, Vonsattel JP, Fahn S, Eidelberg D. Differential diagnosis of parkinsonism: a metabolic imaging study using pattern analysis. Lancet Neurol. 2010 Feb;9(2):149-58.

113. Tanji K, Odagiri S, Maruyama A, Mori F, Kakita A, Takahashi H, Wakabayashi K. Alteration of autophagosomal proteins in the brain of multiple system atrophy. Neurobiol Dis. 2013 Jan;49:190-8.

114. Tatebe H, Watanabe Y, Kasai T, Mizuno T, Nakagawa M, Tanaka M, Tokuda T. Extracellular neurosin degrades alpha-synuclein in cultured cells. Neurosci Res. 2010; 67:341–6.

115. Ubhi K, Inglis C, Mante M, Patrick C, Adame A, Spencer B, Rockenstein E, May V, Winkler J, Masliah E. Fluoxetine ameliorates behavioral and neuropathological deficits in a transgenic model mouse of α-synucleinopathy. Exp Neurol. 2012; 234:405–16.

116. Ubhi K, Lee PH, Adame A, Inglis C, Mante M, Rockenstein E, Stefanova N, Wenning GK, Masliah E. Mitochondrial inhibitor 3-nitroproprionic acid enhances oxidative modification of alpha-synuclein in a transgenic mouse model of multiple system atrophy. J Neurosci Res. 2009 Sep;87(12):2728-39.

117. Ubhi K, Low P, Masliah E. Multiple system atrophy: a clinical and neuropathological perspective. Trends Neurosci. 2011 Nov;34(11):581-90.

118. Ubhi K, Rockenstein E, Mante M, Inglis C, Adame A, Patrick C, Whitney K, Masliah E. Neurodegeneration in a transgenic mouse model of multiple system atrophy is associated with altered expression of oligodendroglial-derived neurotrophic factors. J Neurosci. 2010 May 5;30(18):6236-46.

119. Valera E, Mante M, Anderson S, Rockenstein E, Masliah E. Lenalidomide reduces microglial activation and behavioral deficits in a transgenic model of Parkinson's disease. J Neuroinflammation. 2015; 12:93.
120. Valera E, Masliah E. Immunotherapy for neurodegenerative diseases: Focus on α-synucleinopathies. Pharmacol Ther. 2013
121. Valera E, Monzio Compagnoni G, Masliah E. Review: Novel treatment strategies targeting alpha-synuclein in multiple system atrophy as a model of synucleinopathy. Neuropathol ApplNeurobiol. 2016 Feb;42(1):95-106.
122. Valera E, Ubhi K, Mante M, Rockenstein E, Masliah E. Antidepressants reduce neuroinflammatory responses and astroglial alpha-synuclein accumulation in a transgenic mouse model of multiple system atrophy. Glia. 2014; 62:317–37.
123. Vanacore N, Bonifati V, Fabbrini G, Colosimo C, De Michele G, Marconi R, Stocchi F, Nicholl D, Bonuccelli U, De Mari M et al. Case-control study of multiple system atrophy. Mov Disord. 2005 Feb;20(2):158-63.
124. Vanacore N, Bonifati V, Fabbrini G, Colosimo C, Marconi R, Nicholl D, Bonuccelli U, Stocchi F, Lamberti P, Volpe G et al. Smoking habits in multiple system atrophy and progressive supranuclear palsy. European Study Group on Atypical Parkinsonisms. Neurology. 2000 Jan 11;54(1):114-9.
125. Vidal JS, Vidailhet M, Elbaz A, Derkinderen P, Tzourio C, Alpérovitch A. Risk factors of multiple system atrophy: a case-control study in French patients. Mov Disord. 2008 Apr 30;23(6):797-803.
126. Wagner J, Ryazanov S, Leonov A, Levin J, Shi S, Schmidt F, Prix C, Pan-Montojo F, Bertsch U, Mitteregger-Kretzschmar G et al.

Anle138b: a novel oligomer modulator for disease-modifying therapy of neurodegenerative diseases such as prion and Parkinson's disease. Acta neuropathologica. 2013; 125:795–813.

127. Wang W, Perovic I, Chittuluru J, Kaganovich A, Nguyen LT, Liao J, Auclair JR, Johnson D, Landeru A, Simorellis AK et al. A soluble α-synuclein construct forms a dynamic tetramer. Proc Natl Acad Sci U S A. 2011 Oct 25;108(43):17797-802.

128. Wei W, Keogh MJ, Wilson I, Coxhead J, Ryan S, Rollinson S, Griffin H, Kurzawa-Akinibi M, Santibanez-Koref M, Talbot K et al. Mitochondrial DNA point mutations and relative copy number in 1363 disease and control human brains. Acta Neuropathol Commun. 2017 Feb 2;5(1):13.

129. Wilkins A, Majed H, Layfield R, Compston A, Chandran S. Oligodendrocytes promote neuronal survival and axonal length by distinct intracellular mechanisms: a novel role for oligodendrocyte-derived glial cell line-derived neurotrophic factor. J Neurosci, 2003. 23(12): p. 4967-74.

130. Woerman AL, Stöhr J, Aoyagi A, Rampersaud R, Krejciova Z, Watts JC, Ohyama T, Patel S, Widjaja K, Oehler A et al. Propagation of prions causing synucleinopathies in cultured cells. Proc Natl Acad Sci U S A. 2015 Sep 1;112(35):E4949 -58.

131. Woodard CM, Campos BA, Kuo SH, Nirenberg MJ, Nestor MW, Zimmer M, Mosharov EV, Sulzer D, Zhou H, Paull D et al. iPSC-derived dopamine neurons reveal differences between monozygotic twins discordant for Parkinson's disease. Cell Rep. 2014 Nov 20;9(4):1173-82

132. Wullner U, Abele M, Schmitz-Huebsch T, Wilhelm K, Benecke R, Deuschl G, Klockgether T. Probable multiple system

atrophy in a German family. J Neurol Neurosurg Psychiatry. 2004 Jun;75(6):924-5.

133. Xilouri M, Brekk OR, Stefanis L. Autophagy and Alpha-Synuclein: Relevance to Parkinson's Disease and Related Synucleopathies Movement Disorders 31 (2), pp. 178-192

134. Yang SY, Beavan M, Chau KY, Taanman JW, Schapira AH. A Human Neural Crest Stem Cell-Derived Dopaminergic Neuronal Model Recapitulates Biochemical Abnormalities in GBA1 Mutation Carriers. Stem Cell Reports. 2017 Mar 14;8(3):728-742.

135. Yazawa I, Giasson BI, Sasaki R, Zhang B, Joyce S, Uryu K, Trojanowski JQ, Lee VM. Mouse model of multiple system atrophy alpha-synuclein expression in oligodendrocytes causes glial and neuronal degeneration. Neuron. 2005 Mar 24;45(6):847-59.

136. Yu WH, Dorado B, Figueroa HY, Wang L, Planel E, Cookson MR, Clark LN, Duff KE. Metabolic activity determines efficacy of macroautophagic clearance of pathological oligomeric alpha-synuclein. Am J Pathol. 2009 Aug;175(2):736-47.

137. Zhang P, Xia N, Reijo Pera RA. Directed dopaminergic neuron differentiation from human pluripotent stem cells. J Vis Exp. 2014 Sep 15;(91):51737.

138. Zharikov AD, Cannon JR, Tapias V, Bai Q, Horowitz MP, Shah V, El Ayadi A, Hastings TG, Greenamyre JT, Burton EA. shRNA targeting alpha-synuclein prevents neurodegeneration in a Parkinson's disease model. The Journal of clinical investigation. 2015; 125:2721–35.

139. Zuscik MJ, Sands S, Ross SA, Waugh DJ, Gaivin RJ, Morilak D, Perez DM. Overexpression of the alpha1B-adrenergic receptor causes apoptotic neurodegeneration: multiple system atrophy. Nat Med. 2000 Dec;6(12):1388-94.